PROFESSUR FÜR HYDROLOGIE
ALBERT-LUDWIGS UNIVERSITÄT
FREIBURG IM BREISGAU

Simon Brenner

Simulation of Groundwater Inundation during the UK 2012 Floods

Masterarbeit

Referent: Dr. Andreas Hartmann
Korreferent: PD Dr. Jens Lange

Freiburg i. Br., September 2015

Acknowledgements

I would like to express my deepest gratitude for all the people who supported and encouraged me during this work. First of all, I would like thank my first supervisor Dr Andreas Hartmann for his patience, guidance and great engagement and for making this thesis possible. Secondly I want to thank Dr Jens Lange for taking on the second supervision and his constructive feedback. In general, I want to thank the whole Institute of Hydrology for allowing me to be a part in the Master's programme. Thanks also to all the employees and master students in the "blue container" as well as to the "Karst group". For providing data and useful advices I'd like to thank Gemma Coxon and Dr Nicholas Howden from the University of Bristol. A very special thanks to Lukas, Mark and André for their constructive comments and proofreading.

In addition, I would like to thank all my friends who provided welcome distractions. Finally, I'd like to thank my entire family and especially my parents, for making my whole education possible.

Abstract

Groundwater flooding is increasingly recognised as a threat in the UK and throughout Europe. Rapid rising groundwater levels leading to long-lasting groundwater inundation can cause considerable damage and social disruption. The Chalk is particularly susceptible to groundwater flooding due its permeable geology and karstic behaviour. In summer 2012 several areas in southern England experienced groundwater inundations following the wettest June on record. Among these were the Frome and Piddle catchments located in West Dorset.

Comparatively few attempts have been made so far to model groundwater levels in the Chalk on a physical basis and at a high temporal resolution. This study attempted to contribute a simple, process-based groundwater inundation prediction tool based on the karst model VarKarst. VarKarst has a compartment structure considering the different flow paths in karst systems. To model various groundwater levels, matching groundwater storage compartments are chosen and transferred into groundwater levels using a simple linear relationship. Focus was set on the Frome catchment due to the fact that the flooding in July 2012 primarily happened there. In addition, attempts were made to define flood threshold levels. Eventually, future groundwater flooding risk is examined by means of the bias-corrected output of five Global Climate Models (GCMs).

The results indicated that the developed method can offer an alternative to already existing approaches. Groundwater level simulations showed high efficiencies of over 0.80 in the calibration period with only slight decreases in the validation period. Optimised parameters during calibration showed a karstic behaviour dominated by the matrix which is in accordance with other studies of the Chalk. Nevertheless, due to considerable under- and overestimations further improvement of the presented method is demanded. Thereby assumptions regarding the porosity and the assumed linear relationship are possible starting points. The threshold level was defined based on a rather coarse dip approach and an event analysis and needs further verification.

Climate predictions of groundwater flooding occurrences showed a positive trend throughout the century 2000-2099. However, GCM output differed substantially from reality so that results should be interpreted with caution. To cope with the vastly different GCM output, a model threshold had to be introduced. In order to improve the reliability of the climate projections, an application of other bias-correction or downscaling methods should be considered in the future.

Key words: Chalk, UK, groundwater flooding, groundwater inundation, hydrological modelling, flood threshold, climate change, GCM-output, future flood risk

Zusammenfassung

Sowohl im Vereinigten Königreich, als auch in ganz Europa wird "Groundwater Flooding" zunehmend als Gefahr erkannt. Ein "Groundwater Flooding" findet statt, wenn schnell ansteigende Grundwasserspiegel über die Geländeoberkante treten. Karstsysteme mit durchlässigem Gestein wie der englische "Chalk" sind dabei besonders anfällig. Im Sommer 2012 führten starke Regenfälle zu Überflutungen durch aufsteigendes Grundwasser in mehreren Gebieten im Süden Englands, darunter die Einzugsgebiete der Frome und der Piddle im westlichen Dorset.

Bislang gibt es nur wenige hochaufgelöste, prozess-basierte Modelle zur Simulation von Grundwasserspiegeln im englischen "Chalk". Die Bestrebung dieser Arbeit ist daher eine einfache, physikalisch basierte, alternative Methode beizutragen, welche auf dem Karstmodell VarKarst basiert. Das VarKarst Modell hat eine Struktur mit einer Reihe von Kompartmenten. Mithilfe dieser Kompartmente ist es in der Lage verschiedene Fließprozesse, wie sie im Karst üblich sind, zu berücksichtigen. Um die Grundwasserspiegel zu simulieren wird eine einfache, lineare Beziehung zwischen dem Grundwasserspiegel und einem modellierten Grundwasserspeicherkompartment angenommen. Dabei wird dasjenige Grundwasserspeicherkompartment ausgewählt, das ein möglichst ähnliches Verhalten wie der entsprechende Grundwasserspiegel zeigt. Da es im Sommer 2012 hauptsächlich im Einzugsgebiet der Frome zu einer grundwasserbedingten Überflutung kam, wurde die Modellierung auf das Frome-EZG beschränkt. Zusätzlich zur Modellierung wurde versucht einen Schwellenwert zu bestimmen, ab dem es zu einer Überflutung kommt. Zu guter Letzt wurde das zukünftige Risiko durch aufsteigendes Grundwasser untersucht. Dafür wurde der bias-korrigierte Output von fünf globalen Klimamodellen verwendet.

Die Ergebnisse konnten zeigen, dass die entwickelte Methode eine vielversprechende Alternative zu bisherigen Ansätzen bietet. Die Modellierung ergab hohe Kling-Gupta Efficiencies von über 0.80 in der Kalibrierungsphase und nur geringe Verschlechterungen während des Validierungszeitraumes. Die Modellierung zeigte, wie zuvor bereits andere Studien, ein Karstverhalten welches von der Matrix dominiert wird. Es kam jedoch auch zu großen Unter- und Überschätzungen der jeweiligen Grundwasserspiegel, sodass eine weitere Verbesserung der Methode unerlässlich ist. Dabei sollten die Porosität und das angenommene lineare Verhältnis erste Ansatzpunkte sein. Der ermittelte Schwellenwert basiert auf einem relativ ungenauem Ansatz und einer Eventanalyse und sollte daher weiter verifiziert werden.

Die Modellierung zukünftiger "Groundwater Flooding"-Ereignisse zeigte einen positiven

Trend über das Jahrhundert hinweg. Da der Output der Klimamodelle jedoch stark von den meteorologischen Kennzahlen des Einzugsgebietes abweicht, sollten die Ergebnisse mit Vorsicht interpretiert werden. Infolgedessen musste ein Modellschwellenwert eingeführt werden. Um die Verlässlichkeit der Vorhersagen zu verbessern sollten daher zusätzliche, beziehungsweise andere, bias-Korrekturen oder Downscaling-Methoden in Betracht gezogen werden.

Schlagwörter: Grundwasser, Hochwasser, hydrologische Modellierung, Karst, Chalk, UK, Hochwasservorhersage, GCM-output Zukunftsprognosen

Table of Contents

List of Figures

List of Tables

List of Abbreviations

Notation	Description
BC	Bias Correction
BGS	British Geological Survey
Cal	Calibration
CEH	Centre for Ecology & Hydrology
CFMP	Catchment Flood Management Plan
CMIP	Coupled Model Intercomparison Project
GCM	Global Climate Model
GEM	Groundwater Emergence Maps
GFDL-ESM2M	Geophysical Fluid Dynamics Laboratory - Earth System Model 2
GWL	Groundwater level
HadGEM2-ES	Hadley Global Environment Model 2 - Earth System
hQ-Plot	Plot of groundwater levels against discharges
IPCC	Intergovernmental Panel on Climate Change
IPSL-CM5A-LR	Institut Pierre Simon Laplace Climate Model 5A - Low Resolution
ISI-MIP	Inter-Sectoral Impact Model Intercomparison Project
KGE	Kling-Gupta Efficiency
MCAT	Monte Carlo Analysis Toolbox
MIROC-ESM-CHEM	An atmospheric chemistry coupled version of MIROC-ESM (Model for Interdisciplinary Research on Climate - Earth System Model)

Mod	Modelled ($\widehat{=}$ simulated)
MSE	Mean Squared Error
NOAA	National Oceanic and Atmospheric Administration
NorESM1-M	The Norwegian Earth System Model
NSE	Nash-Sutcliffe Efficiency
Obs	Observed
PET	Potential Evapotranspiration
PSD	Permeable Superficial Deposits
Q	Discharge
Q50	50th Percentile of a discharge time series
RCM	Regional Climate Model
RCP	Representative Concentration Pathway
SCE-UA	Shuffled Complex Evolution (University of Arizona)
SCEM-UA	Shuffled Complex Evolution Metropolis (University of Arizona)
UK	United Kingdom
Val	Validation
VDCN	Vertical Distance to the Channel Network

List of Symbols

Notation	Unit	Description
a_{fsep}	-	Recharge seperation variability constant
a_{GW}	-	Groundwater variability constant
a_{SE}	-	Soil epikarst depth variability constant
$E_{act,i}(t)$	mm	Actual evapotranspiration
$E_{act,i}(t)$	mm	Potential evapotranspiration
$f_{C,i}$	-	Variable seperation factor
h_{GW}	m	Modelled groundwater Level
K_C	d	Conduit storage coefficient
$K_{E,i}$	-	Epikarst storage coefficient
$K_{GW,i}$	d	Variable groundwater storage coefficient
$K_{mean,E}$	d	Epikarst mean storage coefficent
$p_{GW,A}$	-	Ashton Farm groundwater level porosity parameter
$p_{GW,B}$	-	Black House groundwater level porosity parameter
$p_{GW,R}$	-	Ridgeway groundwater level porosity parameter
$\Delta h_{GW,A}$	m	Ashton Farm groundwater level offset parameter
$\Delta h_{GW,B}$	m	Black House groundwater level offset parameter
$\Delta h_{GW,R}$	m	Ridgeway groundwater level offset parameter
$Q_{Epi,i}(t)$	mm	Outflow of the epikarst
$Q_{GW,i}(t)$	$\mathrm{mm\,d^{-1}}$	Groundwater contributions of the matrix
$Q_{GW,N}(t)$	$\mathrm{mm\,d^{-1}}$	Groundwater contributions of the conduit system
$Q_{main}(t)$	$\mathrm{l\,s^{-1}}$	Main spring discharge
$Q_{Surf,i+1}(t)$	mm	Surface flow to the next model compartment

$R_{conc,i}(t)$	mm	Concentrated recharge
$R_{diff,i}(t)$	mm	Diffuse recharge
$R_{Epi,i}(t)$	mm	Recharge to the epikarst
$V_{E,i}$	mm	Epikarst storage distribution
$V_{GW,i}$	mm	Groundwater storage distribution
$V_{max,E}$	mm	Maximum epikarst storage capacity
$V_{max,S}$	mm	Maximum soil storage capacity
$V_{mean,E}$	mm	Mean epikarst storage capacity
$V_{mean,S}$	mm	Mean soil storage capacity
$V_{S,i}$	mm	Soil storage distribution

Chapter 1

Introduction

1.1 BACKGROUND

Worldwide, weather-related disasters account for about 90% of the disastrous events in the last two decades (WDR, 2005, 2014). These disasters include wind storms, droughts and floods. In Europe, floods are the most common fatal disasters. During the 2000-2009 decade, floods are reported to have affected over 3.4 million people and taken at least 1000 lives (JAKUBICKA et al., 2010). In recent years, the United Kingdom faced floods with severe socio-economic consequences (SLINGO et al., 2014). In this context, a special case is "groundwater inundation" or "groundwater flooding" . Groundwater flooding happens when groundwater levels emerge at the ground surface (DEFRA, 2004). The phenomenon appears to be most severe in areas of Chalk outcrop such as in parts of southern England (MACDONALD et al., 2012).

Groundwater Flooding has been increasingly recognised in Europe and throughout the UK (e.g. FINCH et al., 2004; PINAULT et al., 2005; MACDONALD et al., 2007; KREIBICH and THIEKEN, 2008; KORKMAZ et al., 2009; HUGHES et al., 2011; ROBINS and FINCH, 2012). However, the underlying processes still remain insufficiently understood (HUGHES et al., 2011) and an assessment of potential future changes is broadly recommended (JACKSON et al., 2015; JIMENEZ-MARTINEZ et al., 2015).

As reported by the Intergovernmental Panel on Climate Change (IPCC), the world experienced an increase of about 0.6 °C in average global temperatures over the last century (NAKICENOVIC et al., 2000). They further predicted an increase of global temperatures between 2 and 3.5 °C by 2100, depending on the emission scenario. Besides temperatures, rainfall patterns may significantly change in some areas (JIMENEZ-MARTINEZ et al., 2015). Climate change is widely suspected to have significant consequences on groundwater systems (GREEN et al., 2011) with impacts on several groundwater issues (TAYLOR et al., 2013). According to JIMENEZ-MARTINEZ et al. (2015) most researchers appear to agree that there is a trend towards drier summer periods and wetter winter periods in the UK. This will likely increase the occurrence of extreme rainfall events.

So far, comparatively few attempts have been made to establish a simple process-based groundwater inundation tool. With regard to future climatic, social and industrial pressures combined with the complexity of karstic aquifers, there is a substantial need for a better understanding of groundwater flooding processes. The intention of this work is to draw attention to future challenges in the area of groundwater flooding and to contribute a simulation tool which could improve flood risk management.

The present thesis is divided into six chapters followed by the references and appendices. Besides the background information, this introduction comprises a brief overview on karst principles, the process of groundwater flooding and on climate modelling. Additionally, the main objectives of this work are presented. Subsequently, the description of the catchments is provided in Chapter 2. The material and methods used in this study are reviewed in Chapter 3. Chapter 4 presents the results of the study. After discussing the results in Chapter 5, the principal conclusions are set out in Chapter 6.

1.2 STATE OF THE ART

1.2.1 Karst

Karst groundwater provides an important freshwater source for many regions around the world (GOLDSCHEIDER and DREW, 2007). FORD and WILLIAMS (2007) estimated that up to 25% of the world's population obtains water from karstic groundwater resources and around one tenth of the earth's continental area is covered by karst regions. However, karst aquifers are considered as difficult to exploit and highly vulnerable to contamination (BAKALOWICZ, 2005). Additionally, they often show rapid responses to hydrological events due to their intrinsic properties (GOLDSCHEIDER and DREW, 2007). With regard to their evolution and their hydrological behaviour, karst systems differ substantially from other hydrological systems (HARTMANN et al., 2014a). The following section will describe the main hydro(geo)logical peculiarities and their implications for hydrological modelling.

1.2.1.1 Karst Evolution

Primarily, karst develops from carbonate rocks like limestone or dolomite, but also from gypsum and other soluble rocks (BAKALOWICZ, 2005). Karst aquifers are evolving with time, prone to constantly changing their flow and storage characteristics (GOLDSCHEIDER and DREW, 2007). The long-lasting, intense interactions between water with dissolved CO_2 and soluble host rocks result in a characteristic karst landscape with specific underground and/or superficial karst features (HARTMANN et al., 2014a). Often associated with karst evolution is the term "karstification" which is commonly used to describe the process of dissolution in carbonate rocks (BAKALOWICZ, 2005; HARTMANN et al., 2014a).

Karstification can enlarge initial fractures or even change the whole extension and orientation of the flow system (GOLDSCHEIDER and DREW, 2007). HARTMANN et al. (2014a) suggests that there is a "positive feedback" between enlarged fractures, increased water flow and rock dissolution. According to KAUFMANN and BRAUN (2000) fracture flow can increase by several orders of magnitude when initial fractures are enlarged by karstification. These mechanisms can lead to the formation of karst conduits and caves which, in turn, as suggested by GOLDSCHEIDER and DREW (2007): "may collapse or be filled with sediments".

Fractures, conduits and caves are often connected, forming extensive hydraulic networks in the aquifer (HARTMANN et al., 2014a). Consequently, there are two main ways for water flowing through the aquifer: Flow occurring through the hydraulic networks and water flow through the rock matrix.

1.2.1.2 Karst Characteristics

Karst aquifers are highly heterogeneous which is, as identified by GOLDSCHEIDER and DREW (2007), the major problem in analysing karst hydrogeology. They argue that drilling wells in karst aquifers can be problematic due to the fact that water-bearing fractures and conduits may occur directly next to undisturbed rock mass.

Following FORD and WILLIAMS (2007) hydrogeologists distinguish between primary, secondary and tertiary porosity: Primary porosity is attributed to the matrix whereas secondary porosity is attributed to fissures and fractures. Channels or conduits make up the tertiary porosity, although sometimes the latter two porosities are treated as one.

According to GOLDSCHEIDER and DREW (2007) recharge, infiltration, flow as well as storage of karst aquifers are showing dual characteristics: Recharge is either autogenic or allogenic. Whereas autogenic recharge originates from the karst catchment itself, the allogenic recharge is provided by surrounding non-karst catchments. Infiltration occurs either diffusively through the rock matrix or rapidly by point recharge. Flow in the matrix is generally slow and laminar whereas fractures and conduits allow a fast and turbulent flow. Storage is mostly attributed to the matrix and only a small percentage is stored in fractures and conduits.

The uppermost zone of a karst area, usually called "epikarst", is characterised by enhanced permeability and porosity (WILLIAMS, 2008). Hence, it can play an important role in the concentration of vertical flow (AQUILINA et al., 2006). Owing to these characteristics, spring discharges can vary over several orders of magnitudes and water tables in karst aquifers can fluctuate by several meters within short periods of time (HARTMANN et al., 2014a).

Surface water catchments and groundwater catchments are often not coincident. The surface water catchment is controlled by topographical features whereas the groundwater catchment is determined by underground geological structures(HOWDEN, 2006). Sometimes water flow between adjacent catchments occurs through so called piracy routes (JUKIĆ and DENIĆ-JUKIĆ, 2009). In conclusion, Figure 1.1 illustrates the basic karst terms and processes.

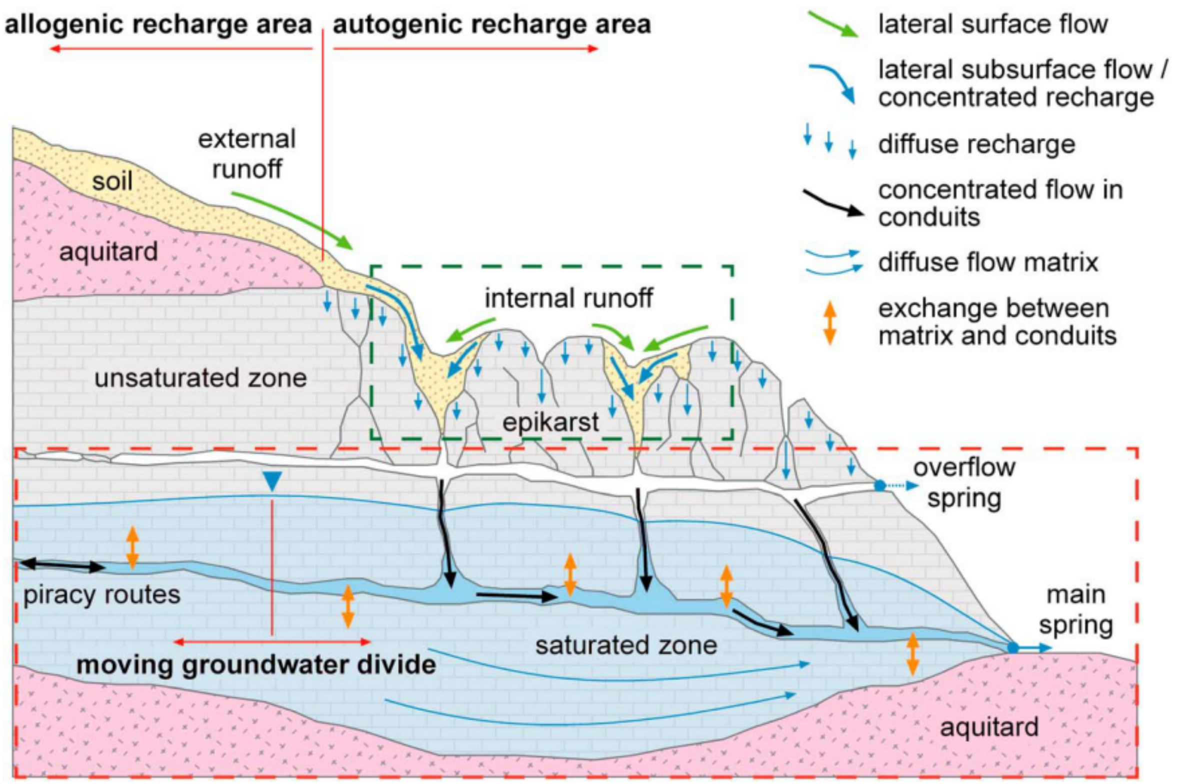

Figure 1.1: Conceptualized karst system. The green dashed lines surround the soil/epikarst system, the red dashed lines surround the groundwater system. Adapted from: HARTMANN et al., 2014a, p.4.

1.2.1.3 The Chalk

The English Chalk extends over large parts of south-east England. Remarkably, Chalk provides about 55% of all groundwater-abstracted drinking water in the UK and is therefore the most important aquifer, particularly in southern England (LLOYD, 1993).

Following the characterisation of PRICE et al. (1993), Chalk-porosities typically range between 20 and 45 percent. Thereby the matrix is primarily composed of small, uniform coccolith particles leading to small effective pore-throat diameters ($0.1 - 1\mu m$). Consequently, matrix permeability is very low ranging from 0.1 to 10 mD. They state, however, that Chalk aquifers are often extensively fissured and prone to dissolution processes and developing fissure networks can increase the transmissivities significantly.

The karstic behaviour of the Chalk in southern England is increasingly being recognised (FITZPATRICK, 2011), even though the Chalk may not be far developed in terms of karstification (MAURICE et al., 2006). ATKINSON and SMART (1981) characterised the English Chalk as a "non-karstic fissured aquifer" but they also suggest that carbonate aquifers should not be considered as wholly karstic or wholly non-karstic, but as holding varying degrees of karstification. LLOYD (1993) points out, that the Chalk in the UK is characterised by the presence of many dry valleys and ephemeral streams. This may indicate the existence of an extensive underground flow network. Chalk soils are largely characterised as shallow (LEE et al., 2006; BRADFORD and CROKER, 2007). BURNHAM and MUTTER (1993) found soil depths over Chalk ranging between 23 and 121 cm whereas JOHNSON et al. (2001) examined depths between 50 and 150 cm.

LEE et al. (2006) reports that previous research suggests that recharge in the Chalk mainly occurs through the matrix. They state, however, that depending on the Chalk type and on the situation significant recharge can occur through fissures. JONES and COOPER (1998) for example examined increased fissure flow during wetter (winter) months. HARIA et al. (2003) found no evidence for rapid preferential flow on an interfluve where the unsaturated zone was approximately 18 meters. Yet, they found evidence at a site located in a valley where the groundwater levels are within 4 meters of the ground surface. Similarly, the study from JOHNSON et al. (2001) suggests that recharge through fissures is enhanced when the water table is close to the surface.

As reported by MACDONALD et al. (1998), rapid groundwater flow occurs throughout the entire Chalk outcrop. He stated, similar to ALLEN et al. (1997) that rapid groundwater flow can be most frequently observed nearby Palaeogene cover and in valley bottoms. Correspondingly, BANKS et al. (1995) observed flow velocities of over 5 kilometres per day in a swallow hole system in the Chalk. WORTHINGTON (1999) examined four different carbonate aquifers in terms of storage and flow properties. He suggests that all unconfined carbonate aquifers demonstrate similar behaviour due similar dissolution and fracturing processes. He attributes disagreements in literature primarily to sampling differences. For all these reasons, the Chalk in the UK can be seen as "karstic".

1.2.1.4 Karst Modelling

There are several ways to model karst systems. "Blackbox" models simply transfer input to output by using transfer functions. Conveniently they are very simple, however, they are not based on physical processes. Considering spatial and temporal variability, process-based karst models have clear advantages (HARTMANN et al., 2014a).

Two main types of process-based karst models can be found in the literature: distributed (eg. KIRALY, 1998; ROZOS and KOUTSOYIANNIS, 2006; BUTSCHER and HUGGENBERGER, 2007) and lumped (eg. RIMMER and SALINGAR, 2006; FLEURY et al., 2007; BUTSCHER and HUGGENBERGER, 2008; FLEURY et al., 2009) modelling approaches. Distributed models represent flow processes in sub-units building a two dimensional or sometimes three dimensional grid. Each sub-unit needs specific parameters allowing spatially explicit flow estimations. (HARTMANN et al., 2013a)

However, as already stated above, karst aquifers are highly heterogeneous and therefore accurate data is rarely available. Thus, mainly lumped modelling approaches are applied on karst systems (JUKIĆ and DENIĆ-JUKIĆ, 2009). HARTMANN et al. (2013a) introduced the VarKarst model which can be seen as a hybrid between lumped and distributed modelling approaches due to its particular model structure (see Section 3.2).

Generally, hydrological modelling is based on conceptualizing real processes (KUCZERA and MROCZKOWSKI, 1998). Direct measurement of model parameters is often not feasible and sometimes impossible. Thus, parameters are estimated indirectly through a calibration procedure (HARTMANN et al., 2014a). They can be estimated manually or automatically (VRUGT et al., 2003). Today, automatic calibration approaches are preferred e.g. MCAT (WAGENER et al., 2001), SCE-UA (DUAN et al., 1992) or SCEM-UA (VRUGT et al., 2003).

Commonly, a goodness of fit measure like the Mean Squared Error (MSE), the Nash-Sutcliffe Efficiency (NSE, NASH and SUTCLIFFE, 1970) or the Kling-Gupta Efficiency (KGE, GUPTA et al., 2009) is used as an objective function to calibrate the model against a runoff time series (KUCZERA and MROCZKOWSKI, 1998). As stated by GUPTA et al. (2009) the NSE and the MSE are widely used but also heavily discussed criteria. They presented the KGE, a result of a decomposition of the NSE (and MSE), emphasizing the importance of the different components of the criteria.

There is a trade-off between relatively simple and more complex models (KUCZERA and MROCZKOWSKI, 1998). As more complex models may include more physical processes (HARTMANN et al., 2014a) and produce better fits during calibration (PERRIN et al., 2001), they have the problem of overparameterization (BEVEN, 1996) leading to parameter unidentifiability (HARTMANN et al., 2014a) and less robustness (PERRIN et al., 2001). A large number of parameters can cause equifinality, meaning that different parameter sets can lead to equally good model results. As early as 1970, the principle of parsimony in hydrological modelling has been promoted by BOX and JENKINS. Parsimony in this context means that the simplest possible model should be selected (BOX and JENKINS, 1970). KUCZERA and MROCZKOWSKI (1998) discussed the assets and drawbacks of parsimonious and complex model approaches. They suggest less than six parameters when calibrating only against streamflow. Multi-objective approaches, with additional information such as hydrochemical data, can relevantly improve parameter identifiability (HARTMANN et al., 2014a).

In order to validate the performance of a model a wide range of techniques is available. KLEMEŠ (1986) proposed several methods including the split-sample test. In the split-sample test available time series are split into two segments. After calibrating against the first segment the second segment is used for validation.

1.2.2 Groundwater Flooding

As stated and characterised in the reports of DEFRA (2004; 2005) there are several types of floods, e.g. (i) fluvial flooding, (ii) pluvial or surface water flooding, (iii) coastal flooding and (iv) groundwater flooding: Whereas (i) and (ii) happen when rivers or soils cannot cope with the amount of water entering it, coastal flooding (iii) occurs as the weather and tidal conditions increase sea levels. Groundwater flooding (iv) appears as a result from rising water tables above the natural surface (see Figure 1.2) driven by intense rainfalls.

Usually, groundwater flooding events are a winter phenomenon and events in summer periods occur very rarely (PARRY et al., 2013). In contrast to fluvial flooding, groundwater flooding events often have longer durations and very low flow velocities (MACDONALD et al., 2008). Thus they are a minor threat to human health but they can produce more than twice as much damage to building fabrics compared to fluvial flooding (COLLIER, 2014). They occur most likely in low-lying areas underlain by permeable strata (DEFRA, 2005; HUGHES et al., 2011). Typically, events last weeks rather than hours leading to substantial social and economic disruption (MACDONALD

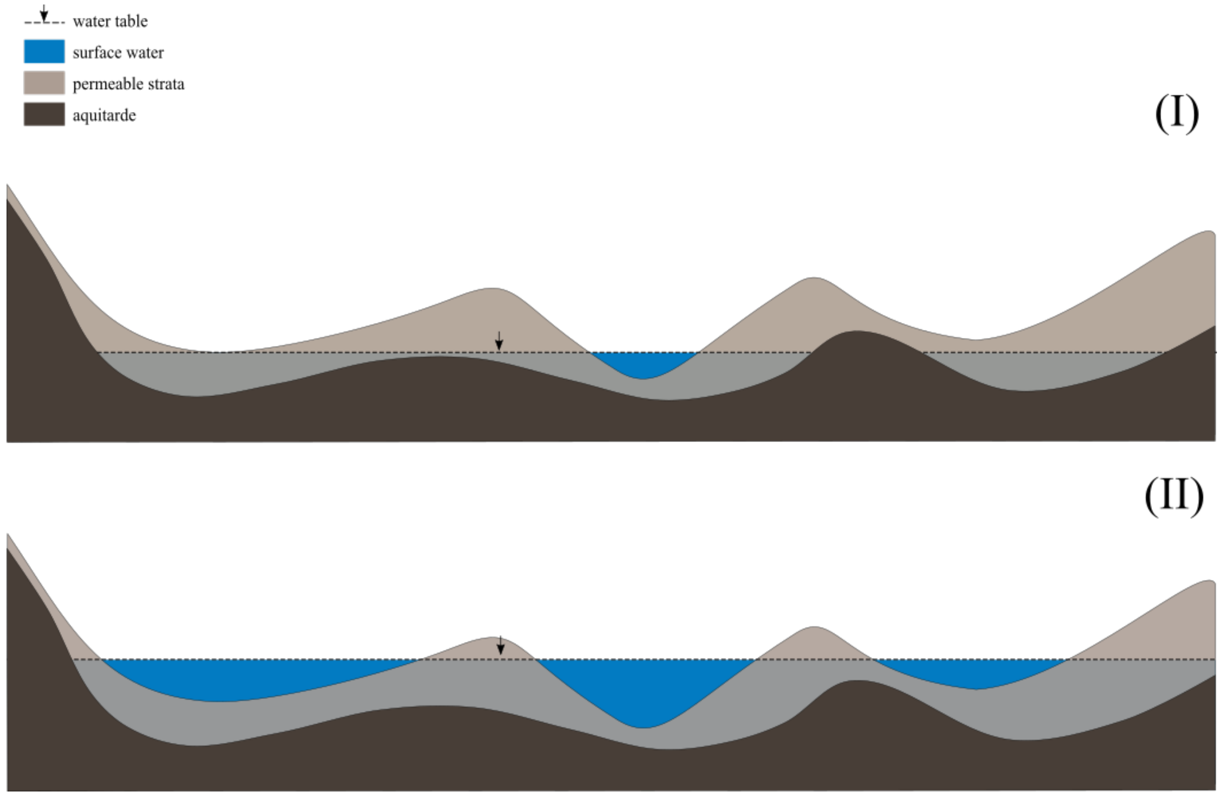

Figure 1.2: Conceptualized Groundwater Flooding

et al., 2008; HUGHES et al., 2011). According to MACDONALD et al. (2008) urban areas are at particular risk since traditional flood protection may be circumvented as the upward flow can occur ubiquitously. In contrast, MCKENZIE and WARD (2015) emphasizes that rural areas are often faced with greater impact because urban areas can mitigate inundation depths through the existence of extensive drain and sewer systems.

FINCH et al. (2004) analysed the spatial distribution of groundwater flooding. The occurrence of emerging groundwater seems to be controlled on how the river valley is oriented to the regional groundwater flow. Zones with increased permeabilities can additionally drive the emergence of groundwater at the ground surface. The paper described two forms of groundwater flooding: Firstly, emergence from saturated alluvial deposits and secondly, emergence from permeable strata, typically located in the upper reaches of streams and rivers.

Following MACDONALD et al. (2008), there are three scenarios of groundwater flooding: (i) long-lasting, regionally extensive groundwater flooding caused by intensive rainfalls, combined with antecedent conditions of high groundwater tables and high soil moisture, (ii) rapid responsive groundwater flooding of shallow unconsolidated sedimentary aquifers and (iii) groundwater flooding due to reduced industrial activities and therefore reduced abstraction.

HUGHES et al. (2011) agreed regarding scenarios (i) and (iii) while suggesting that groundwater flooding can further occur by groundwater flow through the alluvium or caused by geological barriers. MCKENZIE et al. (2010) noted that it is sometimes hard to distinguish between different flood types as they often occur simultaneously. ROBINS and FINCH (2012) emphasized the importance of differentiating between groundwater flood and groundwater induced flood. Whereas the "true groundwater flood" occurs as groundwater levels reach the surface, the groundwater induced flood happens due to increased base flow, leading rivers to burst their banks.

Regardless of the form, scenario or type, groundwater flooding is highly connected to the geological settings and the present topography (COBBY et al., 2009). Several attempts have been made to assess areas which are susceptible to groundwater flooding. JACOBS (2004) created "Groundwater Emergence Maps" (GEMs) by identifying areas where winter groundwater levels are only within 2 meters below the ground surface. He estimated that 1.7 million properties are at risk from groundwater flooding in England. The most vulnerable properties (about 380,000) are located in southern England, where Chalk is the major aquifer type. Following MCKENZIE and WARD (2015) these numbers are probably an overestimate since the used approach was rather course. They add that the procedure by JACOBS does not take into account past flood events. Their estimated number of properties in susceptible areas is around 920,000. Based on the groundwater flooding event in winter 2013/2014, they calculated that only 205,700 properties are at actual risk from groundwater flooding. In addition to endangered properties, the groundwater itself is at risk since superficial damages can lead to water contamination (KREIBICH and THIEKEN, 2008). Besides JACOBS's attempt, the British Geological Society (BGS) has produced groundwater flooding susceptibility maps[1]. They distinguish between "clearwater flooding" from rising groundwater levels and flooding through "Permeable Superficial Deposits" (PSD) e.g. when there is a connection between surface watercourses and the adjacent area through the alluvium (MCKENZIE et al., 2007).

BRADFORD and CROKER (2007) used hQ-plots, a combination of discharge and groundwater head time series to create a fluvial flood alert procedure in the Chalk. They classified the suitability of boreholes for this approach based on their head-flow response. Only boreholes which showed a clear bend in the hQ-plots were considered to be suitable. Moreover this bend corresponded to the respective flood threshold level. For their method they strongly suggest that data from the extreme event in 2000/01 should be incorporated if possible in Chalk catchments of southern England. Regarding groundwater flood risk management COBBY et al. (2009) provided

[1] http://www.bgs.ac.uk/research/groundwater/datainfo/GFSD.html (as of September 24th, 2015)

a notable review of the advances made so far. They believe that determining the inundation depth and its likelihood of occurrence is one of the major challenges of future research. ADAMS et al. (2010) presented a framework for an early warning system. They suggested an approach to model groundwater levels based on a simple linear transfer function.

Furthermore, there are some approaches which include digital elevation models. MCKENZIE et al. (2010) described the use of digital elevation models to predict areas which are susceptible to groundwater flooding. With an extensive borehole dataset they interpolated groundwater levels on a national scale. Where no sufficient data was available they constructed water tables with the help of river networks, lakes and the sea, assuming hydraulic continuity. They concluded that proper borehole data is a crucial requirement for groundwater flood susceptibility mapping.

UPTON and JACKSON (2011) presented an approach to model groundwater inundation extents by simulating a set of hydrographs with a simple lumped parameter groundwater model. They further transposed the modelled hydrograph to a network of boreholes to model groundwater emergence more precisely. However, their approach is only based on monthly values possibly missing shorter groundwater flooding events. BUTLER et al. (2012) notes that one major difficulty when modelling groundwater levels is the parameterization of the unsaturated zone.

According to current climate models, the risk of groundwater flooding will possibly increase (UPTON and JACKSON, 2011). JIMENEZ-MARTINEZ et al. (2015) predicted an increase of future groundwater flooding events in a catchment of the English Chalk. They used transfer functions to avoid modelling the whole karst system and defined a trigger level at which groundwater flooding occurs based on an event in 2000/01. According to their calculations groundwater flooding events will become approximately 7 times more frequent by the end of this century.

1.2.3 Climate Modelling

There is a vast number of Global Climate Models (GCMs) developed by various research groups from all over the world. To study and compare those models the Coupled Model Intercomparison Project (CMIP)[2] was established (MEEHL et al., 2000). Unfortunately, GCM resolutions remain relatively coarse as they are designed for global impact studies (HEMPEL et al., 2013).

EHRET et al. (2012) explains that for using climate models on a regional scale, downscaling and/or bias-correction methods are needed: For downscaling, preferably "dynamical downscaling" is used to improve simulations. It enhances resolution by nesting a Regional Climate Model (RCM) into a GCM. They note, however, that the output of a RCM-GCM may lead to a degree

[2] Now in the fifth phase (CMIP5). URL: http://cmip-pcmdi.llnl.gov/cmip5/ (as of September 24th, 2015)

of error that impedes drawing meaningful conclusions out of impact studies.

Bias-correction (BC) adjusts the GCM output towards historic data (EHRET et al., 2012), building a bridge between GCM output and observed data (HEMPEL et al., 2013). Yet, EHRET et al. (2012) criticise current bias-correction methods as they neglect feedback mechanisms and lack physical justification, rather hiding uncertainties than reducing them. HEMPEL et al. (2013) introduced the Inter-Sectoral Impact Model Intercomparison Project (ISI-MIP) approach for a trend preserving BC. They agree regarding the fact that bias-correction introduces another level of uncertainty. They argue, however, that “impact models (. . .) often require driving climate data that is statistically similar to the observational datasets with which they were calibrated”. For further information about the ISI-MIP approach see Section 3.5.

1.3 OBJECTIVES

In the last 15 years groundwater flooding in the UK has increasingly become a subject of research (COBBY et al., 2009). The English Chalk is profoundly susceptible to groundwater flooding and future climate predictions suggest an increase of intense rain events. This thesis focuses on the modelling of the groundwater levels in the Frome catchment with emphasis on the groundwater flooding event in the summer of 2012.

The intention is to apply an adapted version of the VarKarst model introduced by HARTMANN et al. (2013a) on the catchment to simulate groundwater levels. Subsequently, attempts are made to detect whether and when groundwater inundation happens in the catchment. Finally, the output of five climate models is additionally used as input for the presented model to examine the future risk of groundwater flooding. Consequently, this thesis attempts to answer the following research questions:

Is the developed model able to simulate groundwater levels on a daily time step? Is the presented approach able to adequately detect groundwater inundation? Is it possible to reasonably determine the future frequency of occurrence of groundwater flooding events? And lastly, is the approach a useful alternative to already existing approaches?

Chapter 2

Study site

2.1 GENERAL INFORMATION

The Frome and Piddle catchments are located in West Dorset in the south-west of England (see Figure 2.1). The two rivers drain adjacent chalk catchments and their elevation varies from over 200 m a.s.l. in the north-west to sea level in the south-east. After all, the catchment areas are around 414 and 208 km, respectively. (HOWDEN et al., 2010)
The topography is very flat with a mean slope of 3.9 % and a mean height of approximately 111 meter above sea level. The main urban areas are Dorchester and Wareham. The total population is about 50,000 and is predicted to increase by approximately 10 % by 2035 (DORSET COUNTY COUNCIL, 2011). However, it is a rural region with urban areas making up only a small percentage of the total land use (ENVIRONMENT AGENCY, 2012). Industrial activity is light and focuses mainly on agriculture (HOWDEN, 2006). Hence it is a area of high amenity value, known for its good angling opportunities and remarkable flora and fauna (ADAMS et al., 2003). Agriculture accounts for more than 75 % of the total land use, equally composed of arable and pasture (WESSEX WATER, 2012).

2.2 CLIMATE

Dorset is one of the southernmost counties in the UK. The climate can be defined as oceanic with mild winters and warm summers (DORSET COUNTY COUNCIL, 2009).

The mean winter temperature is about 6 °C and the mean summer temperature is around 20 °C (DORSET COUNTY COUNCIL, 2005). As can be seen from Table 2.1, mean annual precipitation in both catchments lies around 1000 mm exceeding mean annual potential evapotranspiration by approximately 400 mm. Since the area is characterised by mild winters snow is quite rare, particularly in the coastal areas (DORSET COUNTY COUNCIL, 2009).

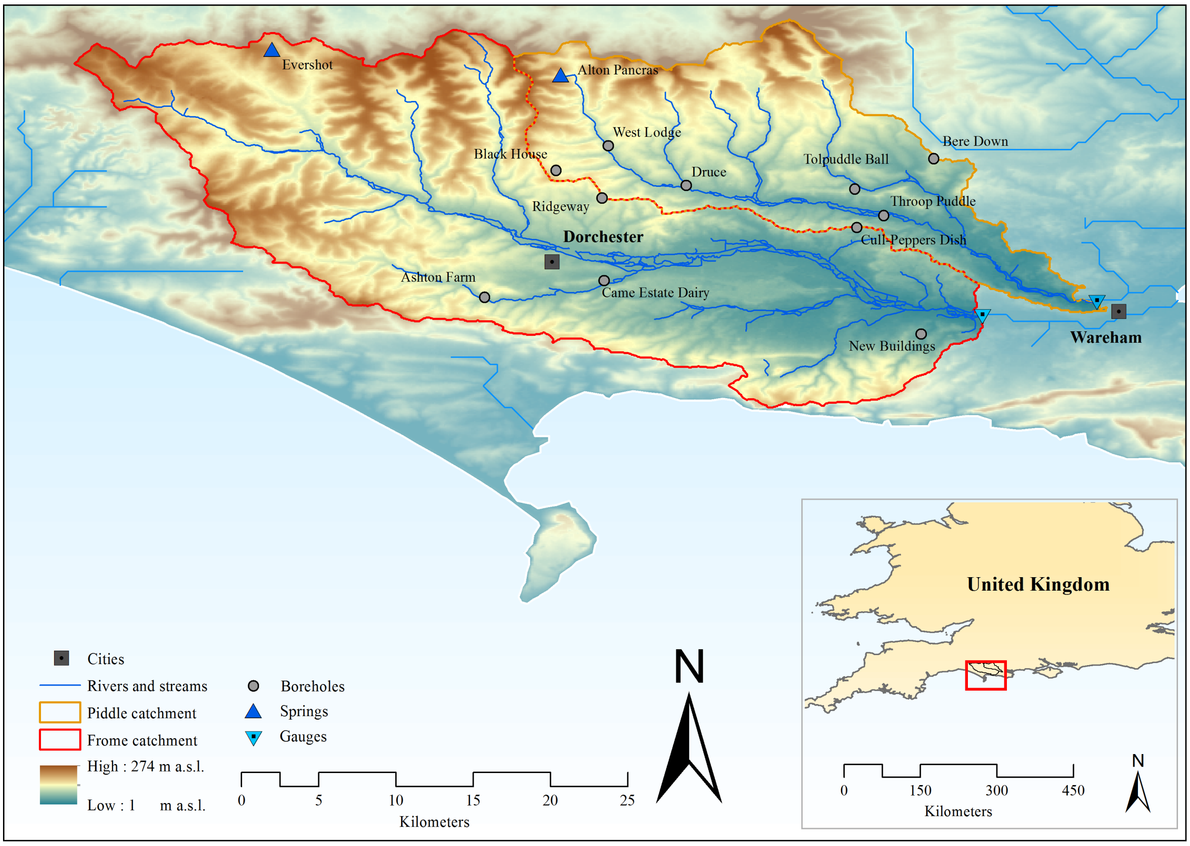

Figure 2.1: The Frome and Piddle Catchment

Table 2.1: Mean, minimum and maximum values of precipitation and potential evapotranspiration in the Frome and Piddle catchments

Parameter	Frome			Piddle		
			Period of time			*Period of time*
Precipitation $[\mathrm{mmy}^{-1}]$	mean	1105	*1900 - 2012*	mean	997	*1900 - 2012*
	min	588		min	522	
	max	1600		max	1464	
PET $[\mathrm{mmy}^{-1}]$	mean	591	*1961 - 2008*	mean	594	*1961 - 2011*
	min	527		min	534	
	max	670		max	669	

Climate projections suggest that the UK will experience increasing temperatures and less rainfall in summer periods and warmer, wetter winter periods (DORSET COUNTY COUNCIL, 2010). According to GOSLING et al. (2011) the total amount of rainfall is predicted to remain unchanged. Hence winter rainfall extremes in the UK are likely to increase in the future.

2.3 HYDROLOGY

The rivers Frome and Piddle arise near Evershot and Alton Pancras, respectively. After flowing south-east to Dorchester, the river Frome turns due east, running through Wool and Wareham. The river Piddle flows south-east through Puddletown before running towards Wareham. (HOWDEN et al., 2010)

Downstream of Wareham, both rivers drain separately into Poole Harbour, which is claimed to be one of the largest estuaries in Europe (MAY and HUMPHREYS, 2005). Like the whole UK Chalk outcrop, the area is characterised by ephemeral groundwater-fed streams, so called (winter-)bournes which normally rise in the wetter winter periods (KEATING, 1982). Notably one tributary of the Frome river is named "South Winterbourne". As can be seen in Figure 2.1, the Frome spring at Evershot is not connected to the river shapefile. The shapefile is provided by the Environment Agency[3] and explicitly intended for chalk streams. However, it seems that the file does not involve the branch to the spring. This can be seen as another indicator of the widespread occurrence of ephemeral streams.

2.3.1 Hydrodynamics

HOWDEN (2006) characterised both rivers as highly groundwater-dominated. For all examined rivers in the catchments he calculated base flow indices of over 0.79. However, he added that local impermeable drift strata could regionally enhance direct run-off proportions. As can be seen in Figure 2.2 both rivers show a similar discharge behaviour. Yet, the mean discharge of the Frome is over twice as high as the discharge of the Piddle (Table 2.2).

[3] http://www.geostore.com/environment-agency/WebStore?xml=environment-agency/xml/ogcDataDownload.xml (as of September 24th, 2015)

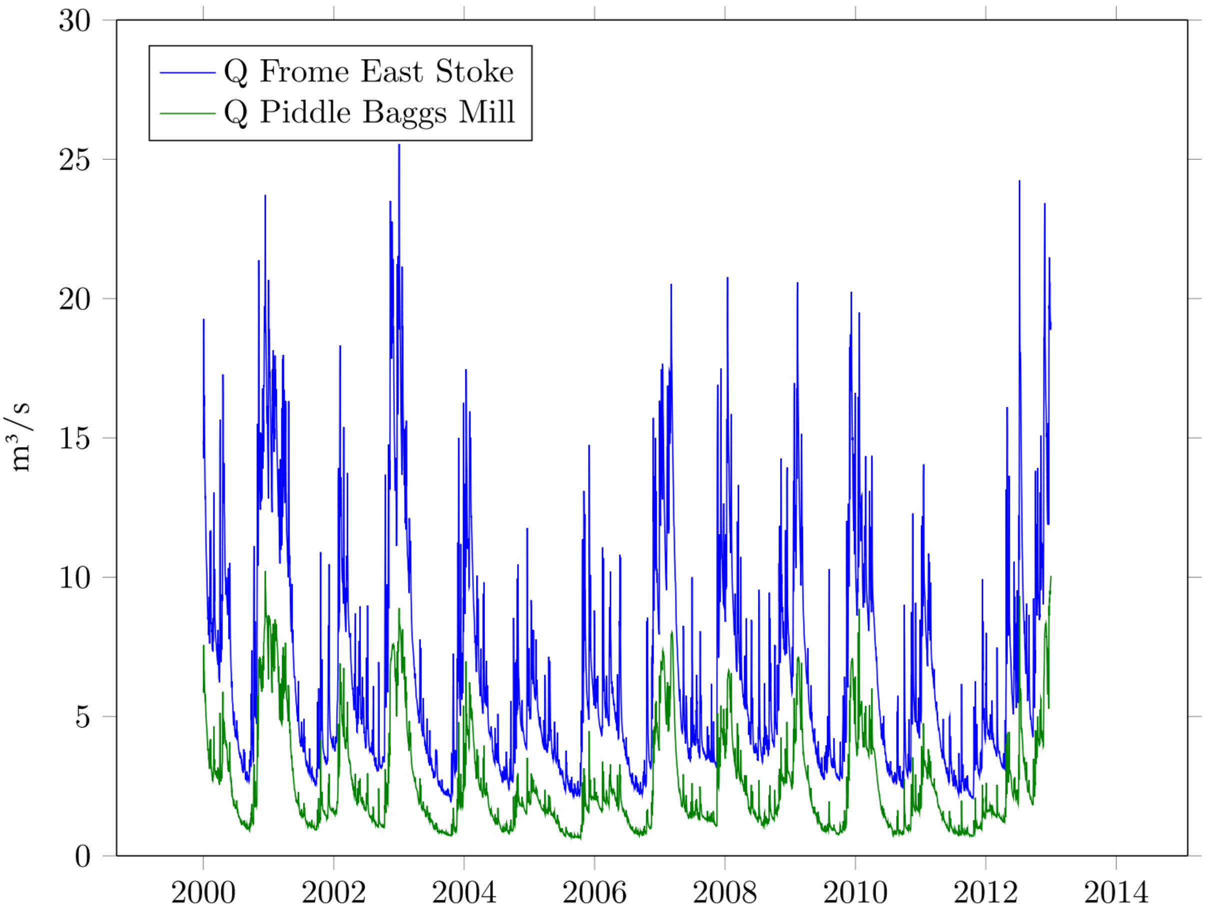

Figure 2.2: Daily discharges [m^3s^{-1}] of the Frome (East Stoke gauging station) and the Piddle (Baggs Mill gauging station) over the modelling period

ADAMS et al. (2003) and HOWDEN (2006) (among others) suggested that there may be groundwater transfers between both catchments. HOWDEN (2006) quantifies water balance losses of 5 % in the Frome catchment (at East Stoke) and 8 % in the Piddle catchment (at Baggs Mill). This may indicate negligible water losses through inter catchment flow. Following the National Rivers Authority (NRA) the catchments are heavily utilised for water abstractions (NRA, 1995). However, they distinguish between surface water abstractions and groundwater abstractions. The total maximum licensed annual water quantity for both catchments is around 128,000 Ml (128 mio m^3) with groundwater accounting for about 50 %. Non-consumptive abstractions (e.g. for fish farming) account for approximately 70 % of the surface water abstracted. Groundwater abstractions are primarily consumptive and either used for public or private water supply. According to MANSELL-MOULLIN (as cited in HOWDEN, 2006, p. 137) groundwater abstractions may be up to 10 percent of the annual runoff in the catchments.

Table 2.2: Hydrological data of the Frome (at East Stoke) and Piddle (at Baggs Mill). Source: CEH, 2015

Parameter	Frome East Stoke	Piddle Baggs Mill	Unit
Period of Record	1965 - 2013	1963 - 2013	y
Base Flow Index	0.86	0.89	-
Mean Flow	6.65	2.44	m^3s^{-1}
95% Exceedance (Q95)	2.45	0.79	m^3s^{-1}
70% Exceedance (Q70)	3.74	1.25	m^3s^{-1}
50% Exceedance (Q50)	5.31	1.85	m^3s^{-1}
10% Exceedance (Q10)	12.65	4.89	m^3s^{-1}

2.3.2 Hydrochemistry

Since this thesis focuses on the hydrodynamics of the system, only some basic hydrochemical information are presented. Further information can be found in the comprehensive work of HOWDEN (2006) and HOWDEN et al. (2010).

All in all, a high quality for both groundwater and surface water has been attested by the NRA in 1995. Conversely, the ENVIRONMENT AGENCY (2009) characterises the quality and quantity of the groundwater as poor at least in the middle reaches of the catchments. Furthermore they predict a future deterioration of both parameters. Following BRUNNER et al. (2010) the biological quality of the river Frome is poor whereas the physico-chemical quality is good. HOWDEN (2006) identifies increased agricultural activity and associated rise of nitrate and potassium concentrations as the major impact on the groundwater quality. According to HOWDEN et al. (2010) the waters of the rivers are nutrient-rich and of a calcium bicarbonate type and therefore characteristic for Chalk-associated agricultural catchments.

2.4 GEOLOGY

The following geological description is mainly based on the doctoral thesis of HOWDEN (2006, p.81 ff) which contains a comprehensive characterisation of the hydrogeological peculiarities.

Historically, the English Chalk was divided into 3 groups: Upper, middle and lower Chalk (JUKES-BROWNE, 1880; JUKES-BROWNE and HILL, 1900, 1903, 1904). During the 1990s a new and more complex lithostratigraphic scheme was developed among others by BRISTOW et al. (1997) dividing the Chalk into ten units. Remarkably, all ten units outcrop in the catchments. Thus, the lithology of the Frome and Piddle catchments can be described as complex.

The geology is predominated by the Cretaceous Chalk outcrop. The Chalk matrix is thereby dominated by the mineral calcite. Approximately 65 % of the catchments are underlain by Chalk. As can be seen from Figure 2.3, the catchments share similar geological features. However, whereas the river Piddle and its tributaries rise primarily from Jurassic limestones and mudstones or the Gault, the headwaters of the Frome include outcrops of the Upper Greensand, often overlain by the rather impermeable Zig-Zag Chalk. The middle reaches of both rivers traverse the Cretaceous Chalk outcrop followed by Palaeogene strata in the lower reaches, eventually draining into Poole Harbour.

Over 40 % of the catchment are covered by drift deposits. Hence, the catchments comprise six main geological units: (i) Jurassic, (ii) Upper Greensand, (iii) Gault, (iv) Chalk, (v) Palaeogene and (vi) Drift. While (i) relies more upon matrix than fracture flow the water movement in (ii) occurs mainly through the matrix. Both units appear in a confined and an unconfined form in the catchments. The Gault (iii) virtually acts as an aquiclude, providing confining layers above Jurassic and impermeable bases to Upper Greensand aquifers. The major aquifer Chalk (iv) appears mainly unconfined. However, in the lower reaches it is overlain by Palaeogene strata, resulting in confined aquifer conditions.

The region around the Frome catchment is known for the highest density of solution features in the UK (EDMONDS, 1983). A considerable number of these features can be observed in the interfluve between the Frome and Piddle (ADAMS et al., 2003). As stated in Subsection 1.2.1.3 Palaeogene strata combined with Chalk is known to enhance karstification. The corresponding soils are often acidic and quite clayey leading acidic runoff to discrete points (ALLEN et al., 1997).

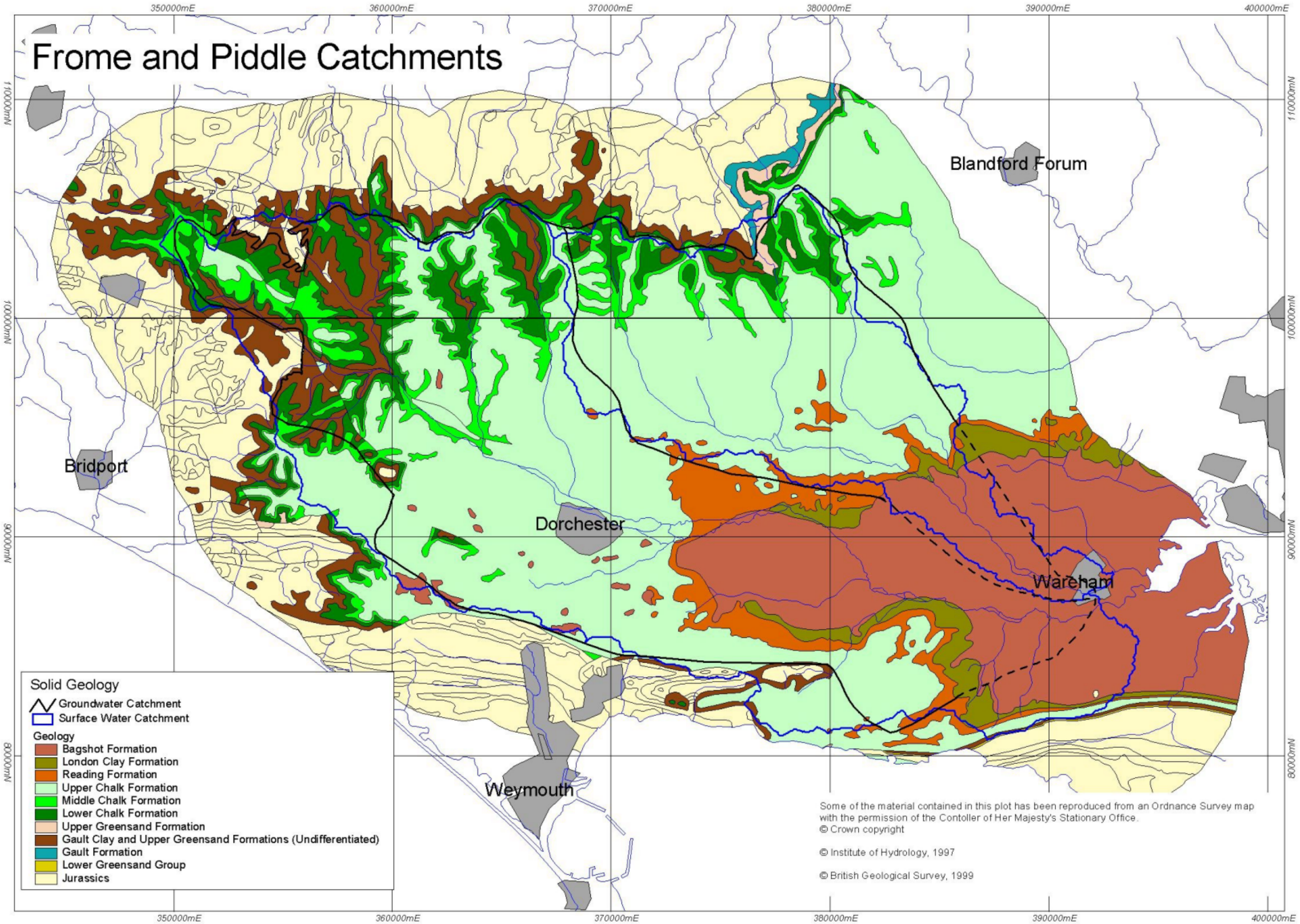

Figure 2.3: Frome and Piddle Catchement Geology. Adapted from: HOWDEN, 2006, p.83.

2.5 SOILS

The distribution of soil types corresponds highly to the underlying geology. Loams over chalk, shallow silts, deep loamy, sandy and shallow clays contribute the lion's share of the soils occurring in the study area (BRUNNER et al., 2010). The soils of the upper parts of the catchments are mainly shallow and well drained (NRA, 1995). In the middle and lower reaches the soils are becoming more sandy and acidic due to waterlogged conditions caused by either groundwater or winter flooding (NRA, 1995; BRUNNER et al., 2010). Generally, soils that develop on carbonate rock are relatively high in clay content (FORD and WILLIAMS, 2007). ALLEN et al. (1997) argues that high clay contents may concentrate runoff to discrete points explaining increased solution activities associated with Palaeogene-covered Chalk.

2.6 GROUNDWATER FLOODING

Exceptionally large amounts of rainfall on 6-7 July in 2012 led to flooding in several areas in the United Kingdom, particularly in southwest England. Following the wettest June on record counties like Devon and Dorset faced over 100 mm of rain in only two days. (ALMOND, 2013)

According to BENNETT (2013) and BUTLER (2013) flooding in the Frome catchment occurred primarily in the South Winterbourne valley and in Maiden Newton. The large precipitation event initially led to flash flooding and resulted in a rapid response of the groundwater levels. The flood in the South Winterbourne valley lasted for approximately two weeks with inundation depths between 500 and 700 mm. 42 properties as well as several roads were flooded during the event. For example, the trunk road A35 between Dorchester and Winterbourne Abbas was closed in both directions due to the flooding (BBC, 2012). The report of BUTLER (2013) suggests that the strongly heterogeneous rainfall pattern led to the localised flooding in the South Winterbourne valley (see Figure A.2 in the Appendix).

The British Geological Society (BGS) produced "Groundwater Flooding Susceptibility Maps" based on rock types and modelled groundwater levels. Figure A.3 (Appendix) shows the areas in the Frome and Piddle catchment which are susceptible emerging groundwater. Generally the Frome catchment comprises larger susceptible areas, particularly around Dorchester and in the South Winterbourne valley.

Figure A.1 in the Appendix shows the behaviour of the borehole Kingston Russell, which is also in the subcatchment South Winterbourne. The borehole has been used by the Environment Agency for flood alert purposes. Unfortunately this borehole is not included in this study. The figure illustrates how frequently the threshold levels have been exceeded between 2004 and 2013.

Research suggests that considerable larger events occurred in the catchment, such as the winter events in 2000/01 and 2013/14. However, due to a lack of data availability, attempts were made to develop a prediction tool based on the event in summer 2012.

Chapter 3

Material & Methods

The following chapter comprises all relevant information about the used data and performed methods. After an overview on the available data and the VarKarst model, the implementation strategy is demonstrated. Following that, methods to define a groundwater inundation threshold are presented. Finally, five climatic scenarios are introduced and hence used for prediction of future groundwater flooding occurences. Figure 3.1 shows the main steps undertaken in a simplified manner.

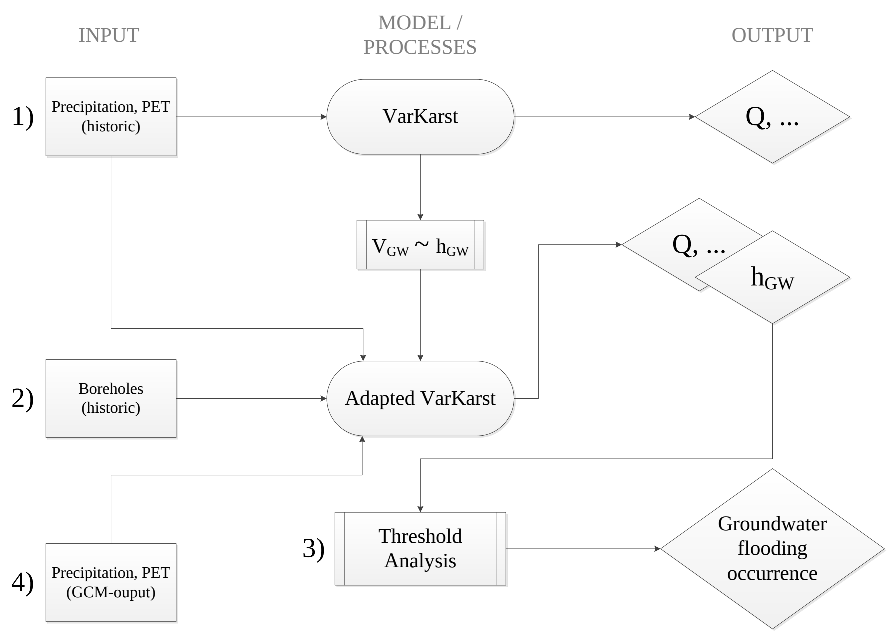

Figure 3.1: Flowchart of the study steps. 1.) Testing of the VarKarst model in the catchment and consequent adaptation 2.) Calibration with the adapted VarKarst model 3.) Threshold Analysis to examine flood occurrences 4.) Using GCM-output for future projections

3.1 AVAILABLE DATA

The discharge data was obtained from the Centre for Ecology & Hydrology (CEH). The daily mean discharges date back to the 1960s and can be downloaded freely from the official website[4]. The borehole data was provided by the Environment Agency (EA) and obtained via the University of Bristol. The digital elevation model was produced by the U.S. Geological Survey[5] (USGS). It is provided in a 3 arc-sec resolution and "void-filled". This means that the recorded raw data which comprise "nodata" areas was corrected with two different filling algorithms (LEHNER et al., 2006). The catchment polygon shapefiles were again provided by the CEH. River network shapefiles were obtained from the EA. The climate scenario data was provided by the Inter-Sectoral Model Intercomparison Project (ISI-MIP)[6].The total data used for modelling in this study can be seen in Table 3.1.

Table 3.1: Data used for modelling

Parameter	Source	Period of time	Resolution	Unit
Precipitation	CEH	01.01.2000 - 31.12.2012	daily	mm d^{-1}
Discharge	CEH	01.01.2000 - 31.12.2012	daily	$m^3 s^{-1}$
Pot. Evapotranspiration	CEH	01.01.2000 - 31.12.2008	daily	mm d^{-1}
Groundwater levels	EA	01.01.2003 - 31.12.2012	daily/monthly	m a.s.l.
Digital Elevation Model[7]	USGS	-	3	arc-sec
Global Climate Model Output[8]	ISI-MIP	01.01.1968 - 31.12.2099	daily	mm & °C

In the beginning, no further information about the temporal resolution and the time spans of the borehole data was available. Unfortunately, only four boreholes provided a high temporal resolution. The high resolution raw data had been collected at a 15-minute interval. For further analysis, the data was aggregated on a daily basis with R. The low resolution boreholes comprised data with roughly one measurement per month. Apart from the gauges and the meteorological stations, Figure 3.2 shows all borehole locations and their measure frequency between 2008 and 2012. Later modelling focusses on the three boreholes "Ashton Farm", "Ridgeway" and "Black House". Only "Ashton Farm" contains a continuous time series without gaps from 2003 to 2012.

[4] http://www.ceh.ac.uk/data/ (as of September 24th, 2015)
[5] http://hydrosheds.cr.usgs.gov/dataavail.php (as of September 24th, 2015)
[6] https://www.pik-potsdam.de/research/climate-impacts-and-vulnerabilities/research/rd2-cross-cutting-activities/isi-mip (as of September 24th, 2015)
[7] The resolution of the available digital elevation models at USGS is stored in the format of arc-seconds. At the equator one arc-second equals approximately 30 meters. In the northern latitudes of the present study site a 3 arc-seconds grid cell measures approximately 60x90 meters. (ARCUSER, 2015)
[8] Spatial resolution 0.5° × 0.5° (see Section 3.5)

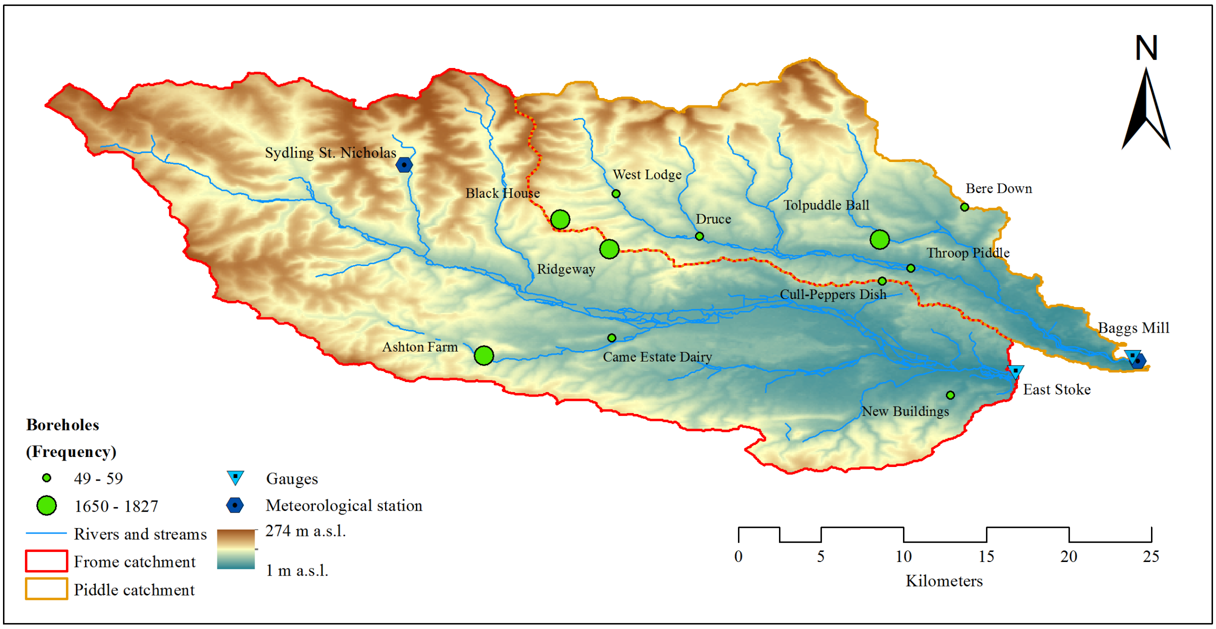

Figure 3.2: Gauges, meteorological stations and borehole locations and their measure frequency between 2008 and 2012

The potential evapotranspiration in both catchments has a strong annual cycle. Since most recent data from years 2009-2012 (Frome) was missing, representative PET-years were calculated on the basis of the last fifty years. These representative years were then attached to time series. The strong annual cycle and the artificial PET-years can be seen in Figure 3.3.

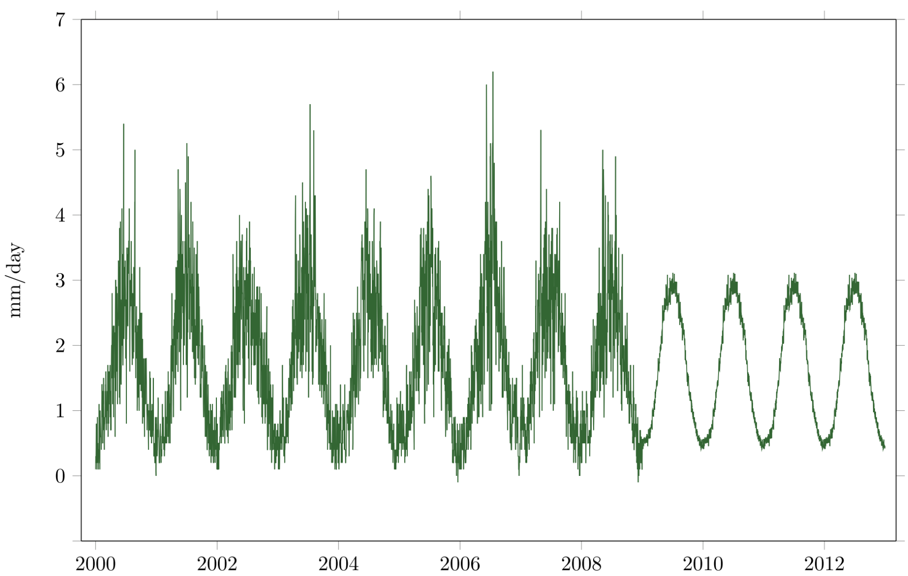

Figure 3.3: Annual cycle of the potential evapotranspiration in the Frome catchment

3.2 THE VARKARST MODEL

In this section the VarKarst model and its functioning will be explained. After some general information about the model a detailed view on the calculation procedure is provided. The major part of this section is based on HARTMANN et al. (2013a) and HARTMANN et al. (2013c). Table 3.2 comprises all relevant equations.

3.2.1 General Information

The VarKarst model is a process-based hydrological karst model programmed in MATLAB® which operates on a daily timestep. It was introduced by HARTMANN et al. (2013a) and was initially applied on a catchment in Southern Spain. Similar to other karst models, it distinguishes between three subroutines representing the soil system, the epikarst system and the groundwater system. The model is able to consider (i) varying soil and epikarst depths, (ii) the duality of recharge (concentrated/diffuse) and the variability of (iii) epikarst hydrodynamics and (iv) groundwater hydrodynamics by using Pareto functions.

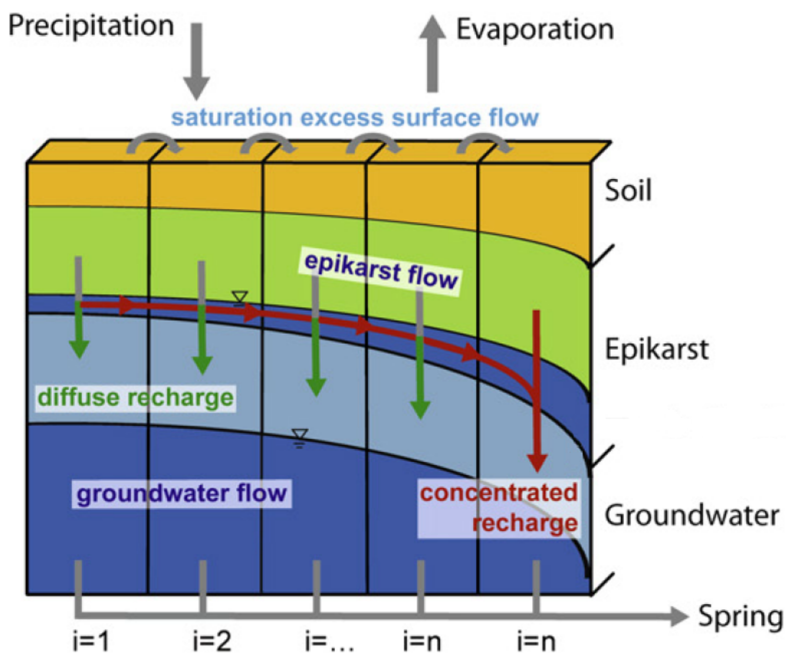

Figure 3.4: The VarKarst model. Modified from HARTMANN et al. (2013a)

Pareto functions are continuous probability distribution functions. They require one distribution parameter and have been broadly used in hydrological modelling (NADARAJAH and ALI, 2008). To attribute the complex karst system behaviour the Pareto functions are applied to a set of $N = 15$ model compartments. The number 15 is not predetermined but has been derived by practical experience from previous studies. Covering the spatial variability this way, the VarKarst model can be seen as a hybrid model since it comprises characteristics of both lumped and distributed modelling techniques. Thus, it combines a high degree of sophistication with a relatively low number of parameters resulting in a parsimonious modelling approach.

VarKarst is able to cope with particular wet and dry conditions due its process-based nature. As reported by HARTMANN et al. (2014b), concentrated recharge in VarKarst increased during extremely wet years whereas diffuse recharge dominated during dry years. They noted, however, that even if the climate shifted towards drier conditions, extreme events still can pose a threat when activating the conduit system. Hence, it is not only the amount of precipitation that is crucial, but also the (spatio-)temporal pattern of the rainfall which influences the model behaviour.

3.2.2 Calculation Procedure

To begin with, some definitions need to be addressed. A mean soil depth $V_{mean,S}$ [mm], a mean epikarst depth $V_{mean,E}$ [mm] and an associated distribution coefficient a_{SE} [-] are defined to assess the variability of soil and epikarst depths. The equations for the storage capacities $V_{S,i}$ and $V_{E,i}$ [mm] for every compartment i can be seen in Table 3.2[9].

After defining the storages, several hydrological processes are simulated in the model. Water entering the model through precipitation can either directly evaporate, flow to the next compartment or percolate to the epikarst system. The actual evapotranspiration from each soil compartment $E_{act,i}$ [mm] is calculated for every time step t by:

$$E_{act,i}(t) = E_{pot}(t)\frac{min[V_{Soil,i}(t) + P(t) + Q_{Surface,i}(t), V_{S,i}]}{V_{S,i}} \tag{3.1}$$

where P [mm] is the precipitation and E_{pot} [mm] is the potential evapotranspiration (PET) provided by the CEH (see 3.1 Available data). The surface inflow $Q_{Surface,i}$ originates from compartment $i - 1$, and is therefore constantly flowing to the next compartment. Water that does not evaporate or flow to the next compartment percolates as recharge $R_{Epi,i}$ [mm] to the epikarst system. The outflow of the epikarst depends on the storage coefficients $K_{E,i}$ [d]

[9] For their derivation see HARTMANN et al. (2013a, Appendix A).

which in turn are controlled by the mean epikarst storage coefficient $K_{mean,E}$ (see Table 3.2[10]). The outflow of the epikarst is then separated into diffuse ($R_{diff,i}$) and concentrated ($R_{conc,i}$) groundwater recharge. Whereas the diffuse recharge arrives the groundwater system below in the compartments $1...N-1$, the concentrated recharge is routed to the last compartment N forming the conduit system.

The groundwater outflow is controlled by the groundwater variability constant a_{GW} and the groundwater storage coefficients for the matrix $K_{GW,i}$ and the conduits K_C. Ultimately, the main spring discharge $Q_{main}(t)$ merges the fast and the slow component by summing up all groundwater flows $Q_{GW,i}$ from the compartments $1...N$.

The groundwater storage V_{GW} is the focus of this thesis. It is regulated by the input ($R_{diff,i}$ & $R_{conc,i}$) and the output ($Q_{GW,i}$). Figure 3.5 vividly shows the behaviour of the groundwater storage separated in the different compartments.

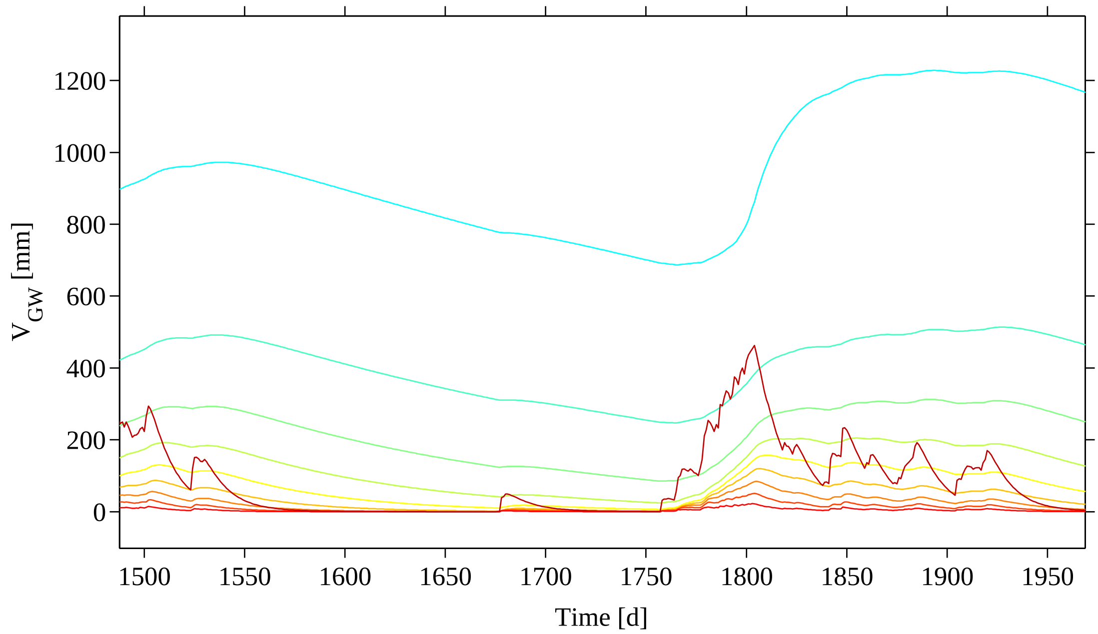

Figure 3.5: Groundwater storage ($V_{GW,i}$) behaviour in the VarKarst model. Every line is a single storage compartment. Note: This is a magnified view that does not show all compartments

[10] For their derivation see HARTMANN et al. (2013a, Appendix A).

Table 3.2: Parameters, descriptions and equations solved in the VarKarst model

Parameter	Description	Equation	Unit
$V_{S,i}$	Soil storage distribution	$= V_{max,S}\left(\frac{i}{N}\right)^{a_{SE}}$	mm
$V_{E,i}$	Epikarst storage distribution	$= V_{max,E}\left(\frac{i}{N}\right)^{a_{SE}}$	mm
$V_{max,S}$	Maximum soil storage capacity	$= V_{mean,S}2^{\left(\frac{a_{SE}}{a_{SE}+1}\right)}$	mm
$V_{max,E}$	Maximum epikarst storage capacity	$= V_{mean,E}2^{\left(\frac{a_{SE}}{a_{SE}+1}\right)}$	mm
$E_{act,i}(t)$	Actual Evapotranspiration	$= E_{pot}(t)\frac{min[V_{Soil,i}(t)+P(t)+Q_{Surface,i}(t),V_{S,i}]}{V_{S,i}}$	mm
$R_{Epi,i}(t)$	Recharge to the epikarst	$= max[V_{Soil,i}(t)+P(t)+Q_{Surface,i}(t)-E_{act,i}(t)-V_{S,i},0]$	mm
$Q_{Epi,i}(t)$	Outflow of the epikarst	$= \frac{min[V_{Epi,i}(t)+R_{Epi,i}+Q_{Surface,i}(t),V_{E,i}]}{K_{E,i}}\Delta t$	mm
$K_{E,i}$	Epikarst storage coefficient	$= K_{max,E}\left(\frac{N-i+1}{N}\right)^{a_{SE}}$	d
$Q_{Surf,i+1}(t)$	Surface flow to the next model compartment	$= max[V_{Epi,i}(t)+R_{Epi,i}(t)-V_{E,i},0]$	mm d^{-1}
$R_{diff,i}(t)$	Diffuse recharge	$= f_{C,i}Q_{Epi,i}(t)$	mm
$R_{conc,i}(t)$	Concentrated recharge	$= (1-f_{C,i})Q_{Epi,i}(t)$	mm
$f_{C,i}$	Variable separation factor	$= \left(\frac{i}{N}\right)^{a_{fsep}}$	-
$Q_{GW,i}(t)$	Groundwater contributions of the matrix	$= \frac{V_{GW,i}(t)+R_{diff,i}(t)}{K_{GW,i}}$	mm d^{-1}
$K_{GW,i}$	Variable groundwater storage coefficient	$= K_C\left(\frac{N-i+1}{N}\right)^{-a_{GW}}$	d
$Q_{GW,N}(t)$	Groundwater contributions of the conduit system	$= \frac{min[V_{GW,N}(t)+\sum_{i=1}^{N}R_{conc,i}(t),V_{crit,OF}]}{K_C}$	mm d^{-1}
$Q_{main}(t)$	Main spring discharge	$= \frac{A_{max}}{N}\sum_{i=1}^{N}Q_{GW,i}(t)$	l s^{-1}

3.3 MODEL ADAPTATION

3.3.1 Multi-objective Approach

The model provides the opportunity for a multi-objective calibration. Besides streamflow, previous studies used hydro-chemical data to increase the model performance. The work of HOWDEN (2006) suggests that hydro-chemical information would be of negligible value in the study area.

Since calibrating only against discharge would lead to a lack of robustness, the adapted model uses the information of discharge and groundwater levels from three boreholes for calibration. The final model comprises two input time series (Precipitation and PET) and four observed time series (Discharge and three boreholes) leading to 13 variable model parameters. All variable parameters and their ranges for calibration are summarised in Table 3.3.

Table 3.3: Variable model parameters, descriptions and ranges for calibration

Parameter	Description	Unit	Ranges	
			Lower	Upper
$V_{mean,S}$	Mean soil storage capacity	mm	0	5000
$V_{mean,E}$	Mean epikarst storage capacity	mm	0	3000
$K_{mean,E}$	Epikarst mean storage coefficient	d	1	50
K_C	Conduit storage coefficient	d	1	10
a_{fsep}	Recharge separation variability constant	-	0.1	5
a_{GW}	Groundwater variability constant	-	0.1	5
a_{SE}	Soil/epikarst depth variability constant	-	0.1	2.5
$p_{GW,A}$	Ashton Farm Groundwater level porosity parameter	-	0.001	0.5
$\Delta h_{GW,A}$	Ashton Farm Groundwater level offset parameter	-	50	150
$p_{GW,R}$	Ridgeway Groundwater level porosity parameter	-	0.001	0.5
$\Delta h_{GW,R}$	Ridgeway Groundwater level offset parameter	-	50	150
$p_{GW,B}$	Black House Groundwater level porosity parameter	-	0.001	0.5
$\Delta h_{GW,B}$	Black House Groundwater level offset parameter	-	50	150

The borehole parameters are introduced to link the modelled groundwater storage to real groundwater elevations. A simple linear relationship is assumed to transfer the modelled storage $V_{GW,i}$ [mm] into a groundwater level h_{GW} [m a.s.l.]:

$$h_{GW}(t) = \frac{V_{GW,i}(t)}{1000 * p_{GW}} + \Delta h_{GW} \tag{3.2}$$

with p_{GW} [-] and Δh_{GW} [m] representing the parameters for the porosity and the offset, respectively. It should be noted that p_{GW} is not equivalent to the real but rather to an effective porosity assuming a vertically constant porosity throughout the aquifer.

3.3.2 Calibration Strategy

The model was previously adapted on a catchment in Spain where the assumption suggested itself that the initial storages were entirely empty. In the present case, this forced the model in an non-stationary state, persistently filling up its storages over the modelling period. Hence, assuming a rather humid climate, the initial storages were set to 100%.

The calibration period ran from 2008 till 2012 and the validation period from 2003 till 2007. Both periods had additional three-year warm-up periods. Calibration was performed against four input time series: discharge (Frome at East Stoke) and the three boreholes (Ashton Farm, Ridgeway and Black House). To improve the groundwater level simulation different weighting schemes were examined.

The Kling-Gupta Efficiency was used as an objective function. To determine which compartment is suitable for the groundwater level simulation the model uses a modified *KGE* which does not include the conditional and unconditional bias (see GUPTA et al., 2009)[11]:

$$KGE_r = 1 - |r - 1| \tag{3.3}$$

Looking only at the correlation (r) between the simulated groundwater storage and observed groundwater level, the appropriate compartment is exclusively chosen based on the right timing.

During this study, different parameter optimization algorithms (MCAT, SCE-UA, SCEM-UA) are tested for their suitability. SCEM-UA tended to produce the highest efficiencies along with relatively short calculation times. Therefore, SCEM-UA was used as the default optimization algorithm. Besides the quantitative measure of efficiency a qualitative visual inspection is carried out. To assess whether parameters are sensitive (or identifiable) cumulative parameter distributions obtained from SCEM-UA were plotted.

In an early phase the model was not able to detect the groundwater flooding event in July 2012 satisfyingly[12]. As a consequence, another time series representing only the event was added. It comprised the groundwater levels at Ashton Farm from 01.07.2012 until 31.08.2012.

[11] For a brief derivation see Appendix C, p. 91
[12] For its performance, see Table B.1 and Figures A.5 & A.6

3.4 THRESHOLD ANALYSIS

3.4.1 Dip Approach

Initially it was thought that a groundwater inundation threshold would be visible in the borehole data. Unfortunately, this was not the case. Therefore attempts were made to detect the threshold or trigger level at which groundwater inundation occurs. It was assumed that there is a linear relationship between the borehole dip (i.e. the distance between the ground surface and the groundwater level) and the vertical distance to the channel network (VDCN). The reason why these two parameters were used is because they are independent from absolute elevations. During high water table conditions the relationship is suspected to change: The smaller the vertical distance to the channel network the bigger the dip to VDCN ratio. The idea is visualised in Figure 3.6.

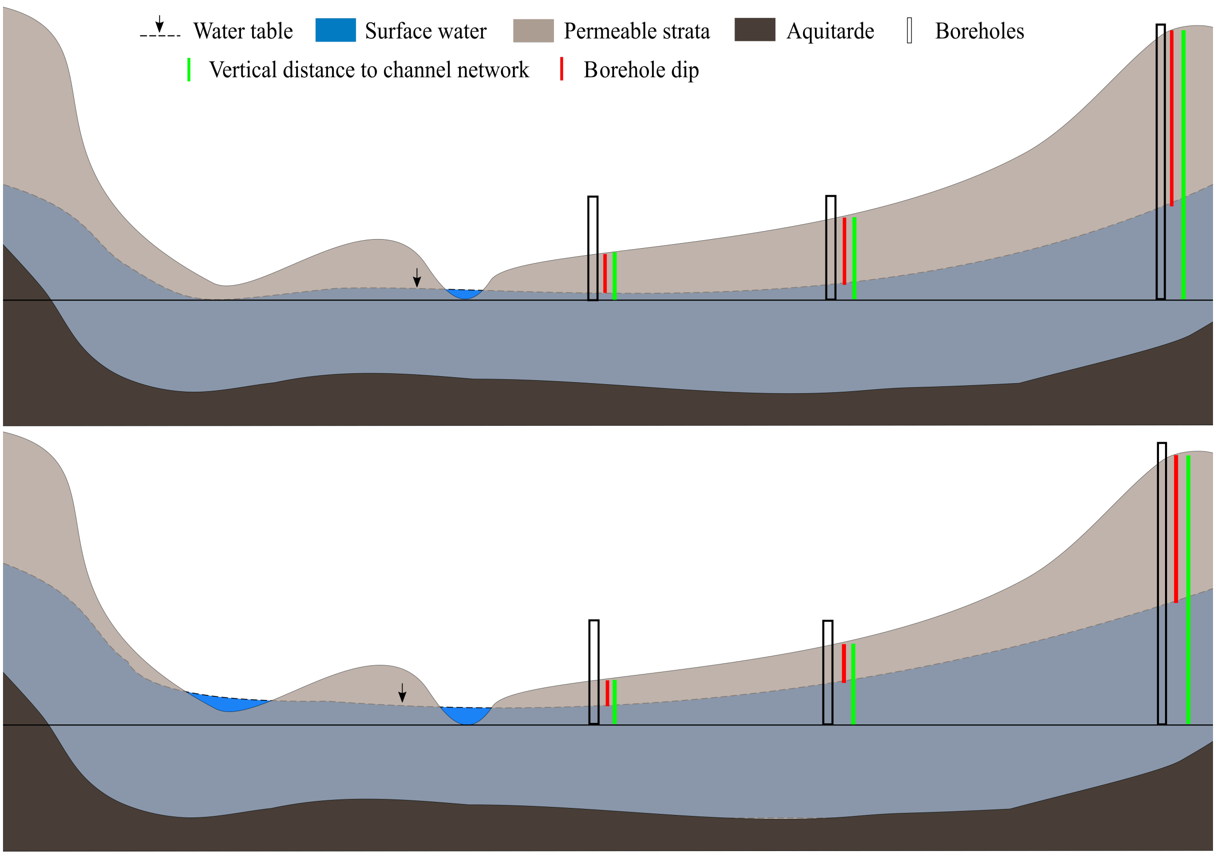

Figure 3.6: Conceptualized groundwater table with varying dips during non-flood conditions (top) and flood-conditions (bottom)

The borehole dips were mostly present in the raw data provided by the EA. Where this was not the case[13], the dip was calculated by subtracting the groundwater levels [m a.s.l.] from the respective borehole elevation [m a.s.l.] obtained from the DEM. The VCDN was calculated with SAGA-GIS. The respective module, written by CONRAD (2003), calculates the vertical distance to a river network by interpolating a river base level which in turn is subtracted from a DEM (CONRAD, 2007). As an input file for the river network the shapefile mentioned in Section 2.3 was used. With mean monthly values from all borehole locations over the period 2008-2012, linear models were set up for every month. Additionally, a model at the time of the flooding, where all boreholes have measured values, was used to examine the relationship during an event. From those boreholes who show a low temporal resolution five were measured on the 16.07.2012 and two were measured on the 17.07.2012. At the four high resolution boreholes the mean of both days is used.

3.4.2 Setting Trigger Levels

Since the dip approach only worked with all available boreholes together but only four boreholes had a daily resolution it was not sufficient for a continuous warning system. However, it may give an indication of the magnitude of the flooding threshold. Based on the dip approach and an event analysis a reasonable threshold was used. Additionally a model threshold was examined. Although three boreholes were modelled, only the borehole at Ashton Farm was used to predict groundwater flooding. This is due to the fact that groundwater inundation primarily took place in the South Winterbourne valley and the other two boreholes are situated in the interfluves where no groundwater flooding is expected. To count the potential groundwater flooding occurrences two criteria were investigated: days over threshold level and events. An event was defined as a series of consecutive days over the threshold level. If two events occur within a range of 3 days, they are counted as one.

3.5 CLIMATE PROJECTIONS

To analyse whether climate change alters the frequency of occurrence of groundwater flooding, the bias-corrected output of five GCMs, provided by the ISI-MIP, was used. According to WARSZAWSKI et al. (2014) ISI-MIP used these five models to span the space of changes in temperature and precipitation as best as possible. Following HEMPEL et al. (2013) the correction

[13] Ashton Farm, Ridgeway, Tolpuddle Ball and Black House

preserves absolute changes in temperature and relative changes in precipitation by (i) adjusting the monthly mean and (ii) adjusting daily variability about the monthly mean. They argue that, in contrast to interpolation methods, their BC approach accounts for expected higher temporal variability at smaller scales. Nevertheless, they concede that BC of daily data with monthly means may neglect weekly variability leading to a misrepresentation of droughts and floods. For further information about the ISI-MIP approach see HEMPEL et al. (2013).

All five models and their origins are listed in Table 3.4. In the following, the models are named from GCM1 to GCM5.

Table 3.4: Naming, original name and institute of all global climate models used

Model	Original Name	Institute name
GCM1	GFDL-ESM2M	NOAA Geophysical Fluid Dynamics Laboratory
GCM2	HadGEM2-ES	Met Office Hadley Centre
GCM3	IPSL-CM5A-LR	Intitut Pierre-Simon Laplace
GCM4	MIROC-ESM-CHEM	Japan Agency for Marine-Earth Science and Technology, Atmosphere and Ocean Research Institute and National Institute for Environment Studies
GCM5	NorESM1-M	Norwegian Climate Centre

The ISI-MIP dataset comprised daily time series of precipitation and air temperature from 01.01.1968 until 31.12.2099 in a $0.5° \times 0.5°$ resolution. Since two cells of the gridded data were present in the study area (see Figure A.4) the average of both was taken for the further analysis. As input data for the adapted VarKarst model daily values of precipitation and potential evapotranspiration from 01.01.2000 until 31.12.2099 are used. The potential evapotranspiration was calculated using the Thornthwaite equation. In the view of the large uncertainties related to climate change projections, different Representative Concentration Pathway (RCP) scenarios are available to obtain from ISI-MIP. In this study the highest scenario (RCP 8.5) is chosen since it is expected to exhibit the most pronounced results (HEMPEL et al., 2013). For further information about emission scenarios see MOSS et al. (2010).

In a first step, the dataset was analysed with regard to their suitability as input for the VarKarst model. Following that, the VarKarst model was used as an impact model to assess the future quantity of groundwater flooding occurrences based on defined threshold levels. To assess the temporal variation the time series were divided into five periods, each 20 years long.

Chapter 4

Results

Is the adapted model able to model groundwater levels in the catchment? Can groundwater inundation be detected? Whether and how will the frequency of groundwater flooding events change in the future? The following chapter is divided into the three parts presenting the results of examining these three questions.

4.1 MODEL ADAPTATION

As stated in the methods section, the model was executed with different weighting schemes. Table 4.1 shows four different weighting schemes and the resulting efficiencies. The $KGEs$ represent the discharge (KGE_Q), the groundwater level at Ashton Farm ($KGE_{GW,A}$) and during the event at Ashton Farm ($KGE_{GW,A_{Event}}$) as well as the groundwater levels at Ridgeway ($KGE_{GW,R}$) and Black House ($KGE_{GW,B}$). They are listed in the same order as indicated by the respective weighting scheme in the squared brackets. The numbers in the round brackets refer to the best found groundwater model compartment.

Table 4.1: Model efficiencies [-] with different weightings in the calbration period (2008-2012) and in the validation period (2003-2007). The numbers in the brackets correspond to the best found groundwater model compartment

Efficiency	Weighting 1		Weighting 2		Weighting 3		Weighting 4	
	[.2 .2 .2 .2 .2]		[.2 .3 .3 .1 .1]		[.2 .4 .2 .1 .1]		[.3 .3 .3 .05 .05]	
	Cal	Val	Cal	Val	Cal	Val	Cal	Val
KGE_Q	0.88	0.82	0.90	0.84	0.89	0.84	0.91	0.85
$KGE_{GW,A}$	0.92 (9)	0.84 (9)	0.91 (9)	0.74 (10)	0.92 (8)	0.82 (9)	0.91 (8)	0.83 (9)
$KGE_{GW,A_{Event}}$	0.80 (9)		0.93 (9)	-	0.91 (8)		0.93 (8)	-
$KGE_{GW,R}$	0.86 (9)		0.88 (9)		0.88 (8)	-	0.88 (8)	-
$KGE_{GW,B}$	0.83 (8)	0.74 (8)	0.85 (9)	0.82(9)	0.85(8)	0.80 (8)	0.85 (8)	0.77 (8)

Overall, efficiencies are higher than 0.80 in the calibration period with all weighting schemes. Mostly compartment 8 or 9 is chosen to model the groundwater levels. Only in the validation period of weighting scheme 2 compartment 10 is used. Sometimes the model compartment increases from calibration to validation period by 1. After all, weighting scheme 2 and 4 show the highest performances. Weighting scheme 4 performs slightly better in the validation period, at least regarding discharge and groundwater levels at Ashton Farm. Therefore , it is chosen as the final model. Table 4.3 shows the resultant optimised values as well as the model performance of the final used model. Without exception, partial efficiencies are high in the calibration period. In the validation period borehole efficiencies decrease by 0.08 and the discharge efficiency decreases by 0.06.

In general, the optimised values are not at the edges of the ranges except for the recharge separation variability constant a_{fsep} which is on the upper edge of its range. Similarly, the other variability constants a_{SE} and a_{GW} are notably high. Mean soil storage and mean epikarst storage capacities are in the middle of their ranges with 2024.8 mm and 2357.6 mm, respectively. The mean epikarst storage coefficient $K_{mean,E}$ is quite low whereas the conduit storage coefficient K_C is rather high. The porosity parameters of the boreholes exhibit similar values at Ridgeway and Black House. The porosity parameter at Ashton Farm is moderately higher. The cumulative parameter distributions differ highly from their uniform distributions as can be seen in Figure 4.1 with $V_{mean,E}$ showing the least deviation.

Figure 4.2 and Figure 4.3 show the observations against simulations in the calibration period and validation period, respectively. Modelled discharge generally matches the observations. In the calibration period the simulated peaks are often below the observed peaks whereas in the validation period it is the other way around. When looking at the groundwater levels, the simulation of Ashton Farm is most fitting. However there are considerable periods which differ clearly from the observations.

It seems that the simulation generally overestimates the groundwater level in the calibration period whereas the simulated values in the validation period are lower than observed. This is supported by the mean observed and modelled groundwater levels in both periods listed in Table 4.2. The table additionally contains the mean annual precipitation and the proportion of modelled diffuse and concentrated recharge in both periods. In average, precipitation in the calibration period is about 56 mm/y higher than in the validation period. Overall, the ratio of diffuse to concentrated recharge is about 80:20. The proportion of diffuse recharge is slightly higher in the validation period.

Table 4.2: Mean values of mean annual precipitation [mm/y], the proportion of modelled recharge (diffuse:concetrated) as well as observed and modelled groundwater levels [m a.s.l.] at Ashton Farm in the calibration and validation period

Period	Precip. [mm/y]	Mod. recharge prop. [%]		GWL Ashton Farm [m a.s.l.]	
		Diffuse	Concentrated	Observed	Modelled
2008-2012	1148	77.5	22.5	67.78	68.61
2003-2007	1092	79.7	20.3	67.43	66.66

All in all, the mean absolute simulation errors in calibration and validation at Ashton Farm are 1.06 m and 0.96 m and the maximum errors are 3.35 m and 3.47 m, respectively. The simulation of Ridgeway is in good accordance with its fragmentary observed time series. The mean absolute error in the calibration period is 2.13 m and the maximum error is 7.69 m. Unfortunately, there were no measurements in the validation period. Simulation of groundwater levels at Black House is slightly worse. Although the course of the simulation is roughly similar to the observations, the simulation fails for example at the peaks in 2008 and 2009 with a maximum error of 11.48 m (mean absolute error: 2.07 m). In the validation period the maximum error is 6.53 m (mean absolute error 2.03 m).

Table 4.3: Model parameters, descriptions, ranges and optimised values

Parameter	Description	Unit	Ranges		Optimised values
			Lower	Upper	
$V_{mean,S}$	Mean soil storage capacity	mm	0	5000	2024.8
$V_{mean,E}$	Mean epikarst storage capacity	mm	0	3000	2357.6
$K_{mean,E}$	Epikarst mean storage coefficient	d	1	50	3.5586
K_C	Conduit storage coefficient	d	1	10	8.8013
a_{fsep}	Recharge separation variability constant	–	0.1	5	4.9657
a_{GW}	Groundwater variability constant	–	0.1	5	4.1629
a_{SE}	Soil/epikarst depth variability constant	–	0.1	2.5	2.2430
$p_{GW,A}$	Ashton Farm groundwater level porosity parameter	–	0.001	0.5	0.0376
$\Delta h_{GW,A}$	Ashton Farm groundwater level offset parameter	m	50	150	64.052
$p_{GW,R}$	Ridgeway groundwater level porosity parameter	–	0.001	0.5	0.0104
$\Delta h_{GW,R}$	Ridgeway groundwater level offset parameter	m	50	150	41.882
$p_{GW,B}$	Black House groundwater level porosity parameter	–	0.001	0.5	0.0167
$\Delta h_{GW,B}$	Black House groundwater level offset parameter	m	50	150	75.585
KGE_Q	Model performance for discharge	–	0	1	0.91/0.85*
$KGE_{GW,A}$	Model performance for groundwater level at Ashton Farm	–	0	1	0.91/0.83*
$KGE_{GW,A_{Event}}$	Model performance for groundwater level at Ashton Farm (Event)	–	0	1	0.93/ – *
$KGE_{GW,R}$	Model performance for groundwater level at Ridgeway	–	0	1	0.88/ – *
$KGE_{GW,B}$	Model performance for groundwater level at Black House	–	0	1	0.85/0.77*

*Calibration/validation

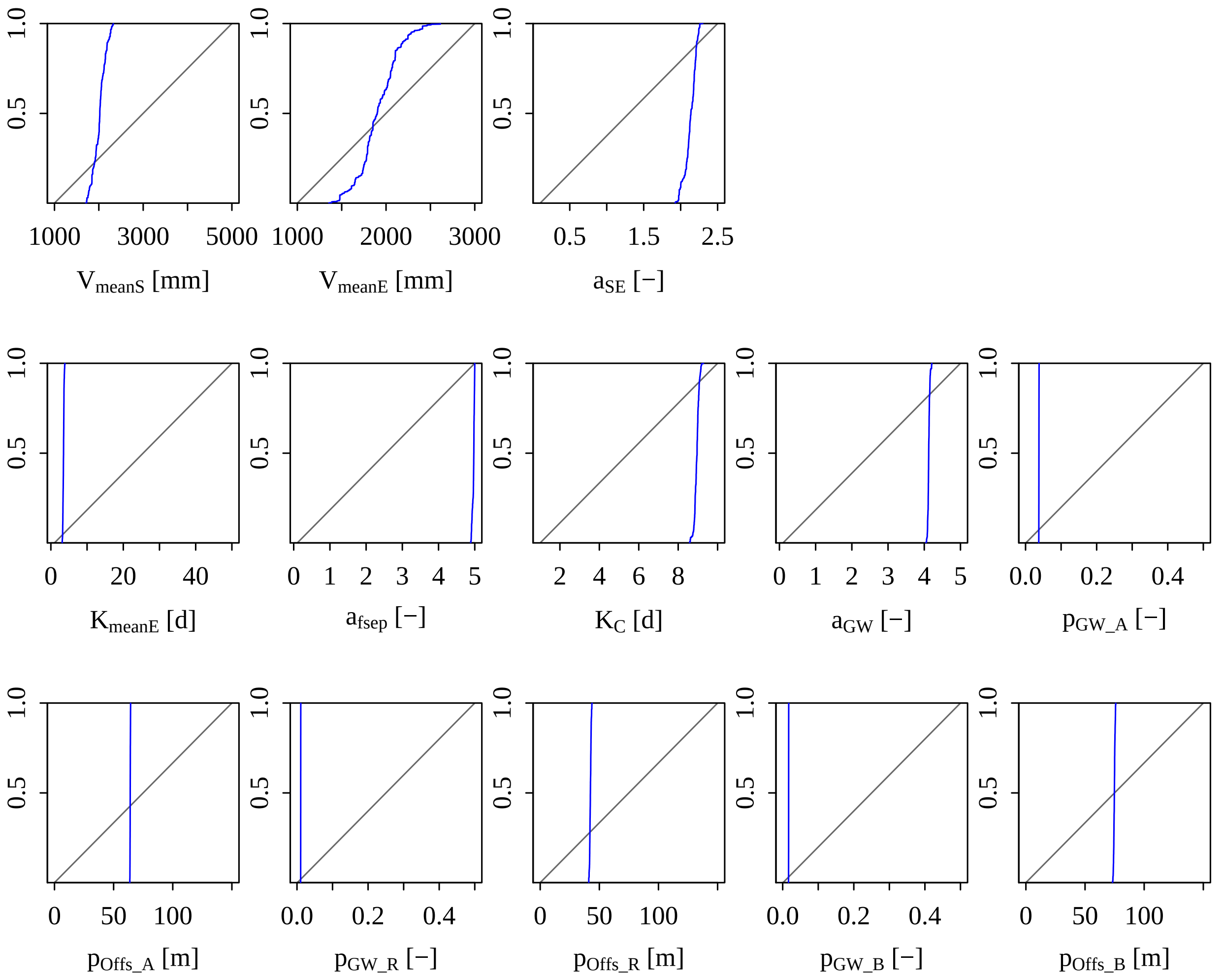

Figure 4.1: Cumulative parameter distributions of the final model. Diagonals represent the uniform distributions.

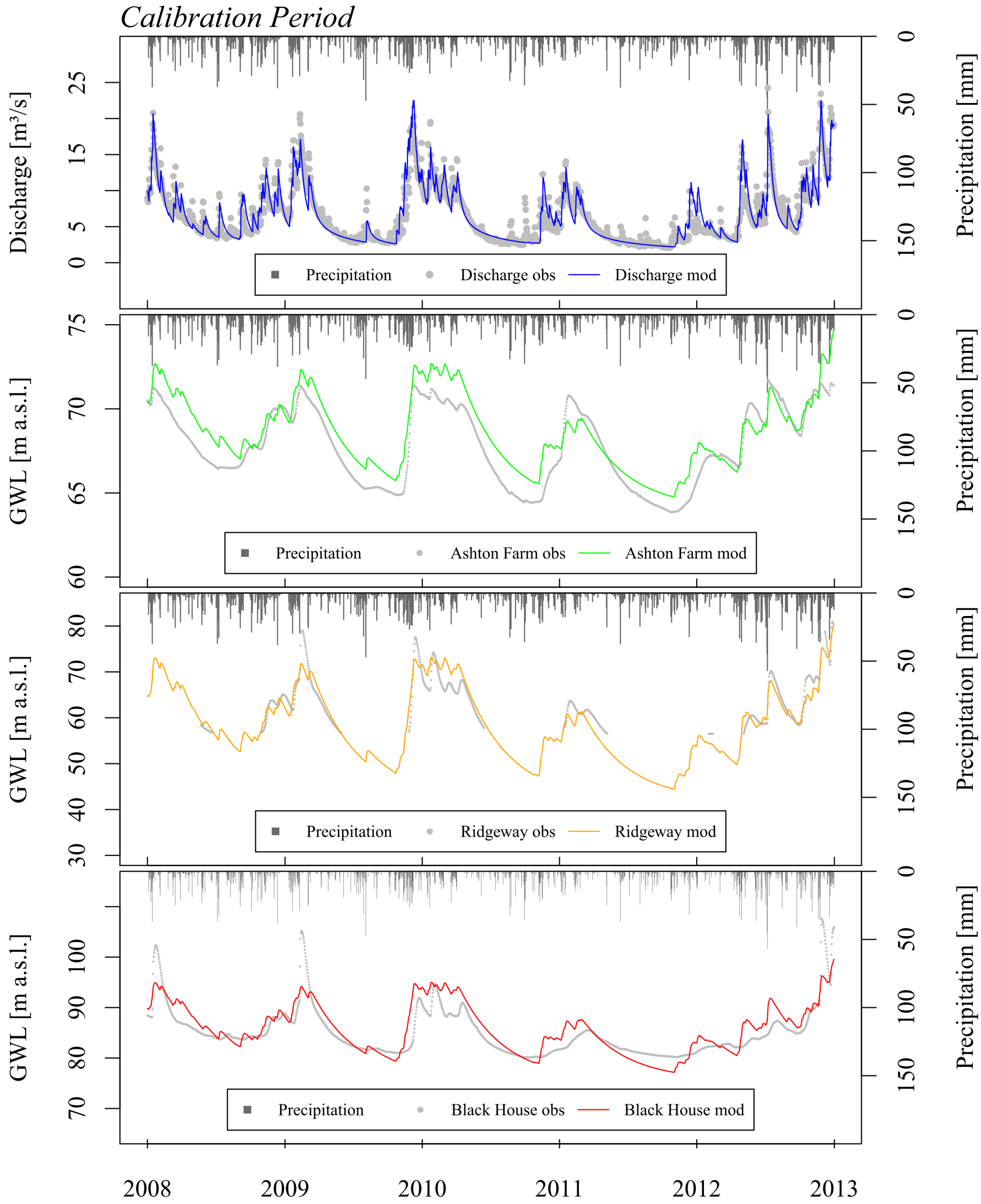

Figure 4.2: Final model run with additional focus on the event in July 2012. Precipitation (Sydling St. Nicholas), observed and modelled discharge (East Stoke) and groundwater levels (Ashton Farm, Ridgeway, Black House) during the calibration period 2008-2012

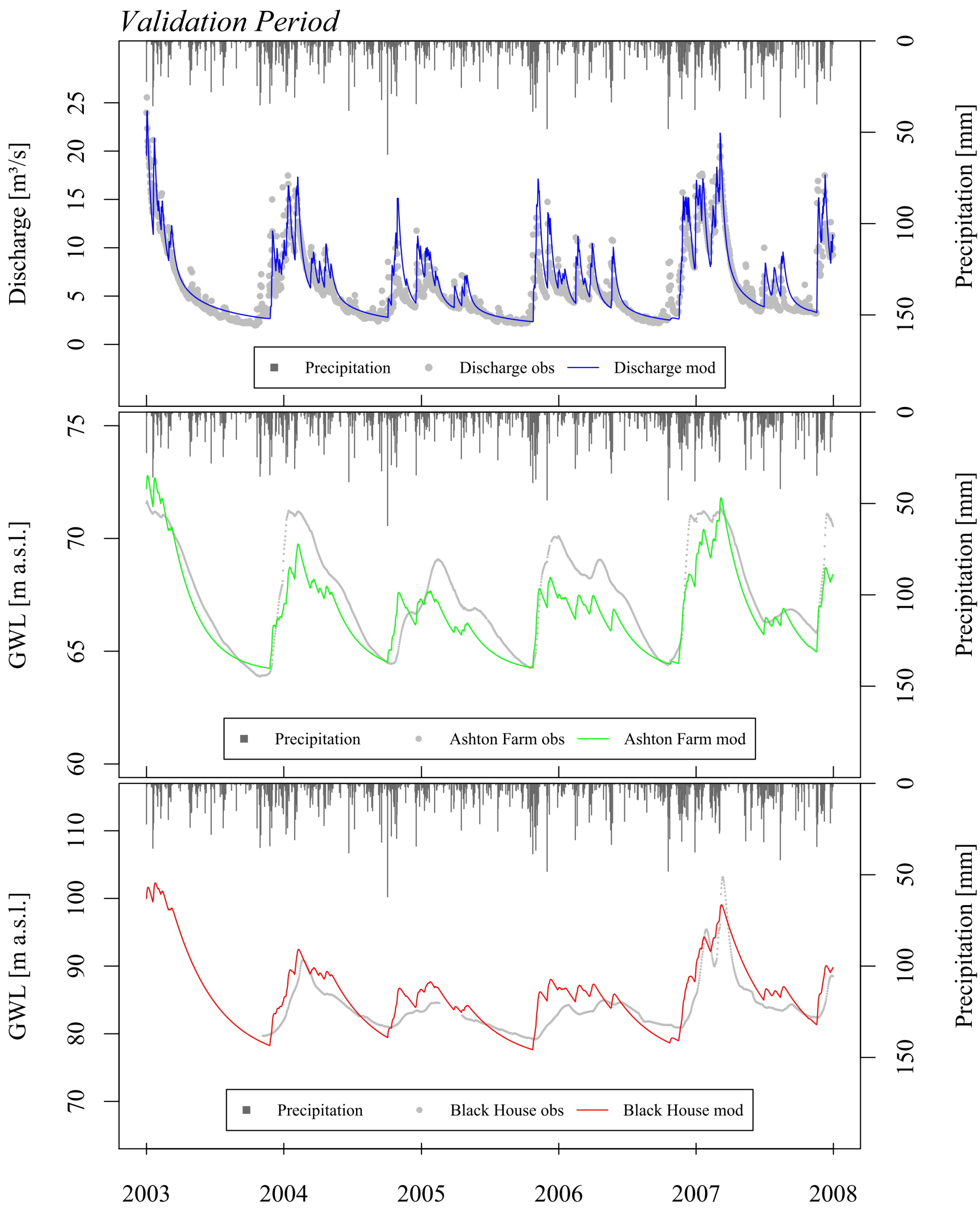

Figure 4.3: Final model run with additional focus on the event in July 2012. Precipitation (Sydling St. Nicholas), observed and modelled discharge (East Stoke) and groundwater levels (Ashton Farm, Ridgeway, Black House) during the validation period 2003-2007

4.2 THRESHOLD ANALYSIS

4.2.1 Dip Approach

Figure A.7 shows the different relationships during all months and their respective y-intercept. The y-intercept represents the mean modelled dip in the catchment. A positive dip means that no groundwater flooding is occurring. The coefficient of determination is always above 0.95. Dips are notably smaller during the winter months. Figure A.8 indicates an inundation depth of 0.53 m during event.

4.2.2 Setting a Threshold level

The dip approach displayed a rough estimation of the inundation depth which is in accordance with the reports of BUTLER (2013) and BENNETT (2013). With that in mind a threshold level of 71.3 m is set at the borehole "Ashton Farm" which is basically half a meter below the maximum groundwater level of the event. Figure 4.4 shows that this is also in good agreement with the length of the flood event (around 2 weeks).

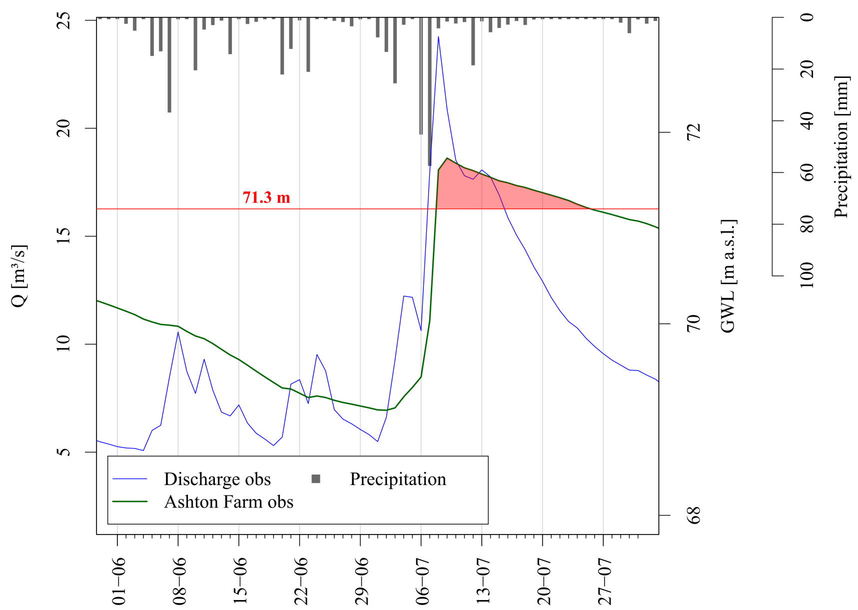

Figure 4.4: Precipitation (grey), discharge (blue) and groundwater level at Ashton Farm (green) during the groundwater flooding event in July 2012 (highlighted red). The lightgrey vertical grid lines indicate weekly intervals. The threshold level is at 71.3 meter

The Figure 4.5 shows clearly a seasonal pattern with highest values in the winter periods. In the year of 2012, however, the threshold level is exceeded during the summer following a winter period with comparably low levels. Both observed and modelled groundwater levels are over the threshold of 71.3 m on 7 occasions. However, the events are not always in accordance. The model suggests an event at the beginning of 2008 which is only almost registered with the observed data. In contrast, the observed groundwater level graph indicates two events at the end of 2012 where the model only counts one.

Generally, as stated in Section 4.1, the model overestimates the peaks clearly, leading to an overestimation of the days over threshold. As the number of events are the same, the model indicates 333 days over the threshold level whereas the observed time series suggest only 60 days.

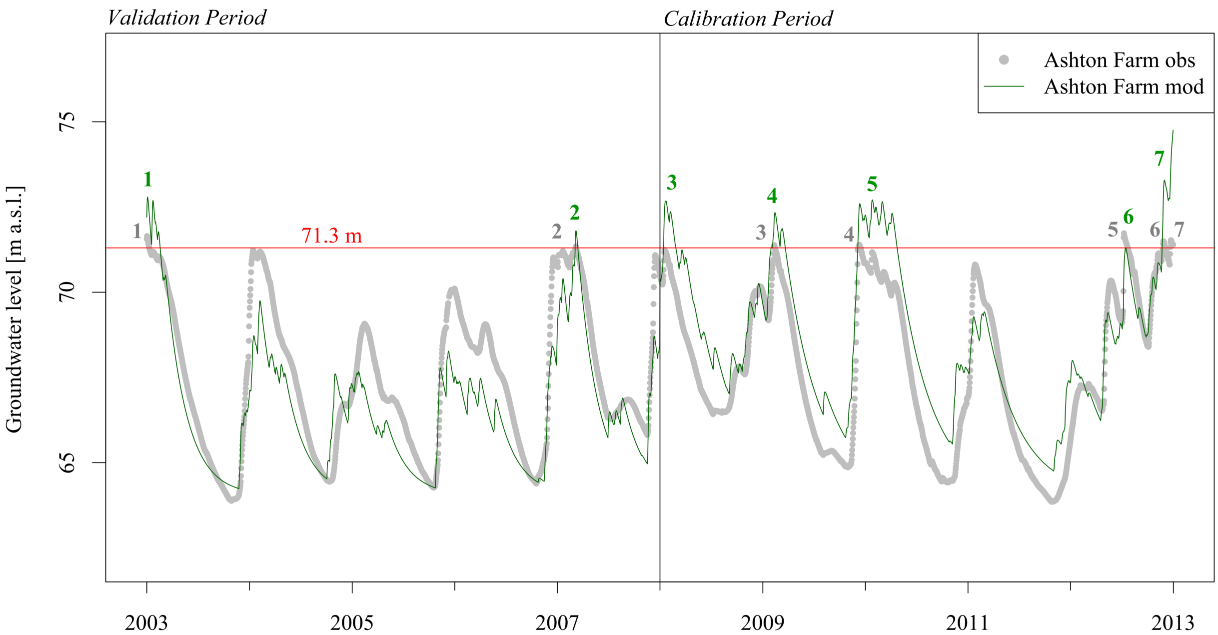

Figure 4.5: Observed (grey dots) and modelled (green line) groundwater level at Ashton Farm, the threshold level (71.3 m) and the resultant count of events

Of all observed groundwater levels 1.64 percent are higher than 71.3 m. Thus 71.3 m corresponds to the 98.36th percentile. This percentile is now applied on the modelled time series resulting in an equivalent model threshold of 72.6 m. Figure 4.6 shows both threshold levels and the resultant count of events.

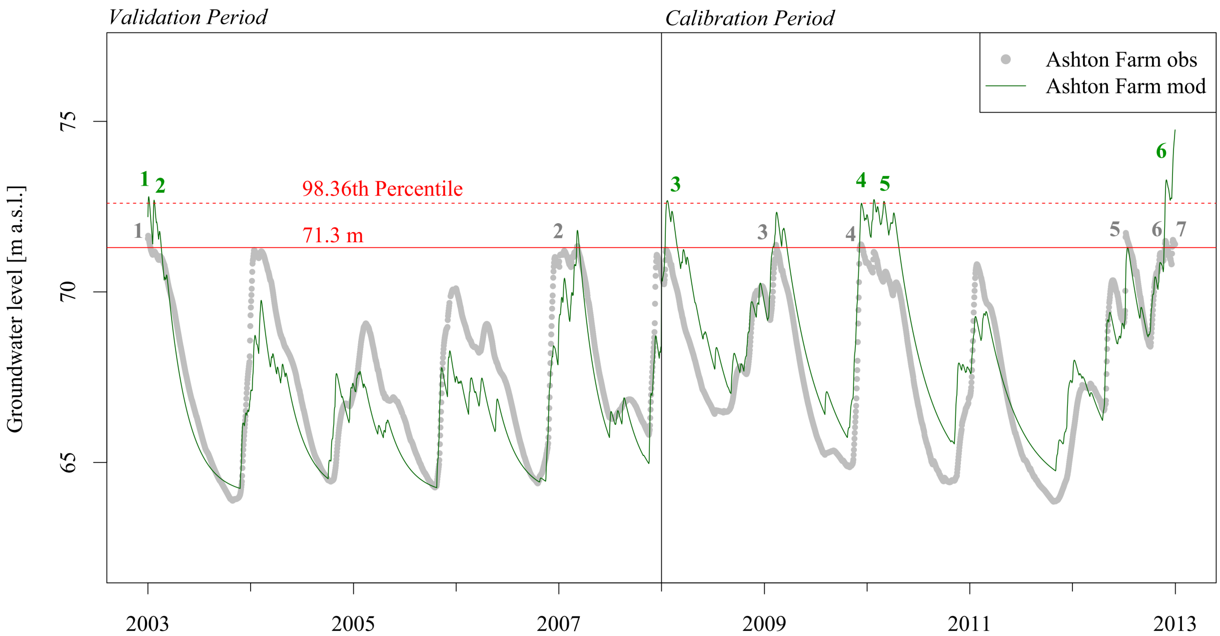

Figure 4.6: Observed (grey dots) and modelled (green line) groundwater level at Ashton Farm, the threshold levels (71.3 and the 98.36th Percentile) and the resultant count of events

As can be seen from the figure, the model now only indicates 6 events. The events 1 and 2 as well as 4 and 5 are very close to each other. The groundwater flooding event in July 2012 (the 5th observed event) is not counted any more. Table 4.4 summarises the counted events and days over threshold. The second numbers are counts with the newly introduced threshold level. The modelled days over the model threshold are in good accordance with the observed days over threshold.

Table 4.4: Counted events and days over threshold in the observed and modelled groundwater levels at Ashton Farm. The second numbers correspond to threshold based on the 98.36th percentile

Period	Observed		Modelled	
	Days	Events	Days	Events
2003-2007	13	2	57 / 8	2 / 2
2008-2012	47	5	276 / 51	5 / 4
Total	60	7	333 / 59	7 / 6

4.3 CLIMATE PROJECTIONS

To analyse the ISI-MIP dataset, calculated mean values of the output data (or rather the input data for the VarKarst model) are listed in Table 4.5.

Table 4.5: Observed (2000-2012) and predicted (1968-2099) mean annual precipitation and mean annual potential evapotranspiration

Parameter	Historic	GCM1	GCM2	GCM3	GCM4	GCM5
Precipitation [mm/y]	1186	934	799	865	887	821
PET [mm/y]	610	376	416	405	420	412

It is apparent that there is a significant difference between the observed historic mean values and the predicted mean values. Predicted values for precipitation and potential evapotranspiration both are substantially lower. On average, predicted mean annual precipitation is 325 mm lower and predicted mean annual PET is 204 mm lower than observed. The difference between the model outputs among each other is lower but also worth mentioning. Nevertheless, all five model outputs are used for the analysis. As in Subsection 4.2.2, the 98.36th percentile is used as the respective threshold level for the future simulations. The percentile is, in each case, applied on the whole modelled time series from 2000 till 2099.

For a comparison, Figure 4.7 shows exceedance probability curves of the simulated groundwater levels in the first period (2000-2019) as well as of the historically observed and modelled groundwater levels (2003-2012). The figure illustrates that the resultant simulated groundwater levels with the GCM output distinctively differ from each other. This is supported by the different threshold levels shown in the legend. The Figure also confirms the above mentioned overestimation of the peaks, as historic modelled groundwater levels (blue) substantially exceed the observed groundwater levels (green) in the upper 5 %.

Though the values vastly differ from reality, they show certain trends. Tables B.2 and B.3 in the Appendix contain the temporal evolvement of the precipitation and potential evapotranspiration of the GCM ouput in average as well as divided into different percentile ranges. The total mean values of precipitation show no trends regardless of the GCM whereas the mean PET values show a positive trend with all GCMs. On closer inspection, highest precipitation values (mean percentile 100-95) show a positive trend throughout the century.

Table 4.6 shows all counted events and days over the respective threshold throughout all periods. GCM1 shows a large number of days over threshold in the first period. In the remaining periods GCM1 no clear trend can be observed. GCM2 shows no discernible trend either, but the last period (2080-2099) exhibits the largest number of days over threshold. Simulations with GCM3 and GCM4 lead to a similar pattern with their maxima in the last period regarding both events and days over threshold. Correspondingly, GCM5 also suggests an increase of events and days over threshold throughout the century. Although most events occur in the last period, most days over threshold occur in the preceding period 2060-2079.

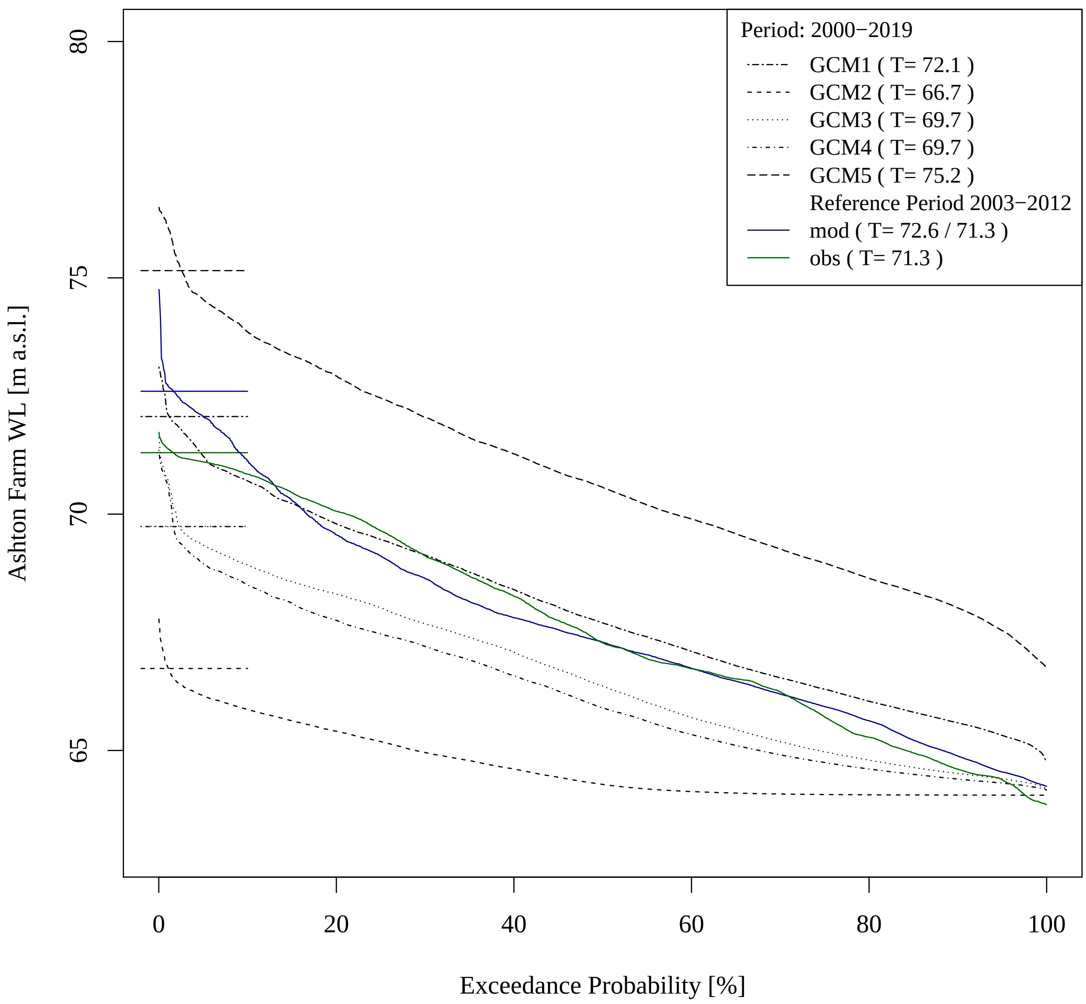

Figure 4.7: Exceedance probability curves of the groundwater levels modelled with all five GCMs (2000-2019) as well as the historically modelled (blue) and observed (green) groundwater levels (2003-2012). The short horizontal lines represent the respective threshold level

Table 4.6: Predicted groundwater flooding events and days over respective threshold at Ashton Farm during 5 periods from 2000 till 2099.

Period	GCM1		GCM2		GCM3		GCM4		GCM5	
	Events	Days	Events	Days	Events	Days	Events	Days	Events	Days
2000-2019	7	263	23	102	2	22	2	48	2	94
2020-2039	4	82	11	123	5	147	2	20	1	7
2040-2059	1	79	13	113	5	54	9	170	3	145
2060-2079	5	85	7	79	4	163	2	122	3	190
2080-2099	2	90	14	181	13	213	14	239	4	163

In addition to the sheer count of events or days over threshold, Figure 4.8 shows boxplots of the respective upper 5 % of all five GCM-output fed models throughout the periods. The plots support the impression that there is a increase of high values throughout the century except with GCM1. Without the first period, GCM1 shows relatively constant boxes, whereas the largest values (upper whisker) seem to increase with time. In the cases of GCM2, GCM3 and GCM4 the median in the last period is at the respective threshold level or above. In addition, the histograms in Figure A.9 mainly confirm the positive trend above the thresholds although less vividly. Yet, they also show the diversity of the resultant groundwater level distributions.

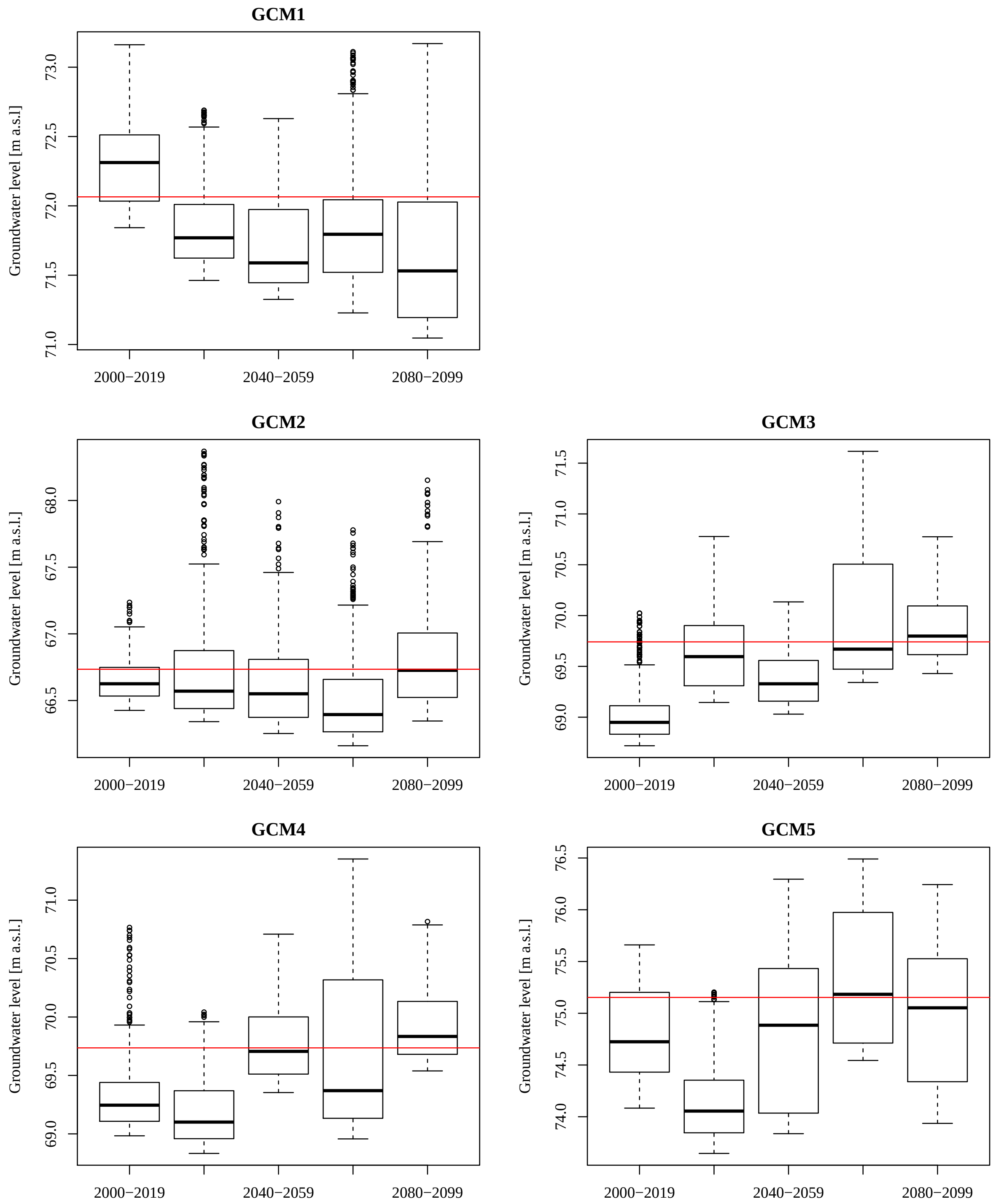

Figure 4.8: Boxplots of the upper 5 % of the future predicted groundwater level at Ashton Farm during the 5 periods. The red horizontal line represents the respective threshold level

Chapter 5

Discussion

This chapter discusses the results of modelling groundwater levels in general and groundwater inundation in particular. The first section reflects on the uncertainties associated with available data and the presented approach. The subsequent section attempts to discuss the results and interpret them in a broader context. Finally the last section deals with the impact and transferability of this study.

5.1 UNCERTAINTIES

In general , uncertainties can have various origins beginning with random or systematic errors in measurements. LIU and GUPTA (2007) note that "[...] input data, parameters, the model structure, initial conditions, and the system boundary represent five major sources of uncertainties in hydrologic modelling.". Uncertainties which relate to this study in particular are described in the following.

5.1.1 Input

The borehole at Ashton Farm is located in the South Winterbourne valley in the Frome catchment. The other two used boreholes are located in the interfluve between the Frome and the Piddle catchment. Strictly speaking they are located in the Piddle catchment and may not be suitable for a simulation. However, the Piddle and Frome catchments are seemingly connected (ADAMS et al., 2003; HOWDEN, 2006) and groundwater levels show very similar behaviour. Moreover, for the purpose of detecting groundwater inundation, only the the borehole at Ashton Farm is used.

The downside of the reported geological connection between the catchments is that groundwater transfer of unknown amounts might occur at times and complicate simulations. In addition, simulations may be affected by irregular surface water and groundwater abstractions. However, as reported by HOWDEN (2006), water loss in the Frome catchment is only around negligible 5 %. Water abstractions might play a role in the Chalk and should not be ignored. Nevertheless, during flood conditions abstraction rates are not expected to be high. In addition, as BENNETT (2013) notes, it would not be feasible to lower groundwater levels during a flood by pumping: Firstly, the amount of water that would needed to be removed from the area would be too big. Secondly, an adequate pumping infrastructure would be too expensive. And lastly, abstracted water would needed to be discharged downstream which in turn would increase the fluvial flood risk. Hence, impairment of the simulated groundwater level peaks is presumably little or non-existent.

The potential evapotranspiration obtained from the CEH was not complete and had to be filled up with artificial data. But, as the PET has a strong annual cycle shown in Figure 3.3, the effect on the modelling is suspected to be negligible. Precipitation data is obtained from the station at Sydling St. Nicholas, located at a medium elevation. Although it may not adequately reflect the spatio-temporal rainfall distribution in the catchment, no other meteorological stations were included. Because the area is comparably flat, high rainfall gradients are rather improbable. In contrast, BUTLER (2013) found a strong heterogeneous rainfall pattern prior to the groundwater flooding event in July 2012. One way or another, including more meteorological stations and obtaining complete time series could reduce possible uncertainties associated with the meteorological input data.

Regarding the dip approach, uncertainties are associated with the rather coarse DEM, the river shapefile and the fact that only a limited number of boreholes were available in the catchment. MCKENZIE et al. (2010), who constructed a water tables using rivers, lakes and boreholes, emphasized the importance of a extensive borehole network. In addition, the dip approach used boreholes from the Frome and the Piddle catchment. The calculated dip would therefore be valid for both catchments. As research suggests, however, only parts in the Frome catchment were flooded during July 2012 (BENNETT, 2013; BUTLER, 2013).

The analysis of the GCM output revealed substantial differences to the real observed meteorological time series. Moreover, the analysis of the GCM output revealed that there is a positive trend in high precipitation values and hence, as several authors noted, a trend towards more extreme rain events. On the one hand, one could argue that data which differ so radically from reality are useless for a hydrological impact model as it has been noted similarly by EHRET et al. (2012). On the other hand, further correction of the GCM output would have presumably introduced additional uncertainties. It is beyond any doubt that modelling with these data can yield only relative rather than absolute results. As a consequence, instead of absolute threshold levels, relative thresholds based on a defined percentile were used.

5.1.2 Modelling

The time series of the borehole at Ridgeway was only fragmentary and did not comprise any values in the validation period. Validation was only possible for discharge and the boreholes at Ashton Farm and Black House. Nevertheless, Ridgeway was included in the results to show that the approach is able to model groundwater levels at different locations. To adequately model the groundwater levels at Ashton Farm, the applied weighting scheme gave little attention to the boreholes at Ridgeway and Black House. Given these circumstances, the associated simulations appear to be quite satisfying.

The relationship between groundwater storage and and groundwater level in the model is assumed to be linear. This might be a too simplistic premise. At the same time, it was tried to keep it as simple as possible and avoid introducing more parameters in order to follow the principle of parsimony (see BOX and JENKINS, 1970). In fact, the described model has 13 variable model parameters. Since it includes four observed time series it is in accordance with the recommendation of KUCZERA and MROCZKOWSKI (1998) who suggested a maximum of six parameters when calibrating only against streamflow. Therefore the approach is suspected to be sufficiently robust because of its multi-objective character. Furthermore, identifiability plots (See Figure 4.1) do not suggest equifinality. All in all, validity could be further increased with a both-sided split sample test as described by KLEMEŠ (1986) and by including larger (complete) time series and more boreholes.

As suggested by EHRET et al. (2012), output from climate models, even after undergoing bias-correction, often is not suitable for hydrological impact models. And as it has been shown, the GCM output is far from reality. However, the focus is only set on the relative trend. Furthermore, unlike the approach by JIMENEZ-MARTINEZ et al. (2015), VarKarst is a process-based model and therefore provides a certain reliability outside the calibration period (KUCZERA and MROCZKOWSKI, 1998).

5.1.3 Groundwater Flooding

The presented approach defines groundwater flooding as threshold exceeeding groundwater levels. Therefore it concerns, after ROBINS and FINCH (2012), only the "true groundwater flooding". This study does not include an analysis whether "groundwater induced flooding" happens in the catchment. According to MCKENZIE et al. (2010) different types of flooding often occur simultaneously. Possible effects of superimpositions of flood types would be worth examining. PARRY et al. (2013) pointed out that groundwater flooding is primarily a winter phenomenon. The question whether and how winter and summer events differ is not discussed in this study, but could be addressed in future research.

The dip approach assumes a linear relationship between the borehole dip and the vertical distance to channel network and a consistently permeable aquifer. This is quite likely for highly permeable aquifers like the Chalk (MCKENZIE et al., 2010). However this is only valid in unconfined aquifers conditions (MCKENZIE et al., 2010) which are only present in the middle and upper reaches of the catchment (HOWDEN, 2006). The VCDN was calculated with a river shapefile which might not be accurate enough for this approach (see Section 2.3). In addition, the dips are partially calculated using the rather coarse DEM, introducing another uncertainty.

Some boreholes are only probed monthly. During the flood event in 2012 some boreholes were probed on the 16th and some were probed on 17th of July. This could have altered the relationship during the flood event (Figure A.8) leading to another y-intercept. Altogether, only 11 boreholes in the Frome and Piddle catchment were used for this approach. Additionally, these boreholes were not equally distributed over the catchment. Nonetheless, the results were in accordance with the reports of BENNETT (2013) and BUTLER (2013) which provides support for the later used threshold level. It should also be mentioned that the threshold level was only selected on the basis of a single event which was, as research suggested, comparably small. BRADFORD and CROKER (2007) suggested that for their approach to define threshold levels the extreme event in winter 2000/01 should be incorporated. Similarly, JIMENEZ-MARTINEZ et al. (2015) defined a threshold level based on the event 2000/2001. However, since several reports suggest similar inundation depths and durations, the threshold level is suspected to be comprehensible.

A model threshold was introduced based on the 98.36th percentile corresponding to the defined threshold at 71.3 meter above sea level. Clearly, a model threshold is rather an artefact which does not help improving the detection of groundwater inundation. In fact, the model threshold was primarily introduced to provide reasonable thresholds for the climate projections. And as the analysis in Subsection 4.2.2 showed, it provided a reasonable number of days exceeding the threshold.

Events were delimited from one another within a range of three days. Presumably, defining other ranges, for example one week, would also be feasible. As shown in 4.6, there are three cases where events were very close to each other (two modelled cases, one observed). In each of these cases, the time between the exceedances was over two weeks. It remains unclear at what point events should be delimited. Considering that, days over threshold might be a more reliable criterion.

5.2 INTERPRETATION

This section covers the interpretation of the results. Accordingly, this section is divided into the model results, the threshold analysis and the climate projections.

5.2.1 Model Results

Overall the model performance is satisfying. Simulations at Ashton Farm are far better than at Ridgeway and Black House. This may on the one hand be attributed to the weighting scheme. On the other hand it could be attributed to the borehole locations. Both Ridgeway and Black House are situated on the interfluve with a borehole dip of approximately 50 meters. As suggested by HARIA et al. (2003) and JOHNSON et al. (2001) recharge through fissures is mainly present when the unsaturated zone is shallow. As the model calibration focusses mainly on the groundwater level at Ashton Farm where the water table naturally is close to the surface, it may fail to reproduce groundwater levels at sites with a deep unsaturated zone.

This discrepancy was not attenuated by a varying selection of model compartments. All three modelled boreholes were simulated using the 8th compartment. Only in the validation period the GWL at Ashton Farm was simulated with the 9th compartment. The increase of the model compartment, which is also present with other weighting schemes (see Table 4.1), can be interpreted in several ways. In general, it shows that calibration and validation period are probably quite different. In particular, choosing another model compartment is related to a better sufficiency of the new compartment either in terms of strength of response or simply in terms of the temporal pattern. However, since it is only a shift of one compartment it should not be overinterpreted.

All in all, simulations show only slight deteriorations in the validation period indicating a good robustness. A look on the parameter values reveals an adequate reflection of the reality. However, $V_{mean,S}$ and $V_{mean,E}$ are quite high considering that initial ranges for these parameters were 0-250/0-500 mm (as in HARTMANN et al., 2013b,c). As previous studies took place in fairly dry catchments, the ranges were extended substantially to deal with the wet climate in southern England. Though, the optimised values might be a little overestimated, at least for the mean soil storage capacity since soils over Chalk tend to be quite shallow (LEE et al., 2006; BRADFORD and CROKER, 2007) as found for example by BURNHAM and MUTTER (1993) or JOHNSON et al.

(2001). This might be due to an underestimation of the potential evapotranspiration. A higher soil storage ultimately leads to a higher actual evapotranspiration (see Equation 3.1). Another reason could also be the lack of an unsaturated zone in the VarKarst structure.

A high a_{SE} leads to a higher proportion of epikarst and soil storage in higher compartments. Additionally, the mean epikarst storage coefficient $K_{mean,E}$ is quite low, indicating a excessive and fast water transport from the epikarst to the groundwater storage. The parameter a_{fsep} is on the upper edge of its range. This implies that a high proportion of the concentrated recharge occurs through the compartment N=15, but most of the recharge, through the other compartments, is diffuse. A high conduit storage coefficient K_C and a high a_{GW} should lead to a discharge reaction dominated by the matrix system. Thus, the parameters suggest large storages and a large proportion of the recharge occurring through the matrix. Analysis of the recharge proportion revealed that the ratio of diffuse to concentrated recharge is roughly 80:20. This is in accordance with the findings of JONES and COOPER (1998) as well as REEVES (1979) who reported 30 % and 10-20 % of the recharge occurring through (macro-)fissures in Chalk catchments, respectively.

Evidently, the validation period was slightly drier than the calibration period which presumably led to overall lower observed groundwater levels at Ashton Farm. This might forced the model to underestimate the (already low) groundwater levels. Conversely, in the wetter calibration period groundwater levels tend to be overestimated. This can not be seen in the simulation of Black House, which might be due to several reasons: Firstly, due to the fact that the simulation itself was not precise because of its low calibration weighting. Secondly, because the rainfall pattern at Black House may differ relevantly from the one obtained from the station at Sydling St. Nicholas. And lastly, it could be due to the above mentioned issues regarding recharge through fissures in a deep unsaturated zone.

In essence, the simulations at Ashton Farm and Black House overestimate high levels and underestimate low levels. The reason for this behaviour might be due to the assumption of a constant vertical porosity. In reality, porosity is likely to decrease with depth, as considered by several models, e.g. TOPMODEL (BEVEN and KIRKBY, 1979) or HillVi (WEILER and MCDONNELL, 2004). Since at low groundwater levels the real porosity is lower than the constant model porosity, simulated levels fall below observed levels. At higher levels it is the other way around. Likewise, BUTLER et al. (2012) emphasized that parameterizing the unsaturated zone correctly is crucial for modelling groundwater levels in the Chalk. A future consideration of this aspect could significantly improve the simulations. For this purpose, the porosity could be incorporated in the storage-level link (Equation 3.2) depending on the borehole dip.

5.2.2 Threshold Analysis

The dip approach delivered an estimation of the inundation depth which was in accordance with the inundation depths reported by BENNETT (2013) and BUTLER (2013). Furthermore, it was supported by the visual analysis of the event. However, visual analysis revealed also that the maximum groundwater level occurred on the 9.07.2015 whereas the dip approach used the values at the 16. and 17. of July. When examined critically, the dip approach turns out to be too limited. In addition to the temporal discrepancy, aforementioned uncertainties associated with the DEM and river shapefile impede drawing meaningful conclusions. Nevertheless, the applied threshold is suspected to be reasonable.

As noted in BENNETT (2013) the EA uses different warning levels (see also Figure A.1) which is also proposed by ADAMS et al. (2010). This might be a meaningful approach to overcome the rigidity of a single threshold level. To define different alert levels, however, more information is needed. Analysing more flood events could enhance the robustness of certain threshold levels. Since the model overestimated the peaks, a model threshold was introduced. The modelled number of days over threshold with the new threshold were in a good accordance with the observations. However, this is only due to the fact that a percentile based threshold applied on a time series with the same length inevitably produces a similar number of exceedances. In summary, it can be said that the approach is not fully developed. However, if simulations could be improved, either by incorporating a depth-depending porosity or by a more extensive calibration, a model threshold could become superfluous.

5.2.3 Climate Projections

The model threshold, however, was essential for the analysis of the climate projections. As it has been shown in the Section 4.3 and discussed in the Subsection 5.1.1, used input data was substantially different from reality. Hence, resultant modelled groundwater levels were mainly unrealistic. The histograms in Figure A.9 emphasize that the use of different climate models results in very different groundwater level distributions. Again, this is an indication for the flexibility of VarKarst regarding different flow paths (as in HARTMANN et al., 2014b). However, as it now impedes realistic values, results can only be seen relatively.

The analysis of the GCM output showed that there is a positive trend in mean potential evapotranspiration values. This is due to the expected increasing temperatures (as also predicted in NAKICENOVIC et al., 2000). Additionally, high precipitation values exhibit a positive trend throughout the century reflecting the presumable increase of extreme rain events (as noted for example in JIMENEZ-MARTINEZ et al., 2015).

In average, groundwater flooding predictions show a moderately upward trend during the century. However, trends among the climate models showed no consistency throughout the periods. Similarly, JIMENEZ-MARTINEZ et al. (2015) found a positive trend regarding future frequency of groundwater flooding events although their findings were more pronounced. However, whereas their results referred to a control period from 1960 until 1990, the reference period in this study is from 2000 until 2019. This may led to a less pronounced trend.

Whether these results are reliable or not remains unclear. The large uncertainties make it very difficult to assess the future groundwater flooding risk. Following EHRET et al. (2012) precipitation as an input for hydrological prediction models needs to be realistic in terms of the mean, the intensity, the intermittency and the spatio-temporal variability. In order to ensure more reliable and realistic input data, other or additional bias-correction or downscaling methods should be considered.

5.3 IMPACT

The presented approach to model groundwater levels uses the process-based karst model VarKarst. The VarKarst model was previously adapted in several settings in Europe and the Middle East (HARTMANN et al., 2013a). In contrast to the models of JIMENEZ-MARTINEZ et al. (2015) and ADAMS et al. (2010), it provides a higher transferability due to its process-based nature. Unlike the approach by UPTON and JACKSON (2011) the presented model simulates groundwater levels on a daily time step.

As has been noted by COBBY et al. (2009), the likelihood and depth of groundwater inundations is one of the major challenges for future research. Since it is a lumped approach it may provide, after BUTLER et al. (2012), "a good indication of the likelihood of groundwater flooding, but do[es] not indicate where the flooding will take place". A spatial determination of groundwater inundation as in UPTON and JACKSON (2011) would be possible but only in catchments where the borehole network is extensive. Thereby, the possibility to model several boreholes with one single calibration, due to compartment structure in VarKarst, might be also an advantage. BUTLER et al. (2012) noted that the parameterization of the unsaturated zone is a major difficulty in the Chalk. Since this study struggles also with the porosity, future work should take a closer look at this subject.

As the current predictions should be interpreted with caution, its usefulness as an groundwater flood prediction model remains to be proven. However, the results showed an overall increasing trend of groundwater level peaks similar to JIMENEZ-MARTINEZ et al. (2015). This emphasizes the importance of further developing reliable flood prediction methods. With further improvement of the method and more reliable input data, the approach is suspected to offer a simple, process-based, high-resolution alternative to the current existing approaches.

Chapter 6

Conclusions

This study focussed on the modelling of groundwater levels in the Frome catchment. An increasing number of groundwater flooding events in the UK has drawn attention of researchers in recent years. Most prior research, however, has been limited to either a low temporal resolution or black box models with no physical basis. Consequently, this study tried to contribute a process-based approach at a daily time step. The VarKarst model, introduced by HARTMANN et al. (2013a), was adapted and used for the groundwater level simulation. After calibration and validation of the model a threshold analysis was undertaken to detect groundwater inundation. Following that, GCM-output was used to derive future groundwater inundation risk.

Despite all assumptions and uncertainties associated with this study, it is a promising approach. The model performs satisfyingly at different borehole locations. However, simulation errors are still quite high and need to be reduced. Thereby, consideration should be given to the porosity parameters. A depth-depending porosity could reduce observed under/overestimations. Further, it is questionable whether a simple linear relationship between groundwater storage and groundwater level is appropriate. The outcomes of the modelling proved the karstic behaviour of the catchment but also the dominance of the matrix system, which is in accordance with previous studies of the Chalk.

The dip approach turned out to be too limited, not least because of limited data. Together with the event analysis, however, it provided an estimation for the threshold level. Owing to the overestimation of the peaks and the unrealistic GCM-output, a model threshold had to be introduced. On the one hand, it provided a reasonable estimation of the days over threshold in the historic modelling period. On the other hand, it was only a workaround which should be avoided in the future.

Climate projection results suggest a probable increase of groundwater flooding events, which is in accordance with the work of JIMENEZ-MARTINEZ et al. (2015). However, since the input data for the impact model were quite far from reality, results should be interpreted with caution. Future climate impact modelling with VarKarst in general and this approach in particular should especially examine the suitability and realism of the input data. A combination with the approach by UPTON and JACKSON (2011) could offer a simple, process-based method to model groundwater inundation spatially. Thereby, it is recommended to apply the model in catchments with a extensive borehole network.

Although there is a considerable amount of uncertainties, the approach is suspected to offer a promising alternative in the field of modelling groundwater inundation. A further development of the model with more appropriate input data could improve simulations and future predictions significantly.

References

ADAMS, B., BLOOMFIELD, J., GALLAGHER, A., JACKSON, C., RUTTER, H., and WILLIAMS, A. (2010). “An early warning system for groundwater flooding in the Chalk”. In: *Quarterly Journal of Engineering Geology and Hydrogeology* **43**:2, pp. 185–193.

ADAMS, B., PEACH, D., and BLOOMFIELD, J. (2003). *The LOCAR hydrogeological infrastructure for the Frome/Piddle catchment*. INTERNAL REPORT IR/03/179, British Geological Survey, 40 pages.

ALLEN, D., BREWERTON, L., COLEBY, L., GIBBS, B., LEWIS, M., MACDONALD, A., WAGSTAFF, S., and WILLIAMS, A. (1997). *The physical properties of major aquifers in England and Wales*. Ed. by D. ALLEN, J. BLOOMFIELD, and V. ROBINSON. Envrionment Agency, 333 pages.

ALMOND, C. (2013). “Heavy rain and flooding in southwest England on the 6. and 7. July, 2012”. In: **68**:7, pp. 171–175.

AQUILINA, L., LADOUCHE, B., and DÖRFLIGER, N. (2006). “Water storage and transfer in the epikarst of karstic systems during high flow periods”. In: *Journal of Hydrology* **327**:3, pp. 472–485.

ARCUSER (2015). *Measuring in Arc-Seconds*. The Magazine for Esri Software Users. As of September 24th, 2015. URL: http://www.esri.com/news/arcuser/0400/wdside.html.

ATKINSON, T. and SMART, P. (1981). “Artificial tracers in hydrogeology”. In: *A Survey of British Hydrogeology, London*, pp. 173–190.

BAKALOWICZ, M. (2005). “Karst groundwater: a challenge for new resources”. In: *Hydrogeology journal* **13**:1, pp. 148–160.

BANKS, D., DAVIES, C., and DAVIES, W. (1995). “The Chalk as a karstic aquifer: evidence from a tracer test at Stanford Dingley, Berkshire, UK”. In: *Quarterly Journal of Engineering Geology and Hydrogeology* **28**:Supplement 1, pp. 31–38.

BBC (2012). *Flooding risk prompts evacuation of Ilford mobile homes*. British Broadcasting Corporation. As of September 24th, 2015. URL: http://www.bbc.com/news/uk-england-dorset-18765793.

BENNETT, C. (2013). *South Winterbourne Flood Investigation*. Parsons Brinckerhoff, 106 pages.

BENNETT, N. D., CROKE, B. F., GUARISO, G., GUILLAUME, J. H., HAMILTON, S. H., JAKEMAN, A. J., MARSILI-LIBELLI, S., NEWHAM, L. T., NORTON, J. P., PERRIN, C., et al. (2013). “Characterising performance of environmental models”. In: *Environmental Modelling & Software* **40**: pp. 1–20.

BEVEN, K. (1996). “Equifinality and Uncertainty in Geomorphological Modelling”. In: *The Scientific Nature of Geomorphology: Proceedings of the 27th Binghamton Symposium in Geomorphology, Held 27-29 September, 1996*. John Wiley & Sons, pp. 289–313.

BEVEN, K. and KIRKBY, M. (1979). “A physically based, variable contributing area model of basin hydrology/Un modèle à base physique de zone d’appel variable de l’hydrologie du bassin versant”. In: *Hydrological Sciences Journal* **24**:1, pp. 43–69.

BOX, G. and JENKINS, G. (1970). *Time series analysis: forecasting and control*. Holden-Day series in time series analysis. San Francisco: Holden-Day. 537 pages.

BRADFORD, R. and CROKER, K. (2007). “Application of head-flow responses to groundwater floods in Chalk catchments”. In: *Quarterly journal of engineering geology and hydrogeology* **40**:1, pp. 67–74.

BRISTOW, R., MORTIMORE, R., and WOOD, C. (1997). “Lithostratigraphy for mapping the Chalk of southern England”. In: *Proceedings of the Geologists’ Association* **108**:4, pp. 293–315.

BRUNNER, P., DENNIS, I., and GIRVAN, J. (2010). *River Frome Geomorphological Assessment and Rehabilitation Plan*. Environment Agency, 128 pages.

BURNHAM, C. and MUTTER, G. (1993). “The depth and productivity of chalky soils”. In: *Soil use and management* **9**:1, pp. 1–8.

BUTLER, A., HUGHES, A., JACKSON, C., IRESON, A., PARKER, S., WHEATER, H., and PEACH, D. (2012). “Advances in modelling groundwater behaviour in Chalk catchments”. In: *Geological Society, London, Special Publications* **364**:1, pp. 113–127.

BUTLER, M. (2013). *Dorset County Council Flood Investigation Report July 2012*. 25 pages.

BUTSCHER, C. and HUGGENBERGER, P. (2007). “Implications for karst hydrology from 3D geological modeling using the aquifer base gradient approach”. In: *Journal of hydrology* **342**:1, pp. 184–198.

– (2008). “Intrinsic vulnerability assessment in karst areas: a numerical modeling approach”. In: *Water Resources Research* **44**:3, pp. 1–15.

CEH (2015). Centre for Ecology and Hydrology. As of September 24th, 2015. URL: http://www.ceh.ac.uk/data/.

COBBY, D., MORRIS, S., PARKES, A., and ROBINSON, V. (2009). “Groundwater flood risk management: advances towards meeting the requirements of the EU floods directive”. In: *Journal of Flood Risk Management* **2**:2, pp. 111–119.

COLLIER, S. (2014). *Groundwater Flood Risk Map Report*. envirep - Environmental Report Specialists. 15 pages.

CONRAD, O. (2003). *ChannelNetwork_Altitude.cpp*. Source code. As of Septmeber 24th, 2015. URL: http://sourceforge.net/p/saga-gis/code-0/2332/tree/trunk/saga-gis/src/modules/terrain_analysis/ta_channels/ChannelNetwork_Altitude.cpp.

– (2007). “SAGA-Entwurf, Funktionsumfang und Anwendung eines Systems für Automatisierte Geowissenschaftliche Analysen”. PhD thesis. Mathematisch-Naturwissenschaftliche Fakultäten, Georg-August-Universität zu Göttingen. 233 Seiten.

DEFRA (2004). *Developing a new Government strategy for floodand coastal erosion risk management in England*. Department for Environment, Food and Rural Affairs, 156 pages.

– (2005). *Taking forward a new Government strategy for flood and coastal erosion risk management in England*. Department for Environment, Food and Rural Affairs, 45 pages.

DORSET COUNTY COUNCIL (2005). *The Dorset Environmental Data Book 2005 - Data and Statistics for the County of Dorset*. Ed. by M. S. PETE JACKSON and J. ELDER. Dorset County Council. 74 pages.

– (2009). *A Local Climate Impacts Profile for Dorset*. Dorset County Council and Dorset District Borough Councils. 153 pages.

– (2010). *Comprehensive Climate Change Risk Assessment*. Dorset County Council & Dorset Districts & Borough Councils. 214 pages.

– (2011). *Dorset Data Book - Data and statistics for the county of Dorset. 57 pages*.

DUAN, Q., SOROOSHIAN, S., and GUPTA, V. (1992). “Effective and efficient global optimization for conceptual rainfall-runoff models”. In: *Water resources research* **28**:4, pp. 1015–1031.

EDMONDS, C. (1983). “Towards the prediction of subsidence risk upon the Chalk outcrop”. In: *Quarterly Journal of Engineering Geology and Hydrogeology* **16**:4, pp. 261–266.

EHRET, U., ZEHE, E., WULFMEYER, V., WARRACH-SAGI, K., and LIEBERT, J. (2012). “HESS Opinions" Should we apply bias correction to global and regional climate model data?"” In: *Hydrology and Earth System Sciences* **16**:9, pp. 3391–3404.

ENVIRONMENT AGENCY (2009). *Interactive Maps*. http://maps.environment-agency.gov.uk/wiyby/wiybyController?ep=maptopics&lang=_e. (as of September 24th, 2015).

– (2012). *Frome and Piddle Catchment Flood Management Plan*. Environment Agency - Summary Report, 26 pages.

FINCH, J., BRADFORD, R., and HUDSON, J. (2004). "The spatial distribution of groundwater flooding in a chalk catchment in southern England". In: *Hydrological Processes* **18**:5, pp. 959–971.

FITZPATRICK, C. (2011). "The hydrogeology of bromate contamination in the Hertfordshire Chalk: double-porosity effects on catchment-scale evolution". 371 pages. PhD thesis. University College London.

FLEURY, P., LADOUCHE, B., CONROUX, Y., JOURDE, H., and DÖRFLIGER, N. (2009). "Modelling the hydrologic functions of a karst aquifer under active water management–the Lez spring". In: *Journal of Hydrology* **365**:3, pp. 235–243.

FLEURY, P., PLAGNES, V., and BAKALOWICZ, M. (2007). "Modelling of the functioning of karst aquifers with a reservoir model: Application to Fontaine de Vaucluse (South of France)". In: *Journal of hydrology* **345**:1, pp. 38–49.

FORD, D. and WILLIAMS, P. D. (2007). *Karst hydrogeology and geomorphology*. John Wiley & Sons. 578 pages.

GOLDSCHEIDER, N. and DREW, D. (2007). *Methods in Karst Hydrogeology: IAH: International Contributions to Hydrogeology, 26*. CRC Press. 273 pages.

GOSLING, S. N., DUNN, R., CARROL, F., CHRISTIDIS, N., FULLWOOD, J., GUSMAO, D. d., GOLDING, N., GOOD, L., HALL, T., KENDON, L., et al. (2011). "Climate: Observations, projections and impacts". In: ed. by M. OFFICE. 154 pages. Met Office. Chap. United Kingdom.

GREEN, T. R., TANIGUCHI, M., KOOI, H., GURDAK, J. J., ALLEN, D. M., HISCOCK, K. M., TREIDEL, H., and AURELI, A. (2011). "Beneath the surface of global change: Impacts of climate change on groundwater". In: *Journal of Hydrology* **405**:3, pp. 532–560.

GUPTA, H. V., KLING, H., YILMAZ, K. K., and MARTINEZ, G. F. (2009). "Decomposition of the mean squared error and NSE performance criteria: Implications for improving hydrological modelling". In: *Journal of Hydrology* **377**:1, pp. 80–91.

HARIA, A. H., HODNETT, M. G., and JOHNSON, A. C. (2003). "Mechanisms of groundwater recharge and pesticide penetration to a chalk aquifer in southern England". In: *Journal of Hydrology* **275**:1–2, pp. 122–137.

HARTMANN, A., BARBERÁ, J. A., LANGE, J., ANDREO, B., and WEILER, M. (2013a). "Progress in the hydrologic simulation of time variant recharge areas of karst systems–Exemplified at a karst spring in Southern Spain". In: *Advances in Water Resources* **54**: pp. 149–160.

HARTMANN, A., GOLDSCHEIDER, N., WAGENER, T., LANGE, J., and WEILER, M. (2014a). "Karst water resources in a changing world: Review of hydrological modeling approaches". In: *Reviews of Geophysics* **52**:3, pp. 218–242.

Hartmann, A., Mudarra, M., Andreo, B., Marín, A., Wagener, T., and Lange, J. (2014b). “Modeling spatiotemporal impacts of hydroclimatic extremes on groundwater recharge at a Mediterranean karst aquifer”. In: *Water Resources Research* **50**:8, pp. 6507–6521.

Hartmann, A., Wagener, T., Rimmer, A., Lange, J., Brielmann, H., and Weiler, M. (2013b). “Testing the realism of model structures to identify karst system processes using water quality and quantity signatures”. In: *Water Resources Research* **49**:6, pp. 3345–3358.

Hartmann, A., Weiler, M., Wagener, T., Lange, J., Kralik, M., Humer, F., Mizyed, N., Rimmer, A., Barberá, J., Andreo, B., Butscher, C., and Huggenberger, P. (2013c). “Process-based karst modelling to relate hydrodynamic and hydrochemical characteristics to system properties”. In: *Hydrology and Earth System Sciences* **17**:8, pp. 3305–3321.

Hempel, S., Frieler, K., Warszawski, L., Schewe, J., and Piontek, F. (2013). “A trend-preserving bias correction – the ISI-MIP approach”. In: *Earth System Dynamics* **4**:2, pp. 219–236.

Howden, N., Neal, C., Wheater, H., and Kirk, S. (2010). “Water quality of lowland, permeable Chalk rivers: the Frome and Piddle catchments, west Dorset, UK”. In: *Hydrology Research* **41.2**: pp. 75–91.

Howden, N. J. K. (2006). “Hydrogeological controls on surface/groundwater interactions in a lowland permeable chalk catchment: implications for water quality and numerical modelling”. PhD thesis. Imperial College London (University of London).

Hughes, A., Vounaki, T., Peach, D., Ireson, A., Jackson, C., Butler, A., Bloomfield, J., Finch, J., and Wheater, H. (2011). “Flood risk from groundwater: examples from a Chalk catchment in southern England”. In: *Journal of Flood Risk Management* **4**:3, pp. 143–155.

Jackson, C. R., Bloomfield, J. P., and Mackay, J. D. (2015). “Evidence for changes in historic and future groundwater levels in the UK”. In: *Progress in Physical Geography* **39**:1, pp. 49–67.

Jacobs (2004). *Strategy for Flood and Coastal Erosion Risk Management: Groundwater Flooding Scoping Study (LDS 23) Final Report Volume 1 of 2*. Department for Environment, Food and Rural Affairs (DEFRA), 85 pages.

Jakubicka, T., Vos, F., Phalkey, R., Marx, M., and Guha-Sapir, D. (2010). *Health impacts of floods in Europe*.

Jimenez-Martinez, J., Smith, M., and Pope, D. (2015). “Prediction of groundwater induced flooding in a chalk aquifer for future climate change scenarios”. In: *Hydrological Processes*, pp. 1–38.

Johnson, A. C., Besien, T. J., Bhardwaj, C., Dixon, A., Gooddy, D. C., Haria, A. H., and White, C. (2001). “Penetration of herbicides to groundwater in an unconfined chalk aquifer following normal soil applications". In: *Journal of Contaminant Hydrology* **53**:1–2, pp. 101–117.

JONES, H. and COOPER, J. (1998). "Water transport through the unsaturated zone of the Middle Chalk: a case study from Fleam Dyke lysimeter". In: *Geological Society, London, Special Publications* **130**:1, pp. 117–128.

JUKES-BROWNE, A. (1880). "II.—The Subdivisions of the Chalk". In: *Geological Magazine (Decade II)* **7**: (06), pp. 248–257.

JUKES-BROWNE, A. and HILL, W. (1900). *The Cretaceous Rocks of Britain: The Gault and Upper Greensand of England*. Memoirs of the Geological Survey of the United Kingdom Bd. 1. 499 pages. H.M. Stationery Office.

– (1903). *The Cretaceous Rocks of Britain: The Lower and Middle Chalk of England*. Memoirs of the Geological Survey of the United Kingdom. 198 pages. H.M. Stationery Office.

– (1904). *The Cretaceous Rocks of Britain: The Upper Chalk of England*. Memoirs of the Geological Survey of the United Kingdom. 584 pages. H.M. Stationery Office.

JUKIĆ, D. and DENIĆ-JUKIĆ, V. (2009). "Groundwater balance estimation in karst by using a conceptual rainfall–runoff model". In: *Journal of hydrology* **373**:3, pp. 302–315.

KAUFMANN, G. and BRAUN, J. (2000). "Karst aquifer evolution in fractured, porous rocks". In: *Water Resources Research* **36**:6, pp. 1381–1391.

KEATING, T. (1982). "A Lumped Parameter Model of a Chalk Aquifer-Stream System in Hampshire, United Kingdom". In: *Groundwater* **20**:4, pp. 430–436.

KIRALY, L. (1998). "Modelling karst aquifers by the combined discrete channel and continuum approach". In: *Bulletin d'Hydrogéologie* **16**: pp. 77–98.

KLEMEŠ, V. (1986). "Operational testing of hydrological simulation models". In: *Hydrological Sciences Journal* **31**:1, pp. 13–24.

KORKMAZ, S., LEDOUX, E., and ÖNDER, H. (2009). "Application of the coupled model to the Somme river basin". In: *Journal of hydrology* **366**:1, pp. 21–34.

KREIBICH, H. and THIEKEN, A. H. (2008). "Assessment of damage caused by high groundwater inundation". In: *Water Resources Research* **44**:9, p. 14.

KUCZERA, G. and MROCZKOWSKI, M. (1998). "Assessment of hydrologic parameter uncertainty and the worth of multiresponse data". In: *Water Resources Research* **34**:6, pp. 1481–1489.

LEE, L., LAWRENCE, D., and PRICE, M. (2006). "Analysis of water-level response to rainfall and implications for recharge pathways in the Chalk aquifer, SE England". In: *Journal of hydrology* **330**:3, pp. 604–620.

LEHNER, B., VERDIN, K., and JARVIS, A. (2006). "HydroSHEDS technical documentation, version 1.0". In: *World Wildlife Fund US, Washington, DC*, pp. 1–27.

LIU, Y. and GUPTA, H. V. (2007). “Uncertainty in hydrologic modeling: Toward an integrated data assimilation framework”. In: *Water Resources Research* **43**:7.

LLOYD, J. (1993). “The Hydrogeology of the Chalk in North-West Europe”. In: ed. by R. DOWNING, M. PRICE, and G. JONES. Clarendon Press, Oxford. Chap. The United Kingdom, pp. 220–249.

MACDONALD, A., BREWERTON, L., and ALLEN, D. (1998). “Evidence for rapid groundwater flow and karst-type behaviour in the Chalk of southern England”. In: *Geological Society, London, Special Publications* **130**:1, pp. 95–106.

MACDONALD, D., BLOOMFIELD, J., HUGHES, A., MACDONALD, A., ADAMS, B., and MCKENZIE, A. (2008). “Improving the understanding of the risk from groundwater flooding in the UK”. In: *FLOODrisk 2008, European Conference on Flood Risk Management, Oxford, UK, 30 Sept - 2 Oct 2008. The Netherlands*: 10 pages.

MACDONALD, D., DIXON, A., NEWELL, A., and HALLAWAYS, A. (2012). “Groundwater flooding within an urbanised flood plain”. In: *Journal of Flood Risk Management* **5**:1, pp. 68–80.

MACDONALD, D., HALL, R., CARDEN, D., DIXON, A., CHEETHAM, M., CORNICK, S., and CLEGG, M. (2007). *Investigating the interdependencies between surface and groundwater in the Oxford area to help predict the timing and location of groundwater flooding and to optimise flood mitigation measures*. 12 pages.

MAURICE, L., ATKINSON, T., BARKER, J. A., BLOOMFIELD, J., FARRANT, A., and WILLIAMS, A. (2006). “Karstic behaviour of groundwater in the English Chalk”. In: *Journal of Hydrology* **330**:1, pp. 63–70.

MAY, V. and HUMPHREYS, J. (2005). *The Ecology of Poole Harbour*. Proceedings in Marine Science. 282 pages. Elsevier Science.

MCKENZIE, A., BLOOMFIELD, J., HULBERT, A., and RUTTER, H. (2007). *Confidence and Groundwater Flood Susceptibility Mapping*. British Geological Survey. 7 pages.

MCKENZIE, A., RUTTER, H., and HULBERT, A. (2010). “The use of elevation models to predict areas at risk of groundwater flooding”. In: *Geological Society, London, Special Publications* **345**:1, pp. 75–79.

MCKENZIE, A. and WARD, R. (2015). *Estimating numbers of properties susceptible to groundwater flooding in England*. 16 pages.

MEEHL, G. A., BOER, G. J., COVEY, C., LATIF, M., and STOUFFER, R. J. (2000). “The coupled model intercomparison project (CMIP)”. In: *Bulletin of the American Meteorological Society* **81**:2, pp. 313–318.

MOSS, R. H., EDMONDS, J. A., HIBBARD, K. A., MANNING, M. R., ROSE, S. K., VAN VUUREN, D. P., CARTER, T. R., EMORI, S., KAINUMA, M., KRAM, T., et al. (2010). “The next generation of scenarios for climate change research and assessment”. In: *Nature* **463**:7282, pp. 747–756.

NADARAJAH, S. and ALI, M. M. (2008). “Pareto random variables for hydrological modeling”. In: *Water resources management* **22**:10, pp. 1381–1393.

NAKICENOVIC, N. et al. (2000). “Emissions scenarios”. In: *Intergovernmental Panel on Climate Change (IPCC)*. 608 pages.

NASH, J. and SUTCLIFFE, J. V. (1970). “River flow forecasting through conceptual models part I—A discussion of principles”. In: *Journal of hydrology* **10**:3, pp. 282–290.

NRA (1995). *The Frome & Piddle Management Plan - Consultation Report*. National Rivers Authority - Environment Agency, 114 pages.

PARRY, S., MARSH, T., and KENDON, M. (2013). “2012: from drought to floods in England and Wales”. In: *Weather* **68**:10, pp. 268–274.

PERRIN, C., MICHEL, C., and ANDRÉASSIAN, V. (2001). “Does a large number of parameters enhance model performance? Comparative assessment of common catchment model structures on 429 catchments”. In: *Journal of Hydrology* **242**:3, pp. 275–301.

PINAULT, J.-L., AMRAOUI, N., and GOLAZ, C. (2005). “Groundwater-induced flooding in macropore-dominated hydrological system in the context of climate changes”. In: *Water resources research* **41**:5.

PRICE, M., DOWNING, R. A., and EDMUNDS, W. (1993). “The Hydrogeological of the Chalk in North-West Europe”. In: ed. by R. DOWNING, M. PRICE, and G. JONES. Clarendon Press, Oxford. Chap. The Chalk as an Aquifer, pp. 35–58.

REEVES, M. (1979). “Recharge and pollution of the English Chalk: some possible mechanisms”. In: *Engineering Geology* **14**:4, pp. 231–240.

RIMMER, A. and SALINGAR, Y. (2006). “Modelling precipitation-streamflow processes in karst basin: The case of the Jordan River sources, Israel”. In: *Journal of Hydrology* **331**:3, pp. 524–542.

ROBINS, N. and FINCH, J. (2012). “Groundwater flood or groundwater-induced flood?” In: *Quarterly Journal of Engineering Geology and Hydrogeology* **45**:1, pp. 119–122.

ROZOS, E. and KOUTSOYIANNIS, D. (2006). “A multicell karstic aquifer model with alternative flow equations”. In: *Journal of Hydrology* **325**:1, pp. 340–355.

SLINGO, J., BELCHER, S., SCAIFE, A., MCCARTHY, M., SAULTER, A., MCBEATH, K., JENKINS, A., HUNTINGFORD, C., MARSH, T., HANNAFORD, J., et al. (2014). *The recent storms and floods in the UK*. UK Meteorological Office, 29 pages. UK Meteorological Office, 29 pages.

TAYLOR, R. G., SCANLON, B., DÖLL, P., RODELL, M., VAN BEEK, R., WADA, Y., LONGUEVERGNE, L., LEBLANC, M., FAMIGLIETTI, J. S., EDMUNDS, M., et al. (2013). "Ground water and climate change". In: *Nature Climate Change* **3**:4, pp. 322–329.

UPTON, K. and JACKSON, C. (2011). "Simulation of the spatio-temporal extent of groundwater flooding using statistical methods of hydrograph classification and lumped parameter models". In: *Hydrological Processes* **25**:12, pp. 1949–1963.

VRUGT, J. A., GUPTA, H. V., BOUTEN, W., and SOROOSHIAN, S. (2003). "A Shuffled Complex Evolution Metropolis algorithm for optimization and uncertainty assessment of hydrologic model parameters". In: *Water Resources Research* **39**:8, pp. 1–16.

WAGENER, T., BOYLE, D. P., LEES, M. J., WHEATER, H. S., GUPTA, H. V., and SOROOSHIAN, S. (2001). "A framework for development and application of hydrological models". In: *Hydrology and Earth System Sciences* **5**:1, pp. 13–26.

WARSZAWSKI, L., FRIELER, K., HUBER, V., PIONTEK, F., SERDECZNY, O., and SCHEWE, J. (2014). "The Inter-Sectoral Impact Model Intercomparison Project (ISI–MIP): Project framework". In: *Proceedings of the National Academy of Sciences* **111**:9, pp. 3228–3232.

WDR (2005). *World Disasters Report*. Ed. by J. WALTER. International Federation of Red Cross, Red Crescent Societies, and Centre for Research on the Epidemiology of Disasters, Geneva. 258 pages.

– (2014). *World Disasters Report*. Ed. by T. CANNON and L. SCHIPPER. International Federation of Red Cross, Red Crescent Societies, and Centre for Research on the Epidemiology of Disasters, Geneva. 276 pages.

WEILER, M. and MCDONNELL, J. (2004). "Virtual experiments: a new approach for improving process conceptualization in hillslope hydrology". In: *Journal of Hydrology* **285**:1–4, pp. 3–18.

WESSEX WATER (2012). *Frome & Piddle Catchment Initiative – Framework for Engagement*. Wessex Water - Executive Summary, 10 pages.

WILLIAMS, P. W. (2008). "The role of the epikarst in karst and cave hydrogeology: a review". In: *International Journal of Speleology* **37**:1, pp. 1–10.

WORTHINGTON, S. R. (1999). "A comprehensive strategy for understanding flow in carbonate aquifers". In: *Karst modeling: special publication* **5**: pp. 30–37.

Appendix A

Figures

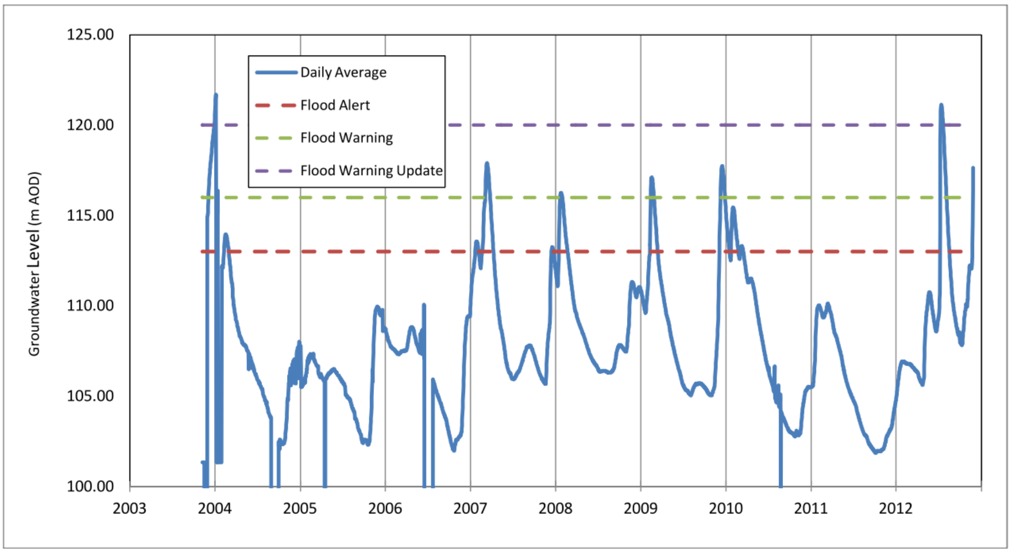

FIGURE B1: GROUNDWATER LEVEL, KINGSTON RUSSELL. 2003 – 2012.

Figure A.1: Behaviour of the borehole at Kingston Russell. Threshold levels refer to different "levels of risk" determined by the Environment Agency. Adapted from: BENNETT (2013, page 66)

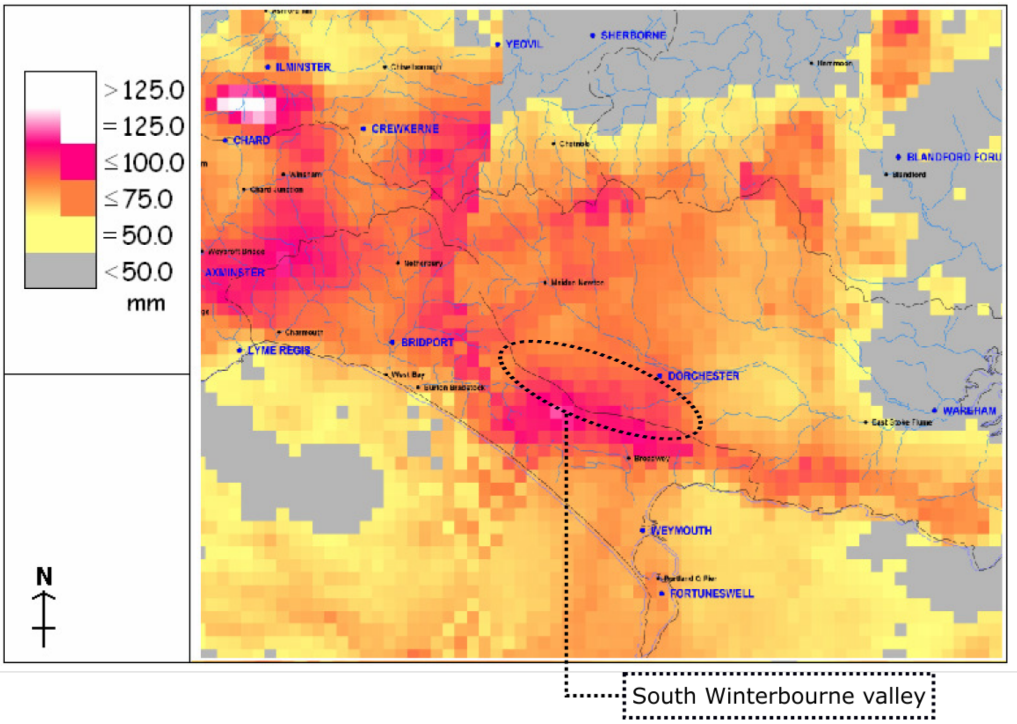

Figure A.2: Rainfall Accumulations on the 6th & 7th July in Dorset. The dashed circle shows the South Winterbourne valley, where most of the flooding occured. Modified from: BUTLER (2013, page 7)

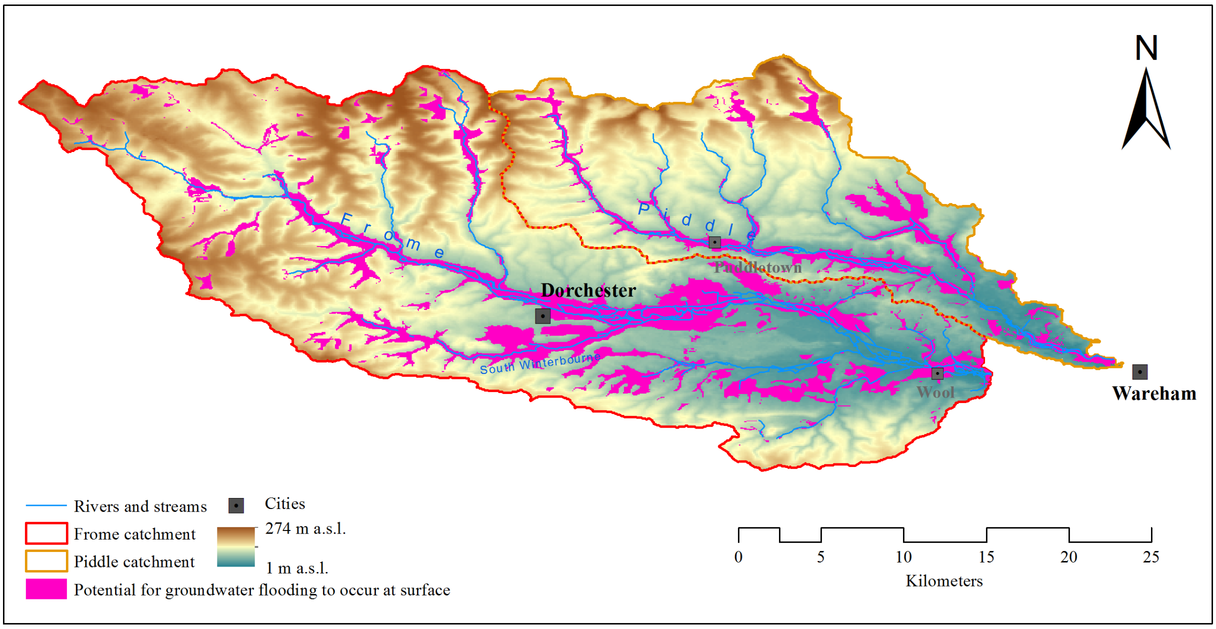

Figure A.3: Frome and Piddle catchment are with areas which are susceptible to groundwater flooding. Shapefile obtained from the BGS

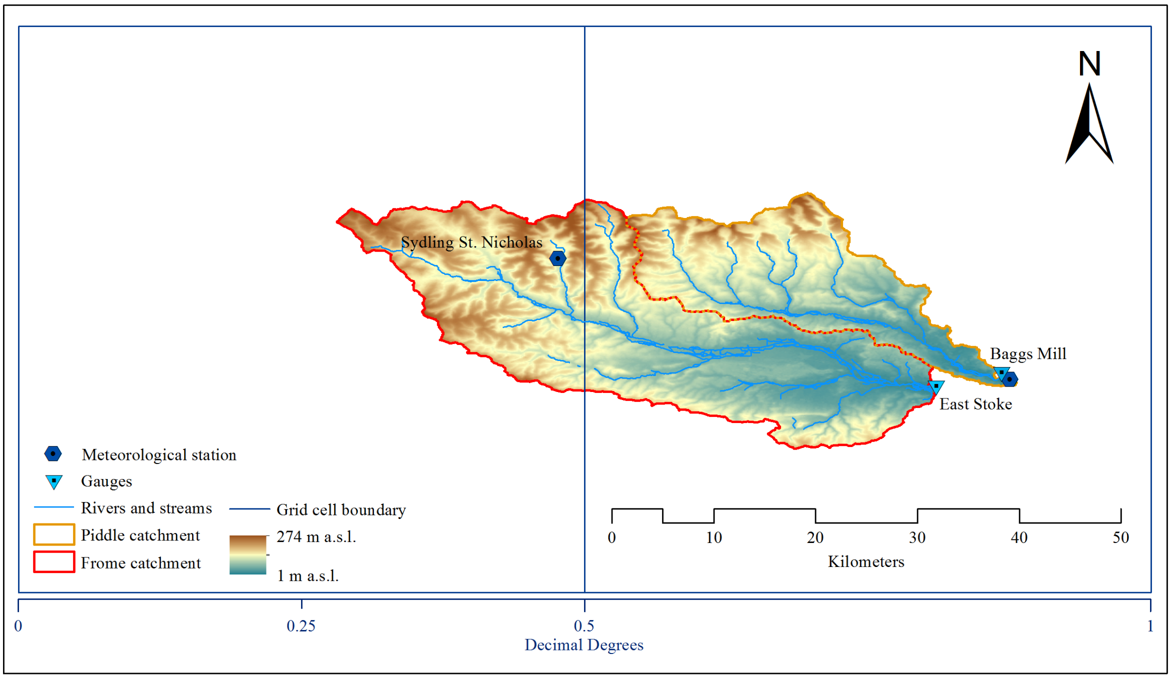

Figure A.4: Study area and size of the GCM grid cells

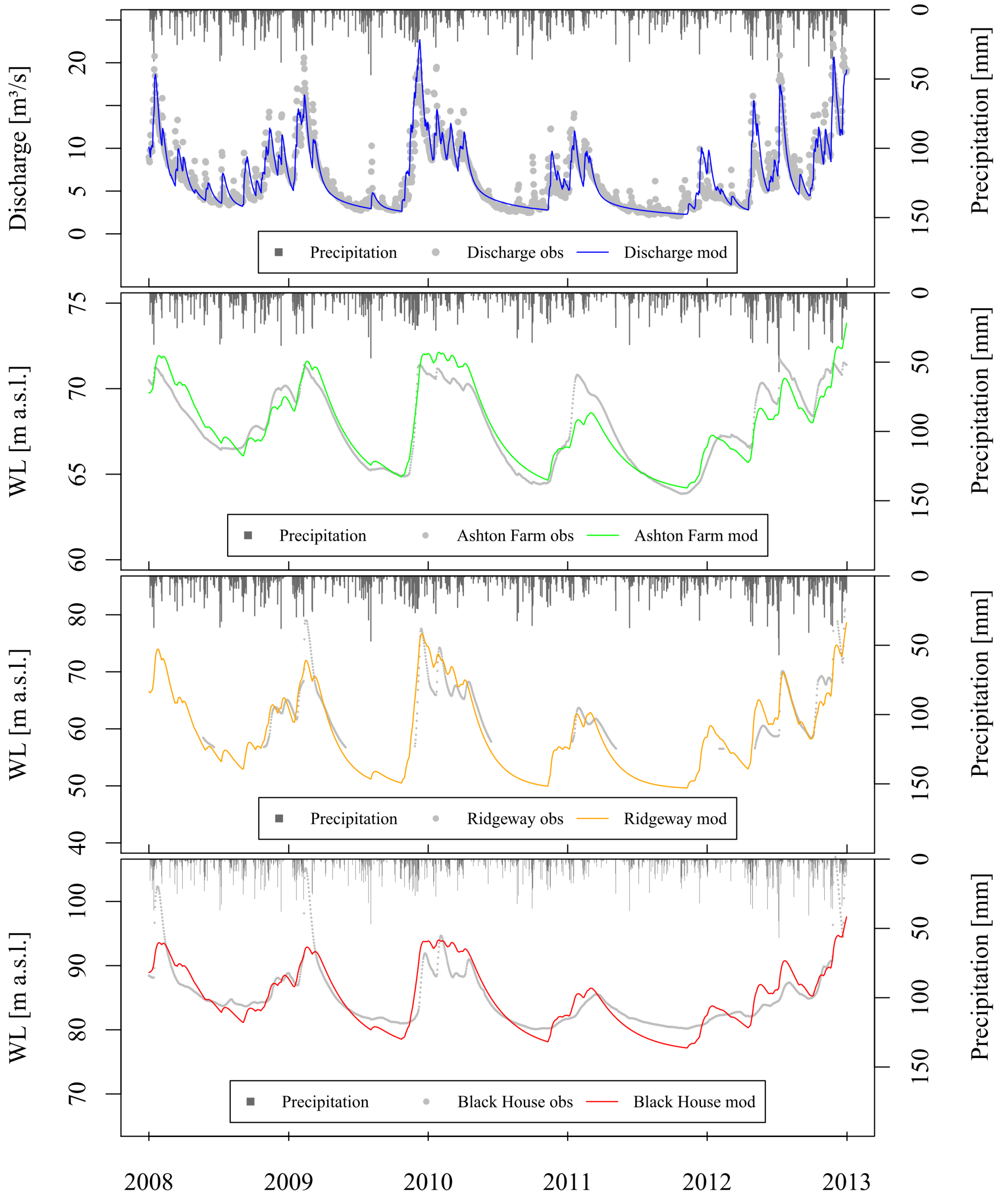

Figure A.5: Early model run without additional focus on the event in July 2012. Precipitation (Sydling St. Nicholas), observed and modelled discharge (East Stoke) and groundwater levels (Ashton Farm, Ridgeway, Black House) during the calibration period 2008-2012

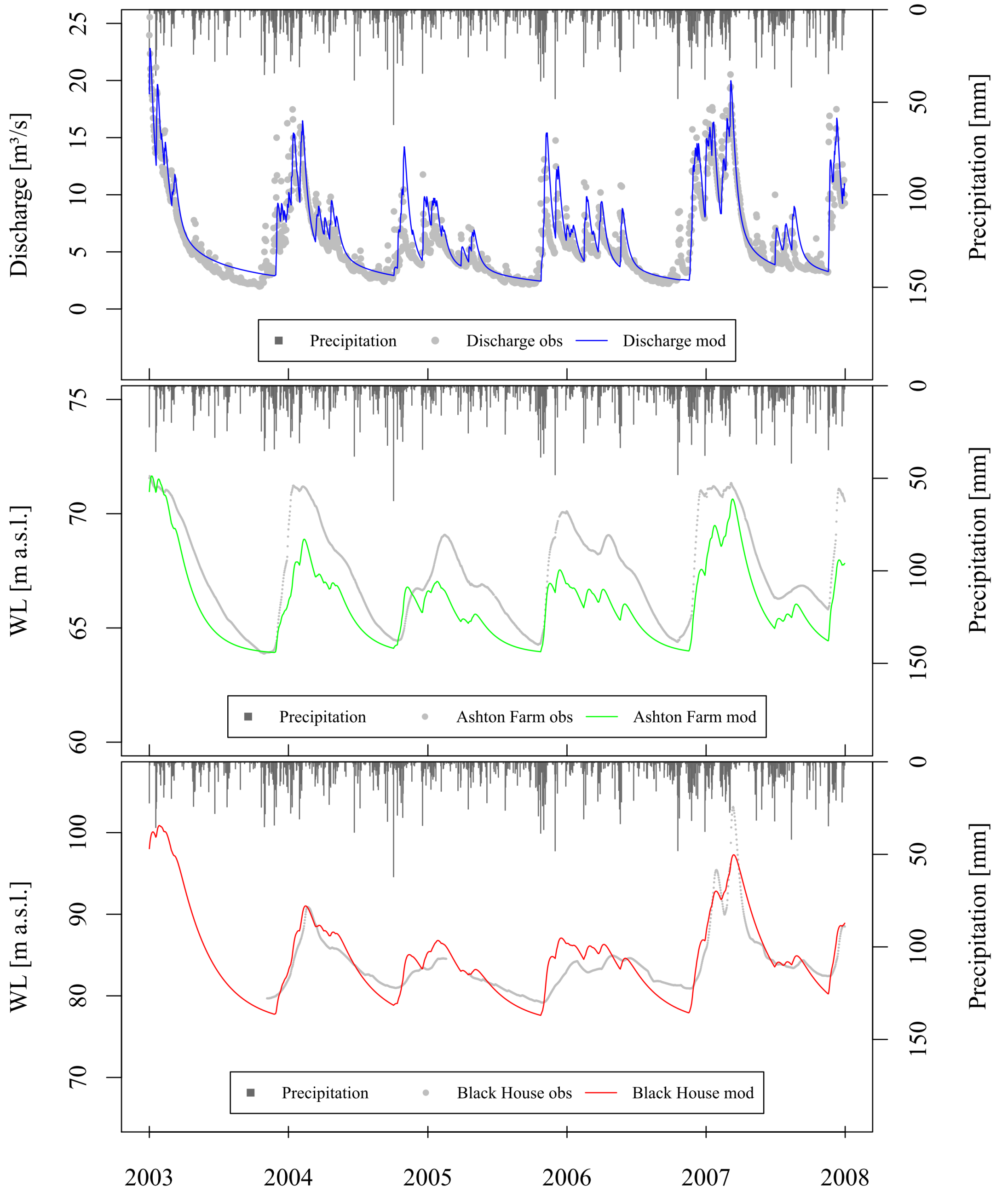

Figure A.6: Early model run without additional focus on the event in July 2012. Precipitation (Sydling St. Nicholas), observed and modelled discharge (East Stoke) and groundwater levels (Ashton Farm, Ridgeway, Black House) during the validation period 2003-2007

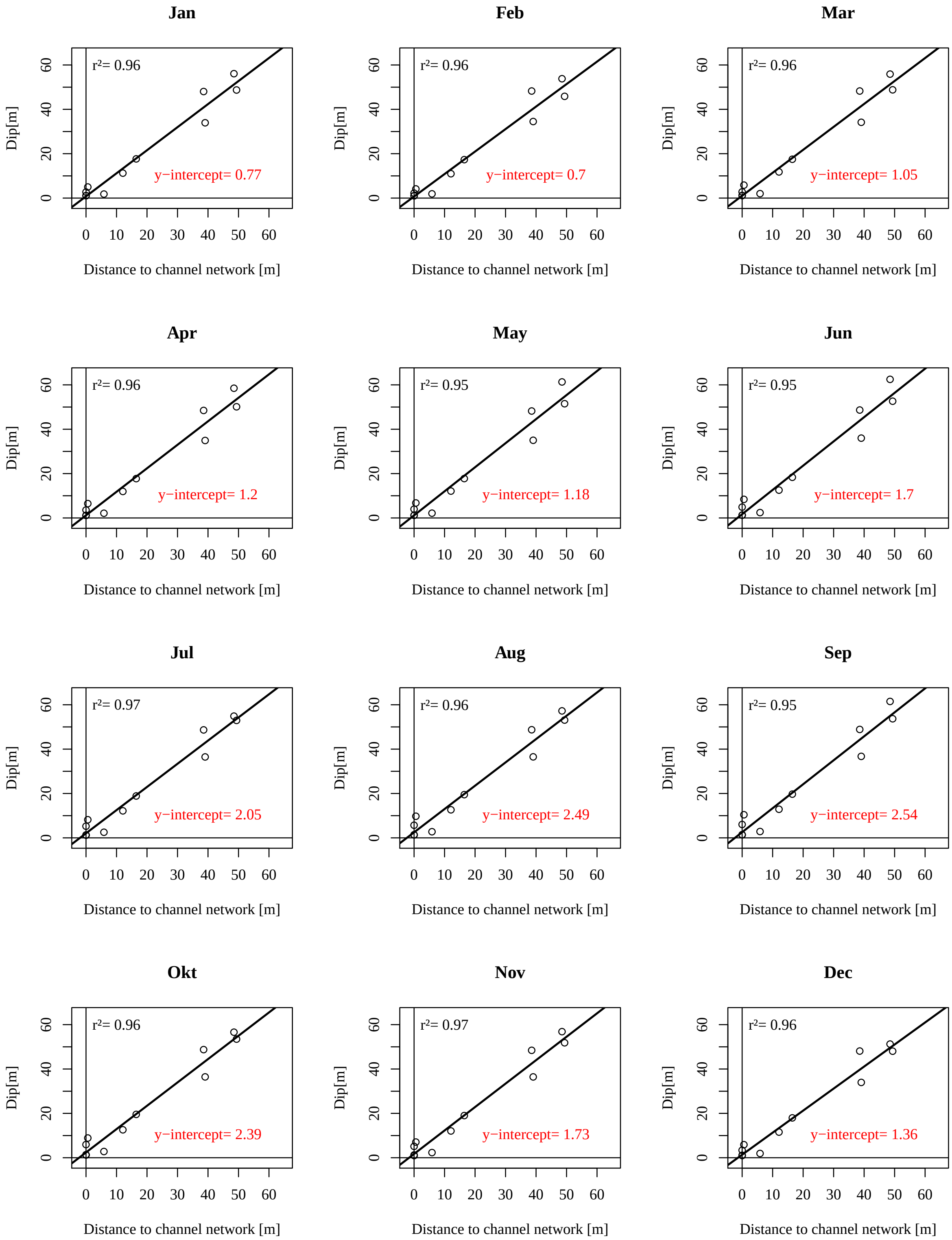

Figure A.7: Linear models of mean monthly values over the time period 2008-2012

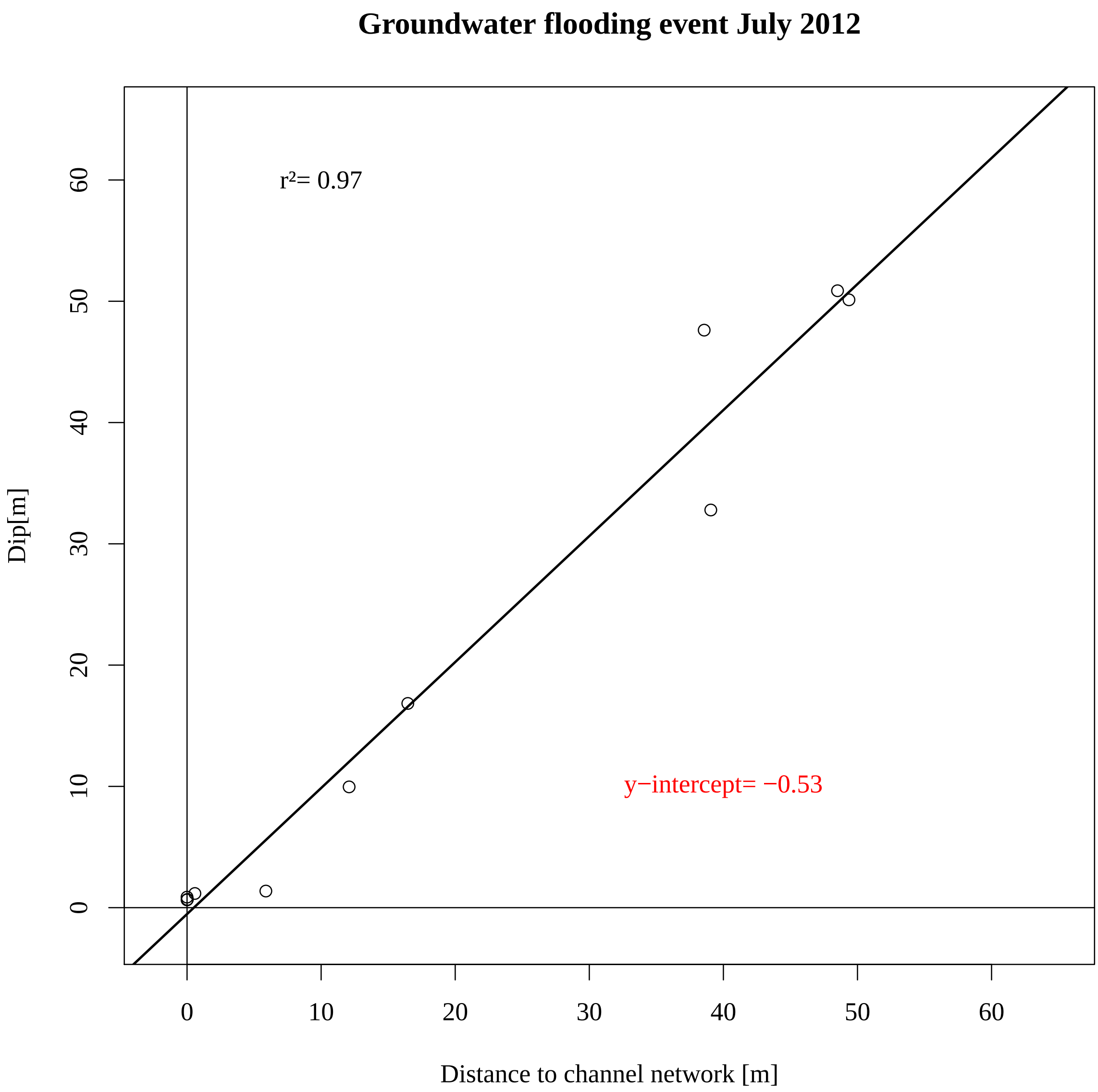

Figure A.8: Linear model at the time of the flooding (Values from the 16th/17th of July)

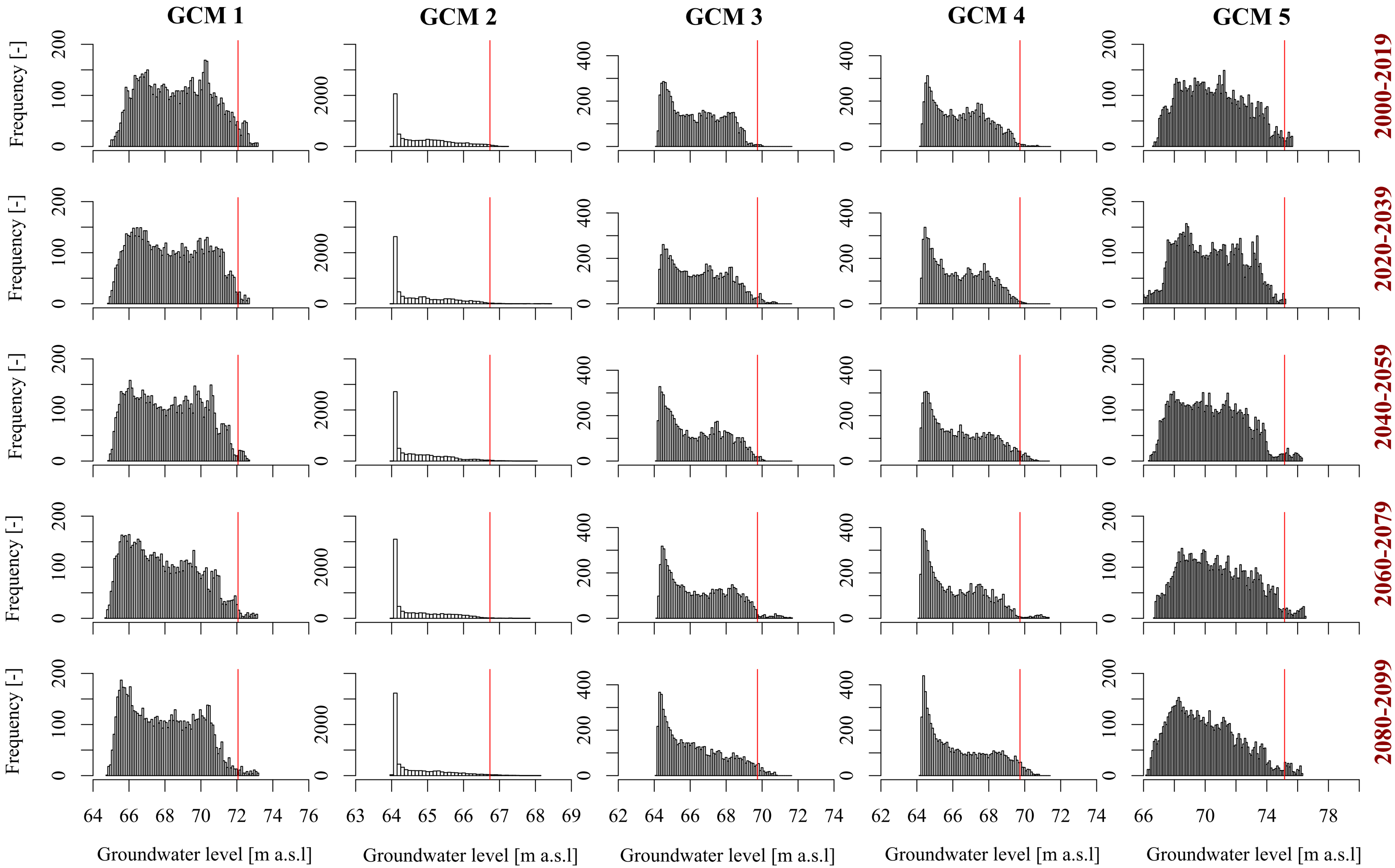

Figure A.9: Histograms of all GCMs over all Periods. The red vertical line represents the respective threshold level

Appendix B

Tables

Table B.1: Early model run: Model parameters, descriptions, ranges and optimised values

Parameter	Description	Unit	Ranges		Optimised values
			Lower	Upper	
$V_{mean,S}$	Mean soil storage capacity	mm	0	5000	4872.1
$V_{mean,E}$	Mean epikarst storage capacity	mm	0	3000	2048.6
$K_{mean,E}$	Epikarst mean storage coefficient	d	1	50	14.086
K_C	Conduit storage coefficient	d	1	10	9.9956
a_{fsep}	Recharge separation variability constant	–	0.1	5	2.6564
a_{GW}	Groundwater variability constant	–	0.1	5	4.3459
a_{SE}	Soil/epikarst depth variability constant	–	0.1	2.5	2.0615
$p_{GW,A}$	Ashton Farm Groundwater level porosity parameter	–	0.001	0.5	0.0248
$p_{Offs,A}$	Ashton Farm Groundwater level offset parameter	m	50	150	63.860
$p_{GW,R}$	Ridgeway Groundwater level porosity parameter	–	0.001	0.5	0.0058
$p_{Offs,R}$	Ridgeway Groundwater level offset parameter	m	50	150	49.436
$p_{GW,B}$	Black House Groundwater level porosity parameter	–	0.001	0.5	0.0117
$p_{Offs,B}$	Black House Groundwater level offset parameter	m	50	150	76.453
$KGE_{weighted}$	Weighted multi-objective model performance	–	0	1	0.89/0.81*
KGE_Q	Model performance for discharge	–	0	1	0.90/0.84*
$KGE_{GW,A}$	Model performance for groundwater level at Ashton Farm	–	0	1	0.93/0.78*
$KGE_{GW,R}$	Model performance for groundwater level at Ridgeway	–	0	1	0.89/ – *
$KGE_{GW,B}$	Model performance for groundwater level at Black House	–	0	1	0.85/0.81*

*Calibration/validation

Table B.2: Means of different percentile ranges of future predicted precipitation [mm] and the observed reference period 2000-2012

Model	Period	Total mean	Percentiles					
			100-95	100-80	80-60	60-40	40-20	20-0
Observed	2000 - 2012	3.25	29.73	17.57	5.47	1.92	0.48	0.01
GCM1	2000 - 2019	2.51	13.20	8.87	4.55	2.73	0.98	0.05
	2020 - 2039	2.42	13.46	8.86	4.38	2.53	0.92	0.04
	2040 - 2059	2.39	13.47	8.85	4.30	2.34	0.77	0.03
	2060 - 2079	2.28	13.49	8.86	4.12	2.11	0.66	0.02
	2080 - 2099	2.30	13.92	9.01	4.10	2.06	0.54	0.02
GCM2	2000 - 2019	2.31	19.09	11.78	4.89	2.59	1.04	0.03
	2020 - 2039	2.26	19.41	12.09	4.97	2.61	1.08	0.03
	2040 - 2059	2.15	19.42	11.94	4.62	2.27	0.67	0.01
	2060 - 2079	2.16	20.26	12.36	4.60	2.27	0.74	0.02
	2080 - 2099	2.17	20.71	12.70	4.68	2.24	0.65	0.01
GCM3	2000 - 2019	2.32	13.30	8.97	4.73	2.90	1.45	0.10
	2020 - 2039	2.50	13.81	9.46	4.91	3.06	1.66	0.12
	2040 - 2059	2.41	13.95	9.54	4.90	2.89	1.46	0.10
	2060 - 2079	2.51	14.29	9.87	5.06	3.03	1.58	0.11
	2080 - 2099	2.46	15.28	10.3	5.22	3.09	1.43	0.07
GCM4	2000 - 2019	2.45	11.88	8.27	4.32	2.59	1.12	0.07
	2020 - 2039	2.53	12.40	8.63	4.56	2.82	1.20	0.07
	2040 - 2059	2.61	13.31	9.13	4.75	2.80	1.14	0.07
	2060 - 2079	2.58	13.13	9.14	4.73	2.79	1.15	0.06
	2080 - 2099	2.71	14.21	9.88	5.09	3.01	1.26	0.07
GCM5	2000 - 2019	2.23	12.50	8.31	4.08	2.35	0.94	0.05
	2020 - 2039	2.20	12.48	8.31	3.89	2.08	0.76	0.04
	2040 - 2059	2.22	12.77	8.48	4.01	2.18	0.73	0.03
	2060 - 2079	2.34	13.28	8.82	4.10	2.32	0.84	0.04
	2080 - 2099	2.20	13.54	8.69	3.83	1.91	0.59	0.03

Table B.3: Means of different percentile ranges of future predicted potential evapotranspiration [mm] and the observed reference period 2000-2012. Potential evapotranspiration is calculated with the Thornthwaite equation

Model	Period	Total mean	Percentiles					
			100-95	100-80	80-60	60-40	40-20	20-0
Observed	2000 - 2012	1.67	4.81	3.17	2.27	1.50	0.90	0.46
GCM1	2000 - 2019	1.04	3.50	2.94	1.87	1.02	0.41	0.04
	2020 - 2039	1.07	3.55	2.98	1.95	1.06	0.43	0.04
	2040 - 2059	1.08	3.66	3.06	1.95	1.05	0.40	0.04
	2060 - 2079	1.08	3.73	3.08	1.93	1.02	0.40	0.04
	2080 - 2099	1.09	3.76	3.11	1.97	1.03	0.40	0.04
GCM2	2000 - 2019	1.14	3.47	3.01	2.06	1.23	0.51	0.05
	2020 - 2039	1.22	3.63	3.17	2.26	1.34	0.55	0.05
	2040 - 2059	1.25	3.70	3.27	2.29	1.35	0.55	0.05
	2060 - 2079	1.30	3.80	3.34	2.38	1.43	0.58	0.05
	2080 - 2099	1.35	3.96	3.49	2.47	1.48	0.60	0.05
GCM3	2000 - 2019	1.12	3.24	2.92	2.06	1.22	0.49	0.05
	2020 - 2039	1.19	3.41	3.10	2.24	1.28	0.50	0.04
	2040 - 2059	1.21	3.44	3.12	2.25	1.33	0.53	0.05
	2060 - 2079	1.24	3.52	3.20	2.32	1.34	0.54	0.04
	2080 - 2099	1.29	3.56	3.27	2.44	1.41	0.58	0.05
GCM4	2000 - 2019	1.17	4.64	3.61	1.87	1.05	0.48	0.05
	2020 - 2039	1.37	5.07	4.12	2.30	1.26	0.53	0.05
	2040 - 2059	1.40	5.11	4.19	2.33	1.29	0.55	0.05
	2060 - 2079	1.51	5.27	4.44	2.63	1.40	0.57	0.05
	2080 - 2099	1.54	5.33	4.47	2.69	1.46	0.60	0.06
GCM5	2000 - 2019	1.13	3.61	3.07	2.02	1.17	0.49	0.05
	2020 - 2039	1.18	3.64	3.16	2.12	1.25	0.52	0.05
	2040 - 2059	1.22	3.79	3.26	2.19	1.30	0.53	0.05
	2060 - 2079	1.24	3.95	3.38	2.23	1.28	0.53	0.05
	2080 - 2099	1.29	4.07	3.47	2.34	1.34	0.56	0.05

Appendix C

Derivations

Originally, as demonstrated by GUPTA et al. (2009), the KGE comprises three components:

$$KGE = 1 - \sqrt{(r-1)^2 + (\alpha-1)^2 + (\beta-1)^2} \tag{C.1}$$

with the squared expressions corresponding to the linear correlation, the conditional bias and the unconditional bias, respectively. Considering only the correlation the simplified expression is as follows:

$$KGE_r = 1 - \sqrt{(r-1)^2} \tag{C.2}$$

leading to the final equation:

$$KGE_r = 1 - |r-1| \tag{C.3}$$

Ehrenwörtliche Erklärung

Hiermit erkläre ich, dass die Arbeit selbständig und nur unter Verwendung der angegebenen Hilfsmittel angefertigt wurde.

Ort, Datum Unterschrift